VCAM1 expressed by CD8$^+$ CAR T cells promotes T cell activation and tumor cell binding

DISSERTATION ZUR ERLANGUNG DES DOKTORGRADES
DER NATURWISSENSCHAFTEN (DR. RER. NAT.)
DER FAKULTÄT FÜR BIOLOGIE UND VORKLINISCHE MEDIZIN
DER UNIVERSITÄT REGENSBURG

vorgelegt von

Valerie Sophia Bezler

aus

Stuttgart

im Jahr

2024

Das Promotionsgesuch wurde eingereicht am:

08.04.2024

Die Arbeit wurde angeleitet von:

Prof. Dr. Philipp Beckhove

Unterschrift

_____

Valerie Sophia Bezler

Declaration

I herewith declare in lieu of oath that I have composed this thesis without any inadmissible help of a third party and without the use of aids other than those listed. The data and concepts that have been taken directly or indirectly from other sources have been acknowledged and referenced.

Other persons have not helped to produce this work as regards to its content or making. In particular, I have not used the services of any professional agencies in return for payment or those of other persons. Nobody has received payment in kind – neither directly nor indirectly – from me for any work that is connected with the content of this doctoral thesis.

This thesis has not been submitted, wholly or substantially, neither in this country nor abroad for another degree or diploma at any university or institute.

I declare in lieu of oath that I have said nothing but the truth to the best of my knowledge and that I have not withheld any information.

Before the above declaration in lieu of oath had been taken down, I was advised about the significance of a declaration in lieu of oath as well as the legal consequences of an incorrect or incomplete declaration.

Regensburg, 08.04.2024

Valerie Sophia Bezler

Acknowledgements

First and foremost, I want to thank you Hinrich, for teaching the fundamental question of the scientific rational and prioritize science beside all obstacles – thanks for being *super* and *wise* what probably makes you the best supervisor!
Thanks to Philipp Beckhove and Gernot Längst who as mentors invested their time and brain-capacities to support me with constructive feedback. Special gratitude goes to Mike-Andrew Westhoff who escorted my way from the first to the – for now latest rocket-science-thesis!
The whole lit LIT story started with my internship visit in the Schmidl family. Without the base of data of Dania Riegel and Christian Schmidl I could not have built up this story, Manuela and Brigitte likewise helped with the first bricks of FACS, CRISPR and SNACK techniques. New family members joined, and I am very happy to have the philosophically and physiologically embracing Elena around e buone vibrazioni con Marianna & Chiara.
Thanks to the CAR drivers: Marcell with his positive input in form of knowledge and Kimchi, Anja providing a load of help and funny sayings, Jordan with his sense of ease, Astrid taking me to the translational prodigy and her positive-energy-booster, Hong with her beautiful brain (I love the output!), Markus an inspiring example in finding fun and energy for cycling everywhere, Dennis for his late-night-input and paper-output, Sophia for open heart and door, Helena for sharing me-times, Charlotte for optimal organization, Tina for MACSIMAL histo-help and Celine for caring, Linda, Marianna, Maria and Sin-Syue for crossing our CAR driving lane and bringing inspiration.
Melissa Baumeister and Luise Aumüller joined as internship students and mutual support.
Scientists are special colleagues anyway but I am very happy to have found friends among them. I would not want to miss the countless boulder sessions with Jules teaching us "just to grasp up", or the empowering mindset and sailing sessions with Franzi. A special thanks goes to all my dear Pint of Science colleagues, bringing value and fun!
Thanks to all the people helping out and in the LIT for smooth work around the clock.

Härter Kerniger was my survival package since the days I decided to commit to science and they never let me down but rather lifted me over waves and hills, Nancy, Tobi, Uwe, Stäsh, Eva und Chrystl – Danke!

Since I have been small my constant growth was nourished with unwavering support by my family, even that I have grown quite I feel like I can stretch even further because of being backed up. Danke Mama, Papa, Opa & Oma Eva und Felix mit Mädels dass ihr an mich glaubt und für mich da seit!
Well Chris you are the *watt* that powers me through every day – I am grateful and enamoured for each *joule* that you invest in our potential!

Abstract

Chimeric antigen receptor (CAR) T cell therapy has shown extraordinary success in the treatment of B cell leukemia and lymphoma. For treatment of solid cancers, CAR T cell therapy faces many obstacles. Most prominent, the inhibitory tumor microenvironment limits the CAR T cell endurance, and the abundance of cancer cells leads to T cell exhaustion. T cell states have been studied to identify populations with best fitness and long-lasting effector functions. The modulation of immune checkpoint molecules, most prominent PD1, enhances the anti-tumor performance of T cells, at least transiently. Ongoing effort is made to identify further players in the orchestration of CAR T cell functionality.

Our colleagues analyzed tumor infiltrating lymphocytes (TILs) of various solid tumor entities and found the gene activity of VCAM1 (vascular adhesion molecule 1) upregulated in terminal exhausted TILs. So far, VCAM1 is commonly known to be expressed on activated endothelium and to bind VLA-4 on lymphocytes to mediate their adherence and transmigration, however the expression of VCAM1 on T cells was barely reported.

We aimed at defining whether VCAM1 is also expressed on CAR T cells and how VCAM1 modulates CAR T cell function. We found that VCAM1 is indeed upregulated, predominantly on $CD8^+$ CAR T cells, upon activation by either TCR or CAR. Interestingly VCAM1 expression was barely induced on $CD4^+$ CAR T cells or on T cells without CAR. VCAM1 induction was the strongest by the 4-1BB CAR, less by the CD28 CAR. CAR signaling is required to induce early VCAM1 expression since deletion of CAR signaling domains abolished the VCAM1 induction. To address the impact of CAR T cell associated VCAM1 on target cell recognition, we took advantage of BXPC-3 cells that express the VCAM1 ligand VLA-4 but lack VCAM1 expression. We analyzed CAR T cells with CRISPR/Cas9 mediated VCAM1 knockout in co-culture with BXPC-3 cells and found CAR T cells with VCAM1 knockout showed much lower expression of the activation markers CD25 and CD69. Also, the exhaustion molecules PD1, Tim3 and Lag3 were expressed to lower levels on VCAM1 knockout CAR T cells. The VCAM1 knockout in CAR T cells was leading to enrichment of the effector memory phenotype. Markers for degranulation CD107a and intracellular granzyme B and perforin levels were likewise reduced in VCAM1 knockout CAR T cells. However, the in vitro cytotoxicity towards BXPC-3 cells was not altered. We further found reduced avidity of VCAM1 knockout CAR T cells to the target cells compared to the CRISPR-control. These data imply that VCAM1 takes part in the CAR T cell – tumor cell interaction. Our conclusion was sustained by the microscopy observation that CAR and VCAM1 co-localize on the same spot on the T cells and in the contact region to the target cell.

With that we conclude that VCAM1, expressed by CAR T cells, amplifies the avidity in their contact with tumor cells and impacts the activation and exhaustion development of the CAR T cells.

Table of Contents

Abstract ..... **I**

Table of Contents ..... **II**

1. Introduction **1**

1.1. Engineering chimeric antigen receptors 1

1.2. Advancing CAR T cell therapy for application in solid tumors 3

1.3. The immunological CAR synapse 4

1.4. The canonical role of VCAM1 as adhesion molecule 6

1.5. T cell exhaustion with implications for immunotherapy 7

1.6. VCAM1 shows enhanced gene activity and upregulated RNA levels in $CD8^+$ TILs with terminal exhaustion signature 9

1.7. VCAM1 expressed by activated CD8+ T cells - proposing a non-canonical role of VCAM1 11

2. Materials **12**

2.1. Chemicals and reagents 12

2.2. Kits 13

2.3. Buffers & Solutions 13

2.4. DNA preparation 13

2.4.1. PCR reagents 13

2.4.2. Primer 14

2.5. Bacterial strains & culture medium 14

2.6. Plasmid vectors 15

2.7. CRISPR/Cas9 RNA 16

2.8. Cell culture 16

2.8.1. Cell culture medium and supplements 16

2.8.2. Cell lines & primary cells 16

2.9. Antibodies 17

2.10. Software 18

3. Methods **19**

3.1. Bacterial work 19

3.1.1. Heat shock transformation 19

3.1.2. Bacterial culture and expansion 19

3.2. DNA preparation 20

3.2.1. Plasmid design 20
3.2.2. Plasmid isolation 20
3.2.3. Mutagenesis - STOP codon insertion 20
3.2.4. Gibson assembly 21
3.2.5. Sequencing 21
3.3. Cell culture 22
3.3.1. Cell culture of adherent cells 22
3.3.2. Isolation of human peripheral blood mononuclear cells (PBMCs) 22
3.3.3. Cell culture of primary human PBMCs 22
3.4. CAR T cell production 23
3.4.1. Co-transfection of HEK293T cells 23
3.4.2. Retroviral transduction of human T cells 23
3.4.3. Magnetic cell separation (MACS®) 24
3.4.4. CRISPR/Cas9 mediated VCAM1 knockout 24
3.5. Flow cytometry 25
3.5.1. Detection of VCAM1 induction or knockdown/knockout 25
1.1.1. Detection of VLA-4 25
1.1.2. Detection of activation markers CD25/CD69 25
1.1.3. Detection of exhaustion markers PD1/Tim3/Lag3 26
1.1.4. Detection of the memory phenotype 26
1.1.5. Detection of CD107a 26
1.1.6. Detection of Granzyme B/Perforin 26
1.2. Enzyme linked immunosorbent assay (ELISA) 27
1.3. Incucyte cytotoxicity 27
1.4. Rechallenge assay 28
1.5. Cell avidity - zMovi 29
1.6. Confocal microscopy 29
1.7. Statistical analysis 29
2. Results 30
2.1. VCAM1 is upregulated in CD8+ CAR T cells upon stimulation 30
2.2. CAR signaling is required for enhanced VCAM1 induction in T cells 32
2.3. Expression of the VCAM1 ligand VLA-4 34
2.4. VCAM1 knockdown and knockout in CAR T cells 36

2.4.1. shRNA mediated knockdown of VCAM1 in CAR T cells 36
2.4.2. CRISPR/Cas9 mediated VCAM1 knockout in CAR T cells 38
2.5. VCAM1 knockout reduces the activation and exhaustion phenotype in CD8+ CAR T cells 40
2.7. CAR T cell degranulation is decreased upon VCAM1 knockout 43
2.8. VCAM1 co-localizes with the CAR in the T cell - tumor cell contact area. 45
2.9. Avidity of CAR T cells to target cells is reduced upon VCAM1 knockout 47
3. Discussion 49
4. References 57
5. Appendix 73
5.1. List of Abbreviations 73
5.2. List of Figures 74
5.3. List of Tables 75
5.4. VCAM1 exons and target sites 76
5.5. Genomic sequences of CAR constructs 76
5.5.1. #2181 pBullet_Lk_BW431/26scFv_IgG1Fc-CD4TM_41BB_CD3ζ _mir30_shVCAM1-exon2 77
5.5.2. #2182 pBullet_Lk_BW431/26scFv_IgG1Fc-CD4TM_41BB_CD3ζ_mir30_shVCAM1-exon3-early 80
5.5.3. #2193 pBullet_Lk_BW431/26scFv_IgG1Fc-CD4TM_41BB_CD3ζ _mir30_shVCAM1-exon3-late 82
5.5.4. #2210 pBullet_Lk_BW431/26scFv_IgG1Fc-CD4TM_41BB_CD3ζ _mir30_shKanamycin 84
5.5.5. #2602 pBullet_Lk-BW431/26scFv_CD8hinge-CD8TM_41BB_CD3z 86
5.5.6. #2737 pBullet_Lk_BW431/26scFv_IgG1Fc-CD4TM_41BB 88
5.5.7. #2738 pBullet_Lk_BW431/26scFv_IgG1Fc-CD4TM_CD3zeta 91
5.5.8. #2739 pBullet_Lk_BW431/26scFv_IgG1Fc_CD4TM 93

1. Introduction

Cancer is one of the three leading causes of death in industrialized nations besides cardiovascular and infectious diseases[1–3]. The adaptive immune system is capable to control tumor growth to a certain extend but various tumor escape mechanisms can prevail the surveillance of immune cells. First line therapies comprise tumor resection, radiotherapy and chemotherapy with success in some tumor entities. Yet in many cases surgery is unfeasible because of constraint access or disseminated cancer cells that might form metastasis in distant tissues. Radio-and chemotherapy are capable to target cells systemically but come alongside with severe side effects, even though constant progress is being made in this respect. A rather new approach in the toolbox of oncologists is cell-based immunotherapy.

Immunotherapies can support the natural defense, as in case of TIL (tumor infiltrating lymphocyte) therapy or with immune-checkpoint blockade and often serve as an adjuvant procedure to the first line therapy[4,5]. The understanding of the T cell recognition and activation mechanisms has led to the development of more advanced technologies to redirect the immune cells specifically against pre-defined targets. Artificial immune receptors, in early research called "T-bodies"[6] or immunoreceptors, were engineered to be expressed by T cells to provide specificity in targeting and activation. The immune receptors, later called chimeric antigen receptor (CAR), were developed with the aim of arming patient own T cells with an MHC independent antigen recognition domain to detect and eliminate cancer cells.

1.1. Engineering chimeric antigen receptors

Each CAR T cell element needs to be carefully designed for an optimal tumor cell contact, for downstream signaling and subsequent anti-tumor response of the T cell.

The CAR is composed of the antigen targeting domain, usually a single chain variable fragment of an antibody (scFv), followed by a linker that serves also as a spacer to adjust the distance between T cell and target cell. The scFv and linker are the extracellular CAR domain and are connected with a transmembrane domain to the intracellular signaling moiety[7,8]. Other antibody derivates like nanobodies[9,10] or other recognition domains like DARPins[11] can also be used. For the first generation of CAR T cells only a CD3ζ domain transmitted the activating stimulus after binding of target antigen. Adding a co-stimulatory domain in the second generation CAR enabled engineered T cells to overcome the limited persistence of the first generation of CAR T cells[12]. Co-stimulatory domains and the CD3ζ signaling domain are both derived from the T cell receptor (TCR) activation machinery[13]. Most commonly CD28 or 4-1BB cytoplasmatic domains are inserted in addition to the CD3ζ domain for co-stimulation. Molecular structure and membrane organisation[14] differ between co-stimulatory domains and

exhibit different activation patterns of the CAR T cells[15]. CD28 is known to induce stronger activation, whereas 4-1BB provides lower clinical toxicity and longer persitence[15, 16]. Other co-stimulatory domains like ICOS, OX40 or CD40 are under investigation with the aim to modulate expression of certain cytokines, to achieve polarization of the T cell to a certain phenotype and to mediate activation and persistence[17,18].

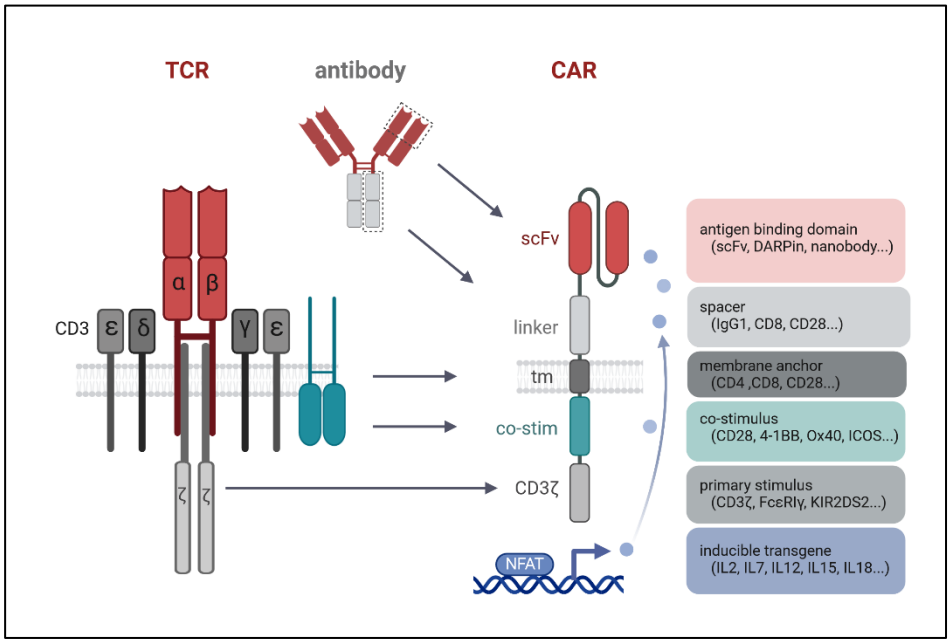

***Figure 1: The Chimeric Antigen Receptor building blocks**. Most common antigen binding domain of CARs are antibody derived scFvs. T cell receptor (TCR) derived signaling domains are added downstream of the receptor to provide the primary and secondary signal, required for T cell activation. In the latest generation of CARs further transgenes are added to provide a third signal by autocrine cytokines or to attract bystander immune cells. Often these transgenes are set under the T cell activation dependent NFAT promoter. scFv = single chain variable fragment, tm = trans membrane.*

A fourth generation of CAR T cells redirected for antigen-unrestricted cytokine-initiated killing (TRUCKs)[19], were engineered to deliver an additional signal for transgenic cytokine secretion. Often the transgenic cytokine is controlled in the expression by the inducible NFAT / IL2 minimal promotor, so it is only produced upon activation of the TCR/CD3 or second-generation CAR signaling cascade. With IL7, IL15, IL18 and IL23 an autocrine stimulus is added to enhance the CAR T cell function[20–23]. IL12 provides a paracrine stimulation, attracting bystander innate immune cells such as NK-cells and macrophages[24,25]. Also other proteins than cytokines can be added as additional transgene to modulate anti-tumor function[26–28].

1.2. Advancing CAR T cell therapy for application in solid tumors

CAR T cell therapies have achieved remarkable success in treating hematologic cancers, even offering cures for patients previously considered untreatable[20,29,30].

B-cell lymphomas present an ideal target for CAR T cell treatment because of the uniform expression of CD19 antigen and the homing of target and effector cells to the same compartment. Success with anti-CD19 CAR cells was achieved with long term remission exceeding in some patients more than ten years in adults and children[31–33]. Challenges remain in the high frequency of relapses and the fine tuning of CAR T cell activity to manage side effects that arise from over activation and antigen escape of cancer cells.

When it comes to solid tumors other challenges additionally come into place, as the great heterogeneity within the cancer cell population impedes the targeting of all entities. Further the cancer cells are not as easily accessible, but often integrated in obstructive tumor stroma and an inhibitory milieu, comprising inhibitory cytokines, chemokines, the expression of checkpoint molecules as well as suppressive cells like Tregs and cancer associated macrophages[34–36]. One example is pancreatic cancer, exhibiting a challenging micro-environment characterized by a dense stroma[37], which allows tumor resection in only 15-20% of all cases[38,39], most probably also hindering the accessibility of CAR T cells. Despite these obstacles, various solid tumor entities have been addressed with targeted CAR T cell therapy among which are colorectal cancer[40], breast cancer[41], non-small cell lung cancer[42], neuroblastoma[43] and glioblastoma[44–47]. Major limitations to success were on target off tumor toxicity, antigen loss and overall limited efficacy[48,49].

To enhance efficacy of CAR T cells they are supported with checkpoint blockade[4,50–52] and small molecule drugs[53]. For enhancing the persistence of CAR T cells, additional cytokine administration or cytokine secretion in the TRUCK system are approached[22,23,54]. With released cytokines also the innate immune system is intended to be recruited to the tumor site. Dual CAR recognition domains are being designed to target the tumor heterogeneity. For less on-target-off-tumor effects, dual recognition CARs with "AND" gating, only providing full T cell activation when both antigens are present, are tested and in clinical exploration[55,56].

First trials have shown clinical safety for applying CAR T cells with additional CRISPR/Cas9 engineering of defined cellular genes, which opens the toolbox for intrinsic fine tuning of the CAR T cell properties[57,58]. To date the knockout approach was used in the clinics to avoid co-expression of the endogenous TCR or the checkpoint molecule PD1[58,59]. The knockdown of other inhibitory signals can be an versatile step towards successful solid tumor clearance; for example CTLA-4 knockout in cytotoxic lymphocytes substantially increases anti-tumor activity[60]. CRISPR technologies can also be used to enhance expression of defined proteins, taking advantage of the dCas9 without catalytic activity by fusion of enzymes for transcriptional

regulation[61,62] . As an alternative for complete knockout the shRNA based knockdown can be used to dampen molecule expression with retaining residual expression[63–65]. Interesting targets for knockdown- or upregulation are immune checkpoint- and adhesion molecules. T cell adhesion molecules also influence the binding properties to target cells. With fine tuning of their expression, the binding and interaction strength in the immunological CAR T synapse can be modulated.

1.3. The immunological CAR synapse

The immunological T cell synapse, formed upon TCR activation, exhibits a well-defined structure with central-, peripheral- and distal- supramolecular activation clusters (SMACs)[66,67]. In the central SMAC (cSMAC) the TCR molecules assemble for MHC dependent antigen recognition. Stimulatory and inhibitory molecules are recruited to the cSMAC[68]. In a secretory synapse the cSMAC contains an area free of surface molecules to allow exocytosis of cytokines, granzymes and perforin[69]. Cell adhesion molecules (CAMs) are organized around the center, in the peripheral SMAC (pSMAC), with LFA-1 being a prominent candidate[70,71]. The integrin α4β1 (VLA-4) is recruited to the pSMAC, in an antigen dependent manner[72]. Beneath the immunological synapse the microtubule organizing center (MTOC) is forming to further support the shape and secretory properties of the T cell[68,73] by stabilizing the actin skeleton. LFA-1 is assumed to control the MTOC orientation and polarization[74]. In the distal SMAC (dSMAC) large proteins like CD45 assemble that can regulate TCR signaling, partially these molecules are on a bystander position within the dSMAC and recruited to the center when needed[75,76]. With this defined structure the T cell signaling network is finely tuned to

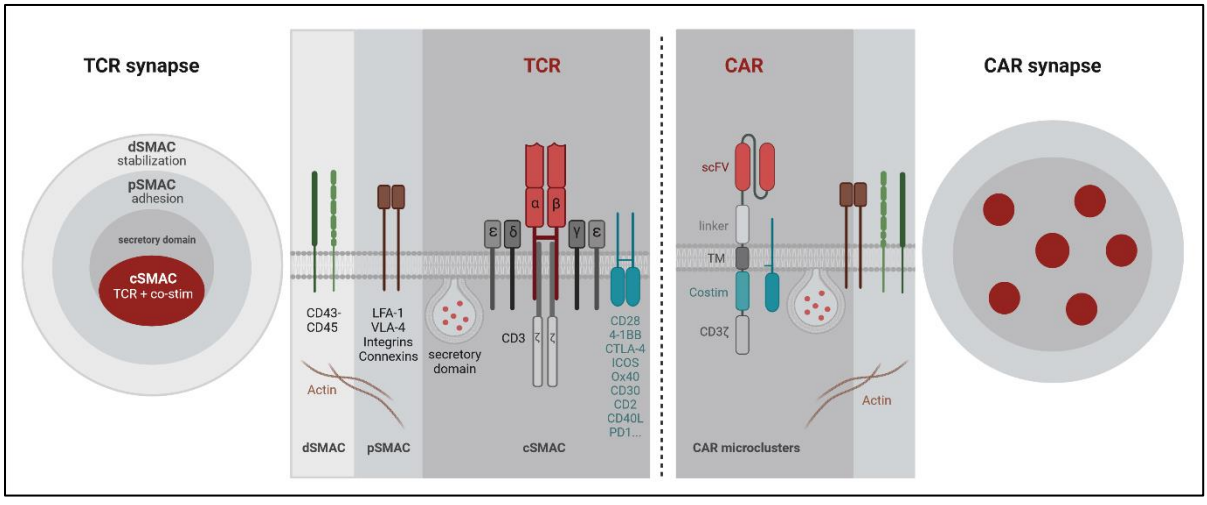

Figure 2: The immunological CAR synapse. *The TCR recruits CD3 and co-stimulatory molecules to the receptor to transmit activation stimuli. These molecules are organized in the cSMAC, neighbored by the secretory domain. Around the cSMAC the pSMAC with adhesion molecules and at further distance the dSMAC with larger molecules are organized, leading to the characteristic bullseye structure. The CAR synapse has a lower degree of organization, assembling the receptor in micro clusters, structural molecules are not excluded from the inner contact region. C = central, d=distal, p=peripheral, SMAC=supramolecular activation cluster.*

orchestrate locomotion, reorganization of the cytoskeleton, attachment and the release of cytokines and lytic granules in a well-orchestrated fashion[34].

In contrast to the physiological TCR synapse, the CAR synapse is characterized by a lower degree of structural organization. The chimeric antigen receptor and adjacent molecules are condensed in several clusters. The larger proteins like CD45 are likewise excluded from the inner core and assemble in the distal periphery of the CAR clusters. Stimulatory molecules are directly integrated as domain into the chimeric antigen receptor. Our group reported that there is no cross activation in between CAR and TCR synapses on the same cell[77] but complementation in signaling between the endogenous TCR molecules and the CAR still occurs[78]. The signal transmission of the immunological synapses depends not only on the receptor abundance and distribution but also on the avidity of the T cell - tumor cell contact. The latter is further influenced by adhesion molecules which are considered less in modulation of CAR T cell functions. Sufficient adhesion is crucial to allow a productive contact of the CAR T cells with cytotoxic hits towards the tumor cells. Vice versa, cancer cells can send inhibitory molecules through the synapse, that can be taken up by T cells. The optimal CAR T cell acquires strong but not tight adhesion to allow serial killing of multiple tumor cells. Tight adhesion can hinder dissociation from an already tackled target cell and reduce repetitive killing. Further, strong avidity over a certain threshold may lead to exhaustion or even activation induced cell death[79].

Consequently, adhesion molecules recruited to the immunological CAR synapse are pivotal, as they directly impact the therapeutic efficacy by balancing effective tumor cell engagement with the need for T cell dissociation and repeated target interactions.

1.4. The canonical role of VCAM1 as adhesion molecule

Cell adhesion molecules (CAMs) are mediating cell contact, migration, infiltration and homing of T cells. There are five groups of CAMs: integrins, selectins, cadherins, the IgG family and others (including enzymes and mucins)[80].

Integrins are heterodimers, consisting of one of 18 α and one of 8 β subunits[70]. Combination of the respective subunit results in a variety of different integrins which are ubiquitously expressed, as well as their ligands. Lymphocytes rely on the inside out signaling of integrins for mechanical and chemical sensing. Common integrins expressed by T cells are LFA-1 Mac-1 and VLA-4[81]. VLA-4 is composed of the two subunits CD29 (integrin β1) and CD49d (integrin α4)[82] and is strongly expressed after T cell activation, mediating binding of VCAM1 on endothelial cells. Besides its major binding partner VLA-4, VCAM1 was also reported to bind integrin α4β7, αMβ2 and αDβ2.

VCAM1 is a member of the immunoglobulin superfamily, encoded by nine exons, leading to two different splice variants in humans with six or seven immunoglobulin domains respectively[83]. Ig-domain one and four are crucial for VLA-4 dependent adhesion[84,85]. Various cytokines, like TNF-α and IL1 lead to upregulation of VCAM1. Best studied on activated endothelium.

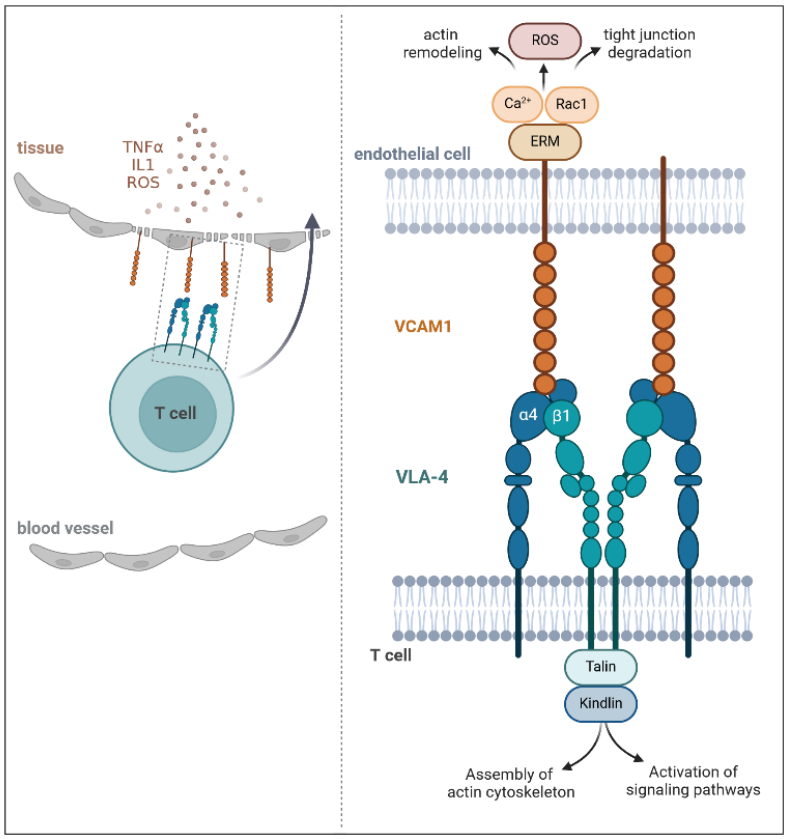

Figure 3: The canonical role of VCAM1. *VCAM1 is expressed upon activation on endothelial cells. Downstream signaling over calcium influx (Ca^{2+}) and Ras-related C3 botulinum toxin substrate 1 (Rac1) leads to actin remodeling and tight junction degradation, both facilitating the lymphocyte transmigration through the endothelium. The main ligand of VCAM1 is VLA-4, a dimer composed of CD29 (integrin β1) and CD49d (integrin α4), which is expressed on immune cells to promote adhesion and initiate migration to adjacent tissue. ERM = ezrin-radexin-moesin family, ROS = reactive oxygen species.*

VCAM1 is also expressed on bone marrow stromal cell, macrophages, dendritic cells and others[86–88]. When expressed by hematopoietic stem cells and leukemic stem cells VCAM1 was also found to reduce phagocytosis, suggesting a role as immune-checkpoint[89]. One single study reported VCAM1 expression in T cells, describing mRNA levels of VCAM1 in $CD8^+$ T cells beeing elevated in HIV infected- compared to HIV-negative individuals[90].
Overall the VCAM1 expression is essential as VCAM1 knockdown in mice leads to embryonic death in most cases [91].

VCAM1 interaction does not only mediate adhesion, the intracellular terminus of VCAM1 binds to Ezrin and Moesin (ERM)[92] which induce Ca^{2+} influx and recruit Rac1[93]. Both, Ca^{2+} and Rac1 trigger NADPH oxidase (NOX) activity. NOX fosters the accumulation of reactive oxygen species (ROS), which induce degradation of tight junction proteins by matrix metalloproteases[94]. Also the phosphorylation of beta-catenin is affected by ROS, leading to endocytosis of cadherins, further reducing the intercellular contact[95]. Both ROS and Ca^{2+} activate PKCα and subsequently PTP1B which is needed for T cell transmigration[96]. Taken together, the extracellular part of VCAM1 mediates adhesion of T cells, the intracellular domain induces pathways to loosen the endothelium and facilitate the subsequent transmigration.

1.5. T cell exhaustion with implications for immunotherapy

Exhaustion is felt after ongoing activity, with some rest the state can usually be reverted, and activity can be taken up again. The concept has been transferred to T cell immunity and "T cell exhaustion" is recently heavily discussed[97]. T cell exhaustion is an altered differentiation lineage, that dampens anti-cancer immunity[98]. Environmental factors like inflammation, regulatory T cell derived cytokines and metabolic stress can potentiate the development of exhaustion. Additionally, activation through either tonic signaling due to CAR aggregation or persisting exposure to antigen are reported to induce this state of malfunction. Exhaustion in T cells is closely related to their activation, the former sets in with or shortly after activation and both conditions run in parallel until the exhaustion takes the lead and dampens the activation potential. There is a point, referred to as terminal exhaustion, when the T cell lose their functional capacity enter activation induced cell death (AICD).

Phenotypic and genotypic analysis of tumor infiltrating cells and T cells of chronic viral infections have revealed surface proteins and transcription factors that correlate with exhaustion and thus characterize the different states of dysfunction[97]. The lineage fate of a T cell is intrinsically set and mediated by transcription regulators[99]. Early exhausted T cells initially express TCF1[100], indicating still a self-renewing capacity, in the later stage Tbet is prominently active[101]. Terminally exhausted T cells show a loss of TCF1 and upregulated levels

of the transcription factor Tox[102]. Immune checkpoint molecules like CTLA-4, PD1, Tim3 and Lag3 come up with early T cell activation and increase their expression along the lineage of exhaustion[103]. Checkpoint molecules are addressed by antigen presenting cells to prevent over-activation, but also tumor cells express the respective ligands and thus dampen the anti-tumor response[104,105]. The blockade of the interaction with CTLA-4 and PD1 enhance and prolong the anti-tumor activity of T cells[106,107].

In contrast to the exhausted subsets, the central memory compartment of $CD8^+$ CAR T cells is reported to provide superior antitumor immunity[108]. Cells being double negative for both, CCR7 and CD45-RO are identified as being in an effector state, typically following initial antigen encounter. The majority of activated cells are present in the effector memory compartment, being single positive for CD45RO[15]. The central memory T cells are assumed to be the long term persisters and are positive for both, CCR7 and CD45RO. To optimize CAR T cell products, researcher distinguished memory T cell subsets even further and described tissue resident CAR T cells that are highly resistant to tumor-imposed dysfunction despite they exhibit epicenetic characterisitcs of exhaustion[109]. This highlights the close connection of activation or functionality to exhaustion related markers, ongoing effort is made to identify further candidates and broaden the knowledge on their roles and interactions.

1.6. VCAM1 shows enhanced gene activity and upregulated RNA levels in CD8$^+$ TILs with terminal exhaustion signature

In order to identify genes that regulate tumor responsive T cells our colleagues performed the "assay for transposase accessible chromatin using sequencing" (ATAC-seq) on CD8$^+$ tumor infiltrating lymphocytes (TILs) of different solid tumor entities[110].

Common signatures for genes that correlate with different T cell states were applied for cluster identification (Figure 4A). Enhances gene activity of VCAM1 also translated to increased mRNA levels of VCAM1 in terminal exhausted TILs (Figure 4B). Treatment with anti-PD1 checkpoint blockade drives the TIL gene activity towards a terminal exhausted cell state (Figure 4C).

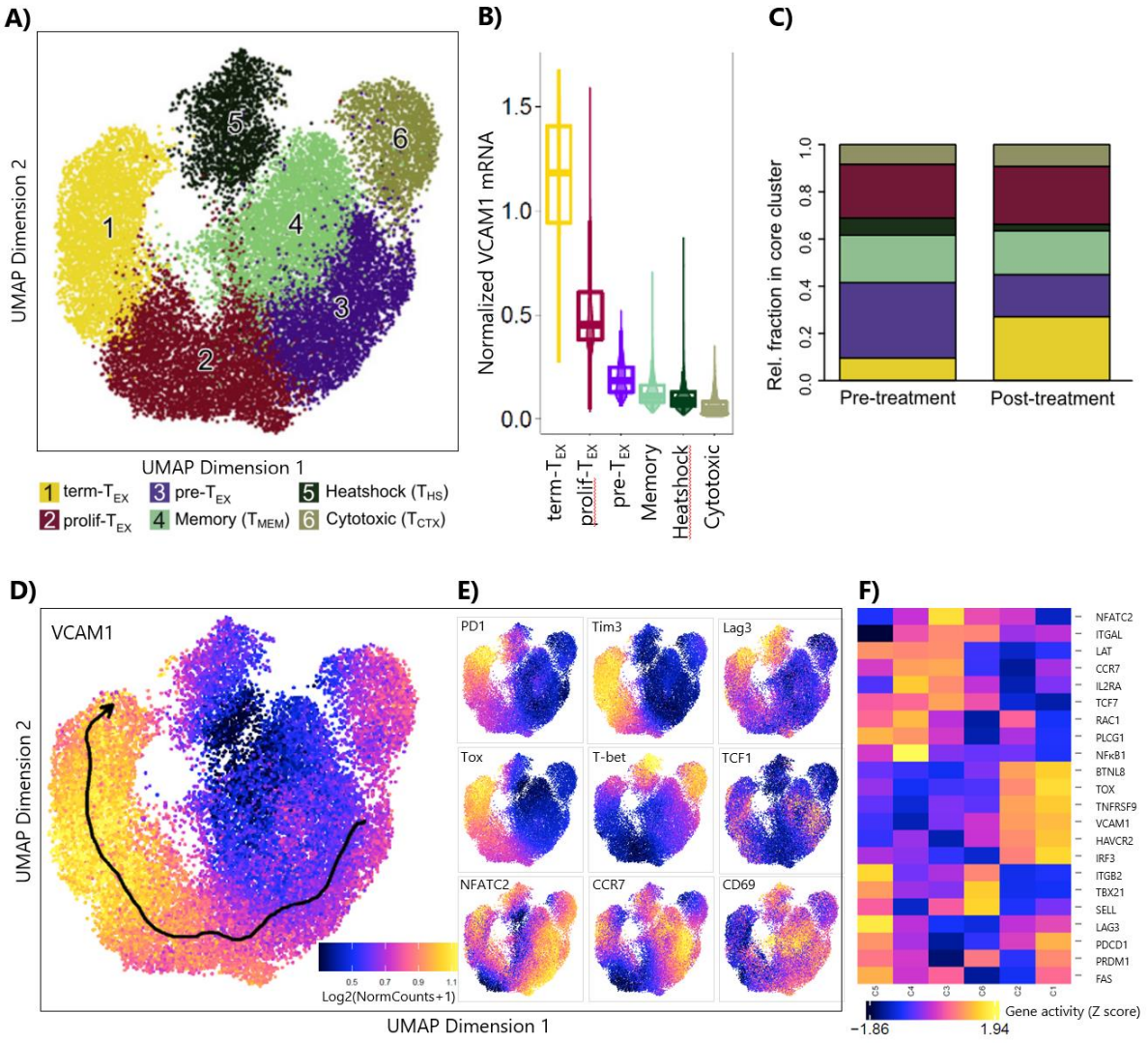

Figure 4: Single-cell ATAC-seq identifies VCAM1 gene activity in terminal exhaustion clusters of primary human CD8$^+$ TILs. A) *UMAP clusters of 21 466 single-cell chromatin profiles of CD8$^+$ T cells from tumor and control tissues. Every dot represents one cell.* ***B)*** *Normalized mRNA expression of VCAM1 in TIL clusters as shown in* ***A)****.* ***C)*** *Distribution of T cells taken from biopsies pre- or post-immunotherapy (aPD1 checkpoint blockade) in basal cell carcinoma samples.* ***D)*** *UMAP of VCAM1 gene activity with supervised dysfunction trajectory from pre-T$_{EX}$ towards term-T$_{EX}$.* ***E)*** *UMAP of per-cell gene activity of marker genes of interest.* ***F)*** *Heatmap of Z score normalized gene activities of selected markers over the TIL core clusters. Figure adapted from Riegel et. al with additional data provided by Dania Riegel and Christian Schmidl.*

Interestingly we observed the gene activity of VCAM1 to increase in clusters along with an increasing exhaustion signature, being the highest in terminal exhausted T cells (Figure 4D). Following the supervised pseudotime trajectory of increasing T cell dysfunction, the gene activity of VCAM1 increases along with the exhaustion markers encoding for (PDCD1; CD279), Tim3 (HAVCR2; CD366) and Lag3 (CD223) and transcription regulators related to exhaustion like Tox, Tbet and IRF4 (Figure E&F). In the VCAM1^{high} clusters low gene activity encoding for activation related proteins like FAS and NFATC2 was found.

In contrast, effector-memory T cells with a high anti-tumor activity and proliferative capacity[111,112] show low levels of VCAM1. Their genetic signature contains naïve like markers such as CCR7 and CD62L/SELL which are present in cluster 4. The findings suggest a strong correlation between the gene activity of VCAM1 and T cell exhaustion.

1.7. VCAM1 expressed by activated CD8+ T cells - proposing a non-canonical role of VCAM1

The common concept states that "enhancing binding interactions between T cells and tumor cells may yield improved responses in solid tumours"[113]. However tight adhesion can hinder repetitive killing and further induce T cell exhaustion[79,114]. Ongoing effort is made to identify drivers of T cell exhaustion, that can potentially be addressed to enhance CAR T cell efficacy as in combined therapy with anti-PD1 checkpoint blockade[4,52].

Upregulation of the adhesion molecule VCAM1 was found by our colleagues in terminal exhausted TILs, in human tumor specimen[110] and murine data sets confirmed these results[115,116]. Asides from these findings the expression of VCAM1 in T cells has not been reported in anti-tumor immune response. The canonical role of VCAM1 on endothelial cells is characterized by its binding capacity of lymphocytes.

The increase in gene activity and mRNA levels of VCAM1 in TILs opens the question of relevance of VCAM1 expression by T cells in the context of solid tumor clearance. We addressed the question in the context of anti-CEA CAR T cells and asked whether VCAM1 expression is induced in CAR T cells upon contact to tumor cells and TCR stimulation.

We further aimed to modulate VCAM1 expression with shRNA mediated knockdown and CRISPR/Cas9 mediated knockout to unravel the impact of VCAM1 on CAR T cell phenotype development and effector functions.

Wit these studies we are aiming to establish whether CAR T cells can interact via VCAM1-VLA-4 with their target cells and whether this interaction potentially impacts the efficacy of anti-tumor cell therapy.

2. Materials

2.1. Chemicals and reagents

Table 1: Chemicals and reagents

Chemicals and reagents	Company
ABTS	Sigma-Aldrich
ABTS Buffer	Sigma-Aldrich
AccuCheck Counting Beads	Invitrogen/Thermo Fisher Scientific
Ampicillin	CalBiochem/Merck
Anti-Biotin MicroBeads Ultra Pure	Miltenyi
Bacto-Agar	Carl Roth
BSA	Carl Roth
CellTrace™ Far Red	Invitrogen/Thermo Fisher Scientific
CFSE	BioLegend
CutSmart® Buffer	New England Biolabs
DMSO	Carl Roth
Fixable Viability Dye eFluor™ 780	eBioscience/Thermo Fisher Scientific
EDTA	GIBCO/Thermo Fisher Scientific
Ethanol	Carl Roth
Glyerin	CalBiochem/Merck
GolgiPlug™ (Brefeldin A)	BD Biosciences
GolgiStop™ (Monensin)	BD Biosciences
Imukin® (IFN-γ standard)	Boehringer Ingelheim
IDTE (10 mM Tris, 0.1 mM EDTA)	Integrated DNA Technologies (IDT)
Ionomycin	Calbiochem/Merck
Isopropanol	Carl Roth
NaOH (1M)	Sigma-Aldrich
Pancoll	PAN-Biotech
Phorbol-12-myristate-13-acetate (PMA)	Calbiochem/Merck
PBS 10x	GIBCO/ Thermo Fisher Scientific
PEIpro® Transfection Reagent	Polyplus transfection
Phusion HF Buffer	Thermo Fisher Scientific
PDL - Poly-D-lysine-hyrobromide	Sigma-Aldrich
Poly-L-Lysine	Sigma-Aldrich
Streptavidin-Peroxidase conjugate	Roche Diagnostics
TrueCut™ Cas9 Protein v2	Invitrogen/Thermo Fisher Scientific
Trypsin/EDTA	PAN-Biotech
Tween20	Merck

2.2. Kits

Table 2: Kits used for bacterial work, DNA extreaction, CRISPR/Cas9 and FACS.

Kit (application)	Company
NucleBond® Xtra Midi Kit (DNA isolation of bacteria)	Macherey-Nagel
P3 Primary Cell 4D-Nucleofector™ X Kit S (CRISPR electroporation)	Lonza
Transcription factor buffer set (intracellular flow cytometry)	BD Pharmingen
QIAquick PCR purification kit	QIAGEN

2.3. Buffers & Solutions

Table 3: Buffers and solutions used for bacterial work, cell culture and ELISA.

Solution	Composition
ELISA blocking buffer	1x PBS, 1% BSA
ELISA blocking buffer-Tween	1x PBS, 1% BSA, 0.05% Tween®-20
ELISA coating buffer	0.1M Na_2HPO_4, pH 9
FACS buffer	1x PBS, 0.5% FCS
LB agar	11 LB medium, 15 g Bacto Agar
LB medium	10 g/l tryptone, 5 g/l yeast extract, 10 g/l NaCl
MACS buffer	1x PBS, 0.5% FCS, 0.4% EDTA (0.5 M)
PBS/Tween (ELISA)	1x PBS, 0.1% Tween®-20

2.4. DNA preparation

2.4.1. PCR reagents

Table 4: PCR reagents for mutagenesis, Gibson assembly and sequencing.

Buffer	Company
BamHI (enzyme)	Thermo Fisher Scientific
CutSmart buffer	New England Biolabs
dNTPs	New England Biolabs
DpnI (enzyme)	New England Biolabs
Gibson Assembly® Master Mix	New England Biolabs
MasterMix Q5	New England Biolabs
PauI (enzyme)	Thermo Fisher Scientific
PhusionTM High-Fidelty DNA Polymerase	Thermo Fisher Scientific
Q5® High-Fidelity 2X Master Mix	New England Biolabs
Quick CP	New England Biolabs
Tango-buffer	Thermo Fisher Scientific

2.4.2. Primer

Table 5: Primers used for mutagenesis, Gibson assembly and sequecing.

Primer ID	target (function)	sequence
1666	IgG-Fc (fw sequencing)	CAAAGCCAAAGGGCAGC
1782	4-1BB (fw mutagenesis)	GGGCTGAAAGAAACTCCTGTAT
1783	4-1BB (rv mutagenesis)	CTTTCAGCCCCGTTTCCTG
1784	CD3 (rv mutagenesis)	AGAGTGTAGTTCAGCAGGAGC
1785	CD3 (fw mutagenesis)	GAACTACACTCTCAGCAGTTCG
1786	IgG (fw Gibson)	AGGTGGAGATCAAAGTG
1787	IgG (rv Gibson)	ACTCTCAGCCTGACACAGAAGAAGA
1788	CD3 (fw Gibson)	TGTGTCAGGCTGAGAGTGAAGTTCAGCA
1789	CD3 (rv Gibson)	CTCGGGGAGCAGAAG

2.5. Bacterial strains & culture medium

For amplification of plasmids the bacterial strain E.Coli DH5α (Woodcock et al., 1989) was used, Genotype: F-, end A1, hsd R17 (rκ-, mκ-), sup E44, thi-1, lambda-, rec A1, gyr A96, Φ 80 d lacZ d M15.

2.6. Plasmid vectors

The shRNA sequences were added at the 3' end of the CAR constructs, embedded in the modified miR-30 backbone[117,118].

Table 6: Plasmids that were used for retroviral CAR transduction. *All expression cassettes were inserted to the pBullet vector plasmid. For unpublished expression cassettes, sequences with annotations are shown in the appendix.*

ID	Plasmid	Characteristics/Reference
#392	pCOLT-GALV	helper plasmid for transduction, containing the gibbon ape leukemia virus envelope (GALV env) protein (Weijtens et al., 1998)[119]
#393	pHIT 60	helper plasmid for transduction, containing Moloney murine leukemia virus (M-MulV) proteins gag and pol (Weijtens et al., 1998)[119]
#607	pBullet_Lk_BW431/26scFv_IgG1Fc-CD28TM_CD28_CD3ζ	expression cassette of the CD28 anti-CEA CAR (Hombach et al., 2001)[12]
#908	pBullet_Lk_BW431/26scFv_IgG1Fc-CD4TM_41BB_CD3ζ	expression cassette of the 4-1BB anti-CEA CAR (Hombach et al., 2011)[120]
#2181	pBullet_Lk_BW431/26scFv_IgG1Fc-CD4TM_41BB_CD3ζ _mir30_shVCAM1-A	expression cassette for the 4-1BB anti-CEA CAR with shRNA targeting exon 2 of VCAM1
#2182	pBullet_Lk_BW431/26scFv_IgG1Fc-CD4TM_41BB_CD3ζ _mir30_shVCAM1-B	expression cassette for the 4-1BB anti-CEA CAR with shRNA targeting early exon 3 of VCAM1
#2193	pBullet_Lk_BW431/26scFv_IgG1Fc-CD4TM_41BB_CD3ζ _mir30_shVCAM1-C	expression cassette for the 4-1BB anti-CEA CAR with shRNA targeting early exon 3 of VCAM1
#2210	pBullet_Lk_BW431/26scFv_IgG1Fc-CD4TM_41BB_CD3ζ _mir30_shKanamycin	expression cassette for the 4-1BB anti-CEA CAR with control shRNA targeting kanamycin
#2602	pBullet_Lk-BW431/26scFv_CD8hinge-CD8TM_41BB_CD3z	expression cassette for the 4-1BB anti-CEA CAR with CD8 hinge and transmembrane domain (built by Sin-Syue Lee)
#2737	pBullet_Lk_BW431/26scFv_IgG1Fc-CD4TM_41BB	expression cassette for the 4-1BB anti-CEA CAR without primary signaling domain
#2738	pBullet_Lk_BW431/26scFv_IgG1Fc-CD4TM_CD3zeta	expression cassette for the 4-1BB anti-CEA CAR without co-stimulatory domain
#2739	pBullet_Lk_BW431/26scFv_IgG1Fc_CD4TM	expression cassette for the 4-1BB anti-CEA CAR without signaling domains

2.7. CRISPR/Cas9 RNA

Table 7: crRNAs and tracrRNA used for CRISPR/Cas9, *the sequences are shown in Table 12.*

RNA	Company
Alt-R® CRISPR-Cas9 tracrRNA	Integrated DNA Technologies (IDT)
Alt-R® Cas9 Negative Control crRNA #1	Integrated DNA Technologies (IDT)
Alt-R® CRISPR-Cas9 crRNA,Hs.Cas9.VCAM1.1.AC	Integrated DNA Technologies (IDT)
Alt-R® CRISPR-Cas9 crRNA,Hs.Cas9.VCAM1.1.AD	Integrated DNA Technologies (IDT)
Alt-R® CRISPR-Cas9 crRNA,Hs.Cas9.VCAM1.1.AF	Integrated DNA Technologies (IDT)

2.8. Cell culture

2.8.1. Cell culture medium and supplements

Table 8: Media and supplements used for cell culture.

Product	Company
D-MEM, High Glucose, GlutaMAX™supplement	GIBCO/ThermoFisher Scientific
FCS (heat-Inactivated 56°C, 30 minutes)	PAN-Biotech GmbH
HEPES	GIBCO/ThermoFisher Scientific
PenStrep	PAN-Biotech GmbH
RPMI1640 GlutaMAX™supplement	GIBCO/ThermoFisher Scientific

2.8.2. Cell lines & primary cells

Primary human PBMCs were provided by the University Hospital Regensburg and permission was obtained (Ethics vote no. 21-2224-101).

Table 9: Cell lines

Cell line	characteristics	Reference
BXPC-3	human pancreatic adenocarcinoma (ATCC CRL-1687)	(Tan et al., 1986)[121]
BXPC-3-GFP$^+$	BXPC-3 cell lines engineered to express GFP with plasmid #1795 - pQCX-eGFP	
HaCaT	human epidermal keratinocytes	(Boukamp et al., 1988)[122]
HEK293T	human embryonic kidney (ATCC CRL-3216™)	(DuBridge et al., 1987)[123]

2.9. Antibodies

Table 10: Antibodies used for cell culture, ELISA, FACS, MACS, microscopy and zMovi.

Antibody	Clone	Company	Dilution	application
Anti-human IFN-γ (Biotin)	4S.B3	BD Pharmingen	1:1000	ELISA detection
Anti-human IFN-γ	NIB42	BD Pharmingen	1:1000	ELISA coating
CCR7 (APC)	2-L1-A	BD Pharmingen	1:40	FACS
CD4 (BV421)	SK3	BioLegend	1:80	FACS
CD8 (BUV805)	SK1	BD Horizon	1:80	FACS
CD8 (BV605)	SK1	BioLegend	1:40	FACS
CD8 (FITC)	BW135/80	Mitlenyi	1:80	FACS
CD25 (PE-Cy7)	BC96	BioLegend	1:30	FACS
CD29 (integrin β1; APC)	TS2/16	BioLegend	1:30	FACS
CD45-RO (BV605)	UCHL1	BD Pharmingen	1:40	FACS
CD49d (integrin α4; PE)	9F10	BioLegend	1:30	FACS
CD66abce (CEA; APC-Vio770)	TET2	Miltenyi	1:40	FACS
CD69 (BV421)	FN50	BioLegend	1:30	FACS
CD106 (VCAM1; APC)	STA	BioLegend	1:30	FACS
CD106 (VCAM1; BV421)	STA	BioLegend	1:30	FACS
CD107a (LAMP1; FITC)	H4A3	BD Pharmingen	1:4	FACS
CD279 (PD1; APC)	EH12.2H7	BioLegend	1:80	FACS
CD366 (Tim3; BB700)	7D3	BD Pharmingen	1:40	FACS
CD223 (Lag3; BV786)	11C3C65	BioLegend	1:40	FACS
Granzyme (PE)	N4TL33	eBioscience	1:20	FACS
hIgG F(ab') (Biotin)	Polyclonal	SouthernBiotech	1:25	MACS
hIgG F(ab') (FITC)	Polyclonal	SouthernBiotech	1:400	FACS
hIgG F(ab') (PE)	Polyclonal	SouthernBiotech	1:400	FACS
Natalizumab	HY-108831	MedChem Express	1:666	zMovi
Perforin (BV421)	δG9	BD Pharmingen	1:20	FACS
TransAct (CD3/CD28)		Miltenyi Biotec	1:100	Cell culture (activation)
Ultra-LEAF™ Purified anti-human CD3	OKT3	BioLegend	1:25,000	Cell culture (activation)
Ultra-LEAF™ Purified anti-human CD28	CD28.2	BioLegend	1:50,000	Cell culture (activation)

2.10. Software

Table 11: Software used for data generation, visualization and analysis.

Software	Company
Biorender	SaaS Man (Science Suit Inc.)
FlowJo 10.10.0	Becton, Dickinson & Company (BD)
GraphPad Prism 10.2.1_1	GraphPad Software
Imaris 9.9.1	Oxford Instruments
IncuCyte 2021C	Essen BioScience
Leica Application Suite X 4.5.0.25531	Leica MICROSYSTEMS
Microsoft 365 Apps for Business	Microsoft
Oceon 1.5.4	Lumicks
SnapGene 7.2.1	GSL Biotech LLC
Zotero 6.9.36	Digital Scholar

3. Methods

Laboratory work was performed at the Leibniz Institute for Immunotherapy (LIT) in Regensburg, previously designated as the Regensburg Center for Interventional Immunology (RCI).

3.1. Bacterial work

3.1.1. Heat shock transformation.

Escherichia coli (E. coli) DH5α competent cells (stored at -80°C) were defrosted on ice and 1-100 ng plasmid/DNA was added. Plasmid DNA and bacteria mix were heat-pulsed at 42°C for 90 s then immediately cooled on ice for 2 min. The bacteria were incubated in 900 µl LB medium (without antibiotic) at 37°C, shaking at 200 rpm for 60 min. The suspension was then centrifuged 5 min at 5000 g, resuspended in 100 µl LB medium containing ampicillin and spread on a LB-agar plate and stored at 37°C overnight for antibiotic selection.

3.1.2. Bacterial culture and expansion

One colony of the LB-agar plate of the heat shock transformation or plasmid-wearing bacteria of a glycerol stock were added to 5 ml LB medium with 100 µg/ml ampicillin. Bacteria were cultured for 8h at 37°C and shaking at 200 rpm. For long term storage, 700 µl bacteria culture was mixed with 300 µl of 87% (v/v) glycerol and stored at -80°C.

3.2. DNA preparation

Plasmid DNA was prepared for retroviral transduction of the CAR in T cells.

3.2.1. Plasmid design

Constructs #2181, #2182 and #2193 were designed with Snapgene 7.2.1. and plasmid DNA ordered with Genscript. Plasmid DNA was dissolved to 10 ng/µl and stored at -20°C or used for heat schock transformation, as described above.

3.2.2. Plasmid isolation

For plasmid DNA isolation of bacteria, the "NucleBond® Xtra Midi Kit" (Macherey Nagel GmbH) was used.
100 ml of plasmid waring LB-bacterial culture was centrifuged 5 min at 8000 g and the supernatant was discarded. The pellet was resuspended with 8 ml RES-buffer. Lysis was induced with addition and inverting of 8 ml LYS-buffer. After 5 min incubation at room temperature the reaction was stopped with adding 8 ml NEU-buffer. The lysate was loaded onto an equilibrated column and topped up with 5 ml EQU-buffer. Sample DNA was eluted with 5 ml ELU-buffer. The DNA was precipitated with 3 ml isopropanol and centrifugated at 4°C for 45 min at 4500 g. DNA was washed with 2 ml 70 % ethanol and dried over night. Finally, the plasmid DNA was diluted in sterile H_2O_{dd} and stored at -20°C.
DNA concentration was measured with the NanoDrop™1000 spectrophotometer (Thermo Fisher Scientific) in 1µl at a wavelength of 260 nm. O.D. ratio is calculated with additional Protein measurement at 280 nm. Purity is given by an O.D. ratio (260nm/280nm) of 1.8.

3.2.3. Mutagenesis - STOP codon insertion

Constructs #2737 was achieved by mutagenesis of #908 with primer 1784 and 1785, adding a stop codon in the start region of CD3ζ. Constructs #2739 was achieved by mutagenesis of #908 with primer 1782 and 1783, adding a stop codon in the start region of 4-1BB.
For the PCR a master mix with 29 µl H_2O, 10 µl Phusion HF Buffer, 5 µl dNTPs, 2.5 µl of each primer, 0,5 µg template DNA and 0.5 µl Phuson High Fidelty DNA Polymerase. PCR reaction was started with 30 s at 98°C followed by 35 cycles with 10 s at 98°C – 30 s at 63.5°C – 4 min at 72°C and ended with 10 min at 72°C. For cleanup of the PCR product the QIAquick PCR Purification Kit was used.

3.2.4. Gibson assembly

For #2738 Gibson assembly was done, to remove the 4-1BB domain.
Digest was done with 27 µl H_2O, 2 µl BamHI, 1 µl Paul, 8 µl Tango-buffer with 2 µg #908 DNA over night. For 5' dephosphorylation the vector digest was incubated with 3 µl H_2O, 2 µl Quick CIP and 5 µl CutSmart buffer for 1 h at 37°C. Inserts were amplified in a PCR mixture containing 9.5 µl H_2O, 12.5 µl MasterMix Q5, 5 ng #908 DNA and 1.25 µl of two primers (for fragment1: 1786 and for fragment2: 1787, or 1788 and 1789). PCR reaction was started with 30 s at 98°C followed by 35 cycles with 10 s at 98°C – 30 s at 58°C – 30 s at 72°C and ended with 120 sec at 72°C. For cleanup of the PCR product the QIAquick PCR Purification Kit was used.
For the Gibson assembly 50 ng of the vector with 3x molar excess of the insert was added to a mixture containing 7.95 µl H_2O, 10 µl Gibson Assembly MasterMix, 0.92 µl vector digest and 0.57 µl fragment1, 0.56 µl fragment2 and incubated for 1 h at 50°C.

3.2.5. Sequencing

Sequencing of plasmid DNA was done to test the integrity of cloned plasmids. 12 µl plasmid DNA (100 ng/µl) and 20 µl (19 ng/µl) primer 1666 was sent to Microsynth for sequencing.

3.3. Cell culture

The culture conditions in the cell culture incubator had a humidified atmosphere (~95%) with 5% CO_2 at 37°C. Cell culture work was carried out in a Biosafety Level S2 laboratory using a laminar flow hood (Class II).

3.3.1. Cell culture of adherent cells

Adherent cells (BXPC-3, HEK293T, HaCaT) were cultured in GlutaMAX™ containing DMEM, supplemented with 10 % FCS, 10 mg/ml streptomycin and 10,000 U/ml penicillin.
For passaging the medium was removed from the flask containing the cells and washed with 1x PBM. 3 ml Trypsin/EDTA was added and incubated at 37°C for 5-10 min. 7 ml fresh culture medium was added to stop trypsinization. Cells were centrifuged in a falcon at 400 g for 5 min. The supernatant was discarded, and cells resuspended in fresh medium. Cells were transferred back to the flask in a ratio 1:4 – 1:20 depending on the growth characteristics of the cell line.

3.3.2. Isolation of human peripheral blood mononuclear cells (PBMCs)

Human PBMCs were isolated from fresh blood of healthy donors, provided by the "Transfusionsmedizin" department of the Universitätsklinikum Regensburg through a ficoll gradient using Pancoll (PAN Biotech). T cells were activated with 1000U/ml IL2 and 200ng/ml activating CD3 and activating 50ng/ml CD28 antibodies for two days and then used for transduction or further cultivated in 200 U/ml IL2.

3.3.3. Cell culture of primary human PBMCs

Suspension cells (PBMCs) were cultivated in GlutaMAX™ containing RPMI1640, supplemented with 10 % FCS, 1 M HEPES, 10 mg/ml streptomycin and 10,000 U/ml penicillin.
For passaging cells were transferred to a falcon and centrifuged at 300 g for 5 min. The supernatant was discarded, and the cells resuspended in fresh culture medium to a density of 0.5 – 1x10^6 cells/ml. T cells were stimulated with 200 – 400 U/ml IL2 if not indicated else.
For long term storage ~10x10^6 cells were frozen in 70 % FCS + 20 % DMEM + 10 % DMSO at -80°C. For defrosting cells were resuspended in 1 ml prewarmed culture medium and immediately transferred to 10 ml prewarmed medium, centrifuged at 300 g for 5 min, supernatant was discarded and cells resuspended and transferred to a culture flask.

3.4. CAR T cell production

The production of CAR T cells with and without VCAM1 modification took one week (Figure 5). On day one primary human PBMCs from healthy donors are isolated and activated.

Retroviral transduction of the CAR by spinfection was performed on two subsequent days. The transduced CAR T cells were enriched by magnetic cell separation (MACS) on day five. For CRISPR/Cas9 mediated VCAM1 knockout the CAR T cells were rested for 3h before electroporation of the targeting guide RNA complex on the same day. After successful transduction the CAR T cells were expanded with 200 - 400 U/ml IL2 for two days. At day eight T cells were analyzed, after resting the cells in fresh medium for 5h stimulation or co-culture was started.

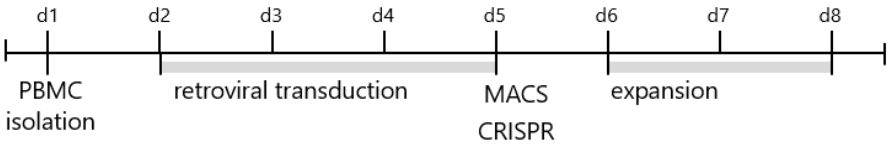

Figure 5: Timeline of the CAR T cell production and VCAM1 modification process.

3.4.1. Co-transfection of HEK293T cells

One day before transfection $2.5x10^6$ HEK293T cells were seeded in 10ml DMEM-culture medium. On the day of transfection medium was replaced with 10 ml un-supplemented RPMI1640. 10 µg plasmid DNA was added with 5 µg of each helper plasmid #392 and #393 to a total volume of 500 µl un-supplemented RPMI1640. 20 µl of the transfection agent PEIpro® (Polyplus) was added, the mixture was vortexed and incubated for 15 min at room temperature. After incubation the DNA/transfection reagent mixture was added dropwise to the HEK293T cells and incubated over night in the cell culture incubator.

3.4.2. Retroviral transduction of human T cells

$5x10^6$ T cells were centrifuged at 300 g for 5 min and resuspended in the 10 ml virus-containing supernatant of the co-transfection, 10% FCS and 200 U/ml IL2 were added to the T cells. The T cells were transferred to a closable cell culture flask, which had been coated with poly-D -lysine (10 µg/ml in 2ml H_2O_{dd}). The T cells were centrifuged in the flask at 1600 g for 1 h at 32°C After the centrifugation cells were incubated for 24 h in the cell culture incubator.
10 ml fresh RPMI1640 with supplements was added to the HEK293T cells for another over night incubation.
The next day the procedure was repeated with the fresh produced virus supernatant.

3.4.3. Magnetic cell separation (MACS®)

For enrichment of the CAR positive T cells magnetic cell separation (MACS®) was performed. Transduced T cells were washed with 1xPBS and ~15x10^6 T cells resuspended in 80 µl MACS buffer incubated with 3.5 µl biotin conjugated hIgG F(ab') antibody (Southern Biotech) for 10 min at 4°C. T cells were washed two times by adding 2 ml MACS buffer and centrifugation at 300 g for 5 min at 4°C. T cells were resuspended in 80 µl MACS buffer and incubated with 20 µl anti-Biotin MicroBeads UltraPure (Miltenyi) for 15 min at 4°C. Cells were washed by adding 2 ml MACS buffer and centrifugation at 300 g for 5 min at 4°C and resuspended in 500 µl MACS buffer. Cells were loaded on a pre-separation filter on an equilibrated MACS column onto a magnetic holder and allowed to flow through. The column was washed three times with 500 µl MACS buffer. The column was removed from the magnetic holder and placed to a fresh falcon and for elution of the CAR positive cells 1 ml supplemented RPMI1640 was added to the column and pressed through with the corresponding plunger.

3.4.4. CRISPR/Cas9 mediated VCAM1 knockout

After MACS enrichment cells were allowed to rest for 4 h in the incubator. For CRISPR/Cas9 1.5x10^6 CAR T cells were used per condition. The laminar flow hood was cleaned with RNAse ZAP before usage

TracrRNA and crRNAs (by Integrated DNA Technologies) were diluted to 200 µM in IDTE buffer. Each crRNA was mixed 1:1 with tracrRNA for stabilization. The resulting guide RNA (gRNA) was incubated for 5 min at 95°C in a Thermo Cycler and afterwards cooled down at room temperature. Per condition 6 µl gRNA was mixed with 2.4 µl TrueCut Cas9 (Thermo Fisher Scientific) and incubated for 20 min at room temperature, if two gRNAs were mixed 3 µl of each was used respectively. T cells were centrifuged at 300 g for 5 min and supernatant pipetted of, cells were resuspended in 500 µl IDTE buffer and centrifuged again. Supernatant was pipetted off entirely, cells were resuspended in 13,2 µl Buffer P3 with 3,8 µl supplement (Lonza). Cas9-gRNA complex was added and cells transferred to a Nucleocuvette™ (Lonza), for electroporation with program CA137 at the 4D-Nucleofector™ (Lonza). After electroporation cells were topped with 100 µl unsupplemented RPMI1640 an rested for 10 min. Then cells were transferred to prewarmed supplemented RPMI1640 at a density of 0.5x10^6 cells/ml with 400 U/ml IL2.

3.5. Flow cytometry

For analysis by flow cytometry 1-3x10^5 cells were stained. Data were gated on living, singulet lymphocytes if not indicated else according to Figure 6. Cells were transferred to a round bottom plate and washed with 200 µl 1x PBS. For surface staining the pellet was resuspended in 80 µl 1x PBS with the respective staining antibodies at suitable concentrations (Table 10) in a master mix and incubated for 15 min at 4°C. Cells were washed another two times before resuspension in 200 µl FACS buffer and transfer to FACS tubes for measurement. Data were analyzed with the FlowJo 10.10.0 software.

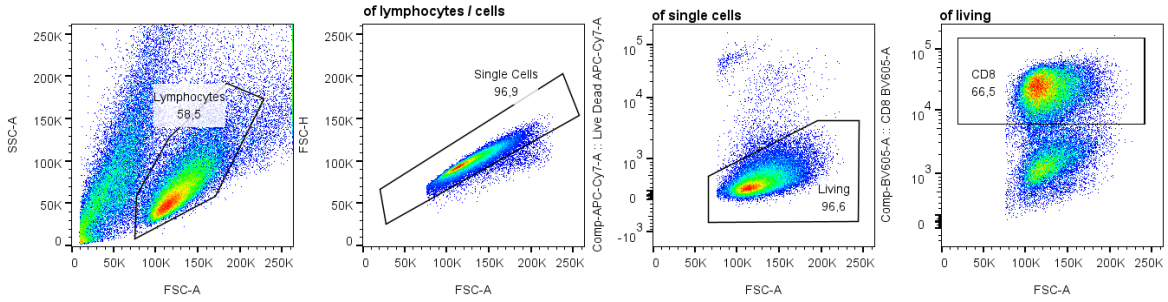

Figure 6: Gating strategy for flow cytometry data *by in the FlowJo 10.10.0 software. If not indicated else, cells were gated on living – singulet – lymphocytes.*

3.5.1. Detection of VCAM1 induction or knockdown/knockout

For measurement of VCAM1 induction and VCAM1 knockdown/knockout T cells were stained with a master mix containing Fixable Viability Dye eFluor™ 780, hIgG F(ab') (PE), VCAM1 (APC), CD4 (BV421) and CD8 (BV605). Expression was measured at the FACSLyric™ (BD).

1.1.1. Detection of VLA-4

For measurement of the CD29 and CD49d, T cells were stained with a master mix, containing CD29 (APC), CD49d (PE) and CD66abce (APC-Vio770). Expression was measured at the FACSLyric™ (BD). For adherent cell lines the first gate was set on the cell population and further subgated to single cells.

1.1.2. Detection of activation markers CD25/CD69

For measurement of the activation markers CD25 and CD69, T cells were stained with a master mix containing Fixable Viability Dye eFluor™ 780, CD8 (FITC), CD25 (PE-Cy7), CD69 (BV421) and VCAM1 (APC). Expression was measured at the FACSLyric™ (BD).

1.1.3. Detection of exhaustion markers PD1/Tim3/Lag3

For measurement of the memory phenotype, T cells were stained with a master mix containing Fixable Viability Dye eFluor™ 780, CD8 (BUV805), hIgG F(ab') (FITC), VCAM1 (BV421), PD1 (APC), Lag3 (BV786), Tim3 (BB700) and CD45RO (BV605). Expression was measured at the FACSymphony™ (BD).

1.1.4. Detection of the memory phenotype

For measurement of the memory phenotype, T cells were stained with a master mix containing Fixable Viability Dye eFluor™ 780, CD8 (FITC), hIgG F(ab') (PE), VCAM1 (BV421), CCR7 (APC), CD45RO (BV605). Expression was measured at the FACSymphony™ (BD).

1.1.5. Detection of CD107a

For measurement of CD107a (LAMP1), T cells were spun down and 100 µl supplemented RPMI1640 containing 1:1500 Golgiplug and 1:1000 Golgistop was added and CD107a (FITC) was added and incubated for 5 h in the cell culture incubator. T cells were spun down at 400 g for 5 min and washed twice with 1x PBS. Cells were stained with a master mix containing Fixable Viability Dye eFluor™ 780, CD4 (BV421), CD8 (BV605), and VCAM1 (APC). Expression was measured at the FACSLyric™ (BD).

1.1.6. Detection of Granzyme B/Perforin

For measurement of granzyme B and perforin, T cells were spun down and 100 µl supplemented RPMI1640 containing 1:1500 Golgiplug and 1:1000 Golgistop was added for 5 h incubation in the cell culture incubator. T cells were spun down at 400 g for 5 min and washed twice with 1x PBS. Cells were stained with a master mix containing Fixable Viability Dye eFluor™ 780, CD8 (BUV805), hIgG F(ab') (FITC), and VCAM1 (APC). T cells were spun down and washed two times with 1x PBS. Cells were fixated with the Transcription Factor Buffer Set (BD Pharmingen) according to the manufacturers protocol. Cells were washed with Perm-wash-buffer of the Set and cells stained with a master mix in 80 µl perm-wash buffer containing granzyme B (PE) and perforin (BV421) for 45 min at 4°C. Cells were washed two times with Perm-wash-buffer. Expression was measured at the FACSymphony™ (BD).

1.2. Enzyme linked immunosorbent assay (ELISA)

To measure secreted cytokines, $0.05x10^6$ T cells were 1:1 co-cultivated with BXPC-3 cells for 48 h and cell culture supernatant was collected. MaxiSorpTM microtiter plates were coated with the IFNγ capture antibody in ELISA coating buffer over night at 4°C. Coating was discarded and 200 µl ELISA blocking buffer added per well for 2 h incubation at room temperature shaking at 300 rpm. Blocking buffer was discarded and plates washed three times with PBS/Tween. Imukin® was added in 12 step serial dilution in 50 µl 1x PBS to the plate and 50 µl sample supernatants were added. Cells were covered to protect from evaporation and incubated over night at 4°C. Sample were discarded and plates washed four times with PBS/Tween. IFNγ detection antibody was added in 200 µl ELISA blocking buffer-Tween (BB-Tween) per well and incubated for 1 h at room temperature, shaking at 300 rpm. Plates were washed four times with PBS/Tween. 1 µl streptavidin-POD was diluted in 10 ml BB-Tween and 50 µl added per well for incubated for 30 min at room temperature, shaking at 300 rpm. Solution was discarded and plates were washed four times with PBS/Tween. 50 µl ABTS solution (10 mg/ml in 1 ml ABTS buffer and 9 ml H_2O_{dd}) was added per well. Signal was detected at 405 nm absorption (1-ref 405 – 490 nm) with the TECAN Spark 20M Microplate Reader after 30/60/90 min.

1.3. Incucyte cytotoxicity

$0.1x10^6$ T cells were co-cultivated 1:1 BXPC-3-GPF^+ tumor cells for four days in the Incucyte SX5® device at 37°C and 5 % CO_2. Every two hours the device acquired images that were analysed for GFP signal in the IncuCyte 2021C software, counting for green positive events over time.

1.4. Rechallenge assay

$0.1x10^6$ T cells were co-cultivated 1:1 with BXPC-3-GPF^+ cells in 12-well plates for 3 days. T cells and the entire supernatant were transferred to falcons, 1 ml 1x PBS was added to the wells and transferred to the respective falcon. 500 µl Trypsin/EDTA was added per well and incubated for 10 min at 37°C, to stop the reaction 1 ml supplemented RPMI1640 was added, and all transferred to the respective falcon. The cell-suspension was centrifuged at 400 g for 5 min and supernatant was removed. Cells were resuspended in 1 ml supplemented RPMI1640. 900 µl of the cell-suspension was on 0.1x106 BXPC-3-GFP+ cells, that have been plated the day before.

The remaining 100 µl were taken for flow cytometry analysis. Therefore, cells were stained with a master mix containing eFluorTM 780, CD4 (PerCP-Cy5.5), CD8 (BV421), hIgG F(ab') (AF647) for 15 min at 4°C and washed two times with 1x PBS. Cells were resuspended in 220 µl FACS buffer and 200 µl transferred to FACS tubes. Directly before measurement 10 µl AccuCheck Counting Beads were added per FACS tube. Expression was measured at the FACSLyrics™ (BD). The procedure was repeated after 3 to four days for 4 rounds.

1.5. Cell avidity - zMovi

For measurement of avidity monolayers with BXPC-3 or HaCaT cells were seeded. Chips were activated and coated the days before the measurement. On the day of experiment Chips were coated with 50 µl Poly-L-Lysine (1:5 in 1x PBS) for 15 min at room temperature. For monolayer seeding $40x10^6$ cells/ml were added in supplemented RPMI1640 to the reservoir of the chip and flushed in and allowed to settle for 2 min. If needed the monolayer was enriched with flushing in cells for a second time. Reservoir was washed and the chips incubated at a 37°C dry chamber for 3 h. T cells were spun down and stained in 250 µl for CellTrace™ Far Red (1:1000 in 1x PBS) for 15 min at 37°C, reaction was stopped with adding 1 ml supplemented RPMI1640 and incubated for 5 min before washing two times with RPMI1640. 10 µl of $10x10^6$ T cells/ml were transferred to the reservoir of the chip and flushed in. After 5 min incubation of the T cells on the monolayer, zMovi analysis was started (acoustic force ramp, increasing incrementally at 10 pN/sec). Analysis was done with the Ocean 1.5.4 software.

1.6. Confocal microscopy

For microscopic analysis $0.15x10^6$ BXPC-3 cells were seeded to µ-Slides 8 well (ibidi). For CFSE staining of BXPC-3 cells were washed in 1x PBS and stained in 500 µl with CFSE (1:1000 in 1x PBS) for 15 min at 37°C, reaction was stopped with adding 1 ml supplemented RPMI1640 and incubated for 5 min before washing two times with RPMI1640 before seeding.
T cells were stained with CellTrace™ Far Red as described above. For staining with VCAM1 (BV421) and hIgG F(ab') (FITC), T cells were resuspended in 80 µl and respective antibodies were added and incubated for 10 min at 4°C, cells were washed once with 1x PBS, before being transferred to the µ-Slides for imaging at the STELLARIS 8 confocal microscope (Leica). Signal intensities were adjusted to single stain controls. T cell objects were generated based on the Celltrace Far Red signal and BXPC-3 objects were generated based on the CFSE signal with the Imaris 9.9.1 software.

1.7. Statistical analysis

Statistics were calculated as indicated with GraphPad Prism version 10.0.2(232).

2. Results

2.1. VCAM1 is upregulated in CD8+ CAR T cells upon stimulation

VCAM1 is known to be expressed by activated endothelial cells and to bind to VLA-4 on T cells. Since tumor infiltrating lymphocytes were found to show a high gene activity score in terminal exhausted clusters[110], we asked whether CAR T cells can also express VCAM1 upon appropriate stimulation.

Human T cells were engineered to express the anti-CEA CAR with the BW431-26 scFv as antigen recognition domain and either CD28-CD3ζ (#607) or 4-1BB-CD3ζ (#908) signaling domains (Figure 8A). Untransduced T cells and anti-CEA CAR T cells (#908) were incubated with CEA$^+$ BXPC-3 tumor cells or stimulated through agonistic CD3/CD28 antibodies or PMA/ionomycin respectively and VCAM1 expression was measured by flow cytometry.

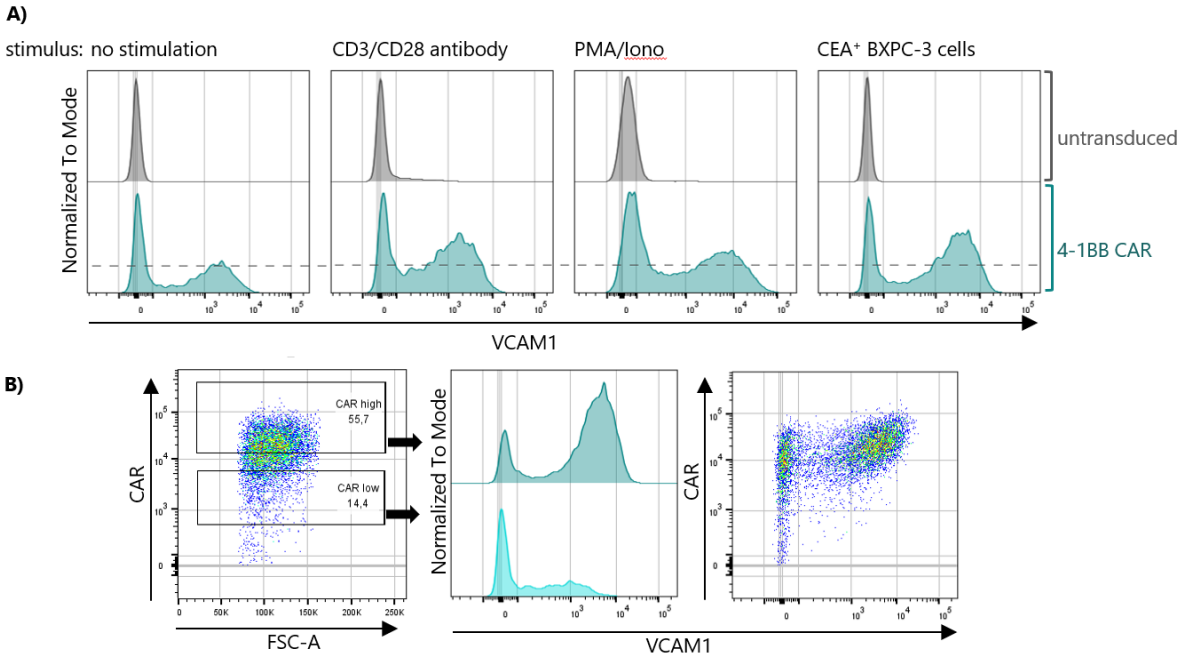

Figure 7: CAR T cells but not untransduced T cells express VCAM1 upon stimulation. A) *0.1x10^6 T cells were stimulated for 3 days with 1:100 Transact, containing activating CD3/CD28 antibodies or 0.05 µg/ml Phorbol-12myristate-13acetate (PMA) and 0.05 µg/ml Ionomycin (Iono) or in 2:1 co-culture with CEA$^+$ BXPC-3 tumor cells. VCAM1 expression was measured by flow cytometry, gated on CD8$^+$ cells. Histograms of one representative donor are shown.* ***B)*** *The CAR T cells stimulated in co-culture with BXPC-3 cells were analyzed with separate gates, set on high and low CD8$^+$CAR$^+$ cells to indicate MFI dependent VCAM1 expression.*

CAR T cells upregulate VCAM1 on their surface, upon stimulation with activating CD3/CD28 antibodies, upon stimulation with PMA plus ionomycin and upon co-culture with the CEA$^+$ BXPC-3 tumor cells respectively (Figure 7A). T cells without CAR express VCAM1 at very low levels, with more than 90% of cells lacking VCAM1 expression, across all three tested stimulatory conditions. T cells with high CAR expression also showed a high expression of VCAM1, indicting a correlation of VCAM1 expression with the CAR level, indicated by the mean fluorescence intensity (MFI) of CAR molecules on surface (Figure 7B).

To further understand the role of different CAR activation stimuli and the kinetics of VCAM1 expression we compared the anti-CEA CAR with 4-1BB and CD28 co-stimulatory domains (Figure 7A).

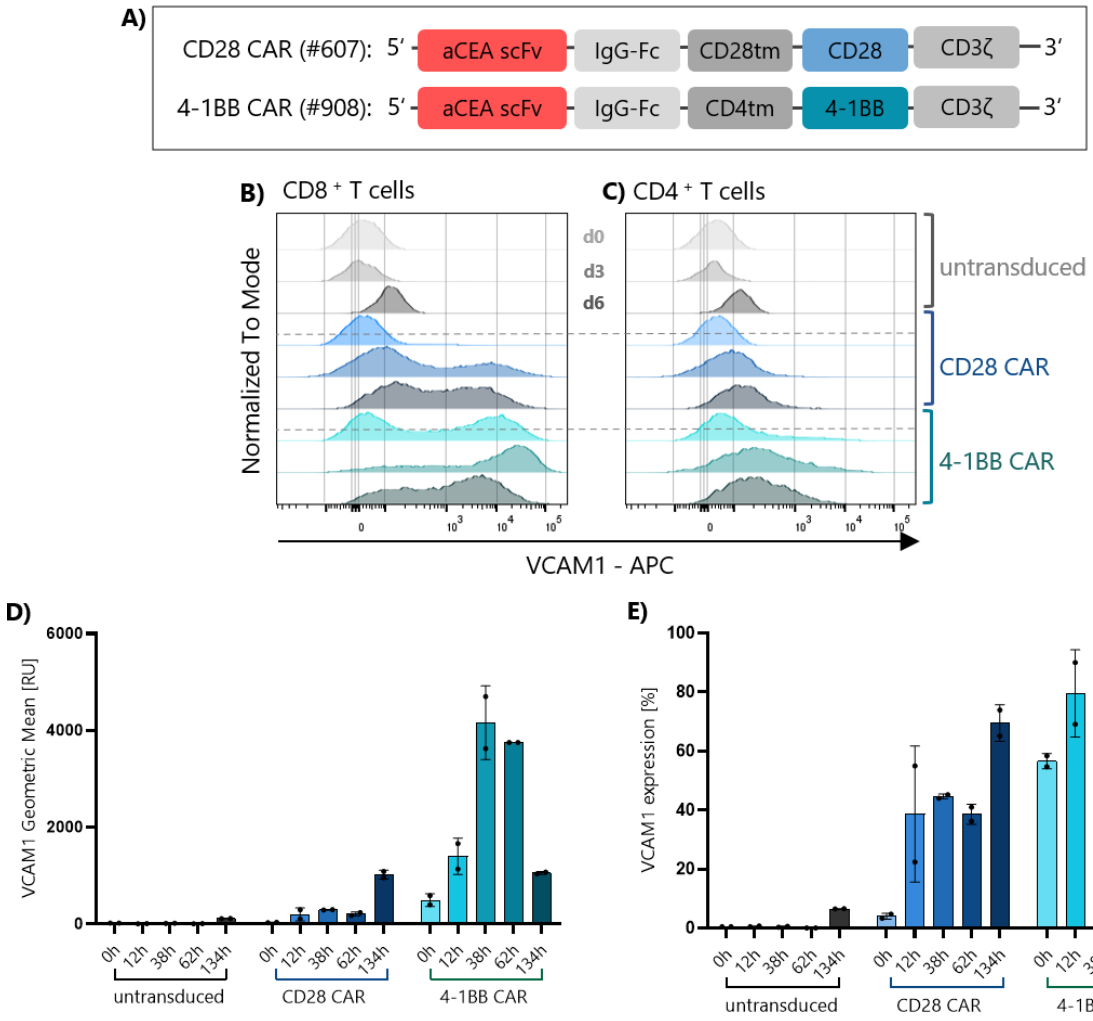

Figure 8: 4-1BB CAR induced stronger VCAM1 expression in CD8⁺ T cells than the CD28 CAR. *After transduction of T cells with the respective CAR, T cells were rested for one day and then 0.05x10⁶ cells co-cultivated 1:1 with BXPC-3 tumor cells for the indicated time. VCAM1 expression on T cells was measured by flow cytometry.* ***A)*** *Schematic structure of the CAR domains.* ***B)*** *&* ***C)*** *Histograms show VCAM1 expression of one representative donor. In* ***D)*** *VCAM1 MFI and in* ***E)*** *VCAM1 positive of CD8⁺ T cells [%] are shown with mean and standard deviation of 2 donors.*

In contrast to CD8⁺ CAR T cells, the CD4⁺ CAR T cells exhibited a marginal increase in VCAM1 expression (Figure 7B&C).

CD8⁺ T cells equipped with the anti-CEA CAR containing the 4-1BB co-stimulatory domain show rapidly upregulation of VCAM1 within 12h and downregulation again after 62h (Figure 7B). In contrast CD8⁺ CAR T cells with the CAR CD28 co-stimulatory domain have a delayed onset of VCAM1 expression and show lower expression levels at maximum. The percentage of cells upregulating VCAM1 is higher in the 4-1BB CAR T cells than in T cells with the CD28 CAR (Figure 7E). This holds also true for the overall expression level per cell (Figure 7D).

Together these data show, that VCAM1 is expressed exclusively on CD8⁺ CAR T cells upon activation. The expression level is strongly dependent on the co-stimulatory domain of the CAR.

2.2. CAR signaling is required for enhanced VCAM1 induction in T cells

To address whether the enhanced VCAM1 expression depends on CAR signaling, we designed anti-CEA CAR constructs with individual domains being exchanged or abrogated (Figure 9A) and found all truncated CARs to be expressed on T cells (Figure 9B).

To discern whether the transduction process itself increases the VCAM1 expression, T cells were "mock" transduced with the helper plasmids only, leaving out the transgene encoding plasmid. Mock transduced T cells did not increase VCAM1 expression over the baseline expression level of untransduced T cells after co-culture with BXPC-3 tumor cells (Figure 9C&D).

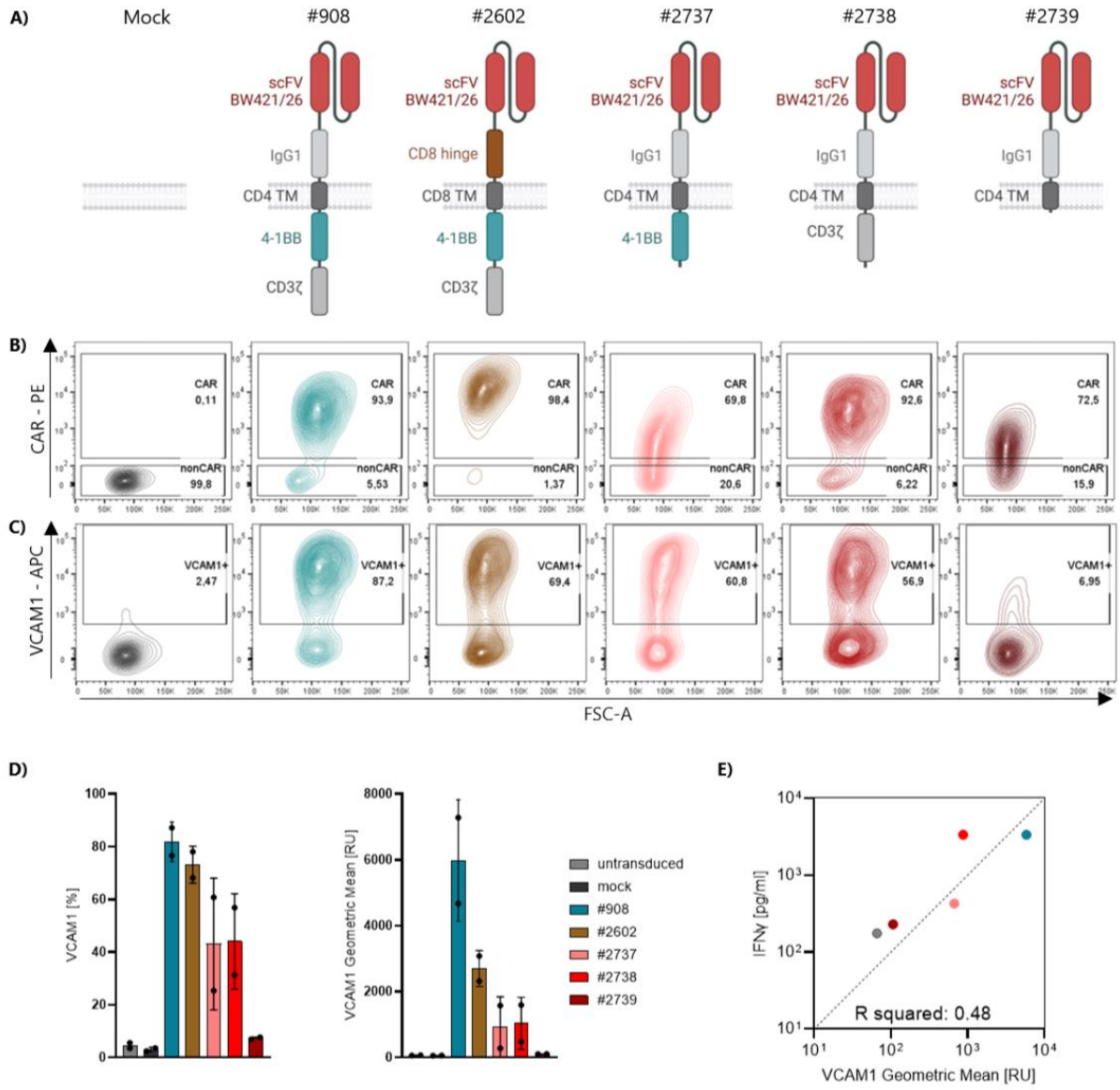

***Figure 9: VCAM1 expression is depended on intracellular CAR signaling domains**. **A)** Construct design with different CAR domains. Mock cells were transduced with helper plasmids only. **B)-E)** 0.1x10^6 T cells were co-cultivated 2:1 with BXPC-3 tumor cells for 2 days. VCAM1 expression was measured by flow cytometry. **C)** For CAR T cells the last gate was set on CD8$^+$CAR$^+$ cells, for untransduced and mock T cells the last gate was set on CD8$^+$ non-CAR cells. **D)** Mean and standard deviation of VCAM1 expression of 2 independent donors. For comparison of #2602 to #908 another set of donors was used, here VCAM1 expression was normalized to #908. **E)** Secreted IFNγ concentration was recorded in the co-culture supernatants by ELISA and plotted against the VCAM1 expression and multiple linear regression was calculated.*

With deletion of the CD3ζ signaling and the co-stimulatory 4-1BB domain (construct #2739) the ability to induce VCAM1 expression was lost in $CD8^+$ CAR T cells. Deletion of the CD3ζ (#2737) or the 4-1BB co-stimulatory domain (#2738) of the CAR also reduced the expression of VCAM1 on the T cells. We concluded that CAR signaling through the primary CD3ζ or the co-stimulatory domain is required for VCAM1 induction.

To further validate whether the IgG1 hinge-CH2-CH3 region also contributes to the induction of VCAM1 in #908 CAR T cells, a CAR differing by the CD8- hinge and transmembrane domain (construct #2602) was tested. #2602 CAR T cells showed a similar expression of the CAR but a lower geometric mean of VCAM1 expression than the #908 CAR T cells. This shows that the CAR "spacer" and transmembrane domains also influence the VCAM1 expression, independent of CAR signaling.

IFNγ secretion of T cells with the different CARs was measured after 48h in the supernatant of a co-culture with BXPC-3 tumor cells. T cell activation, indicated by IFNγ release, increased with VCAM1 expression, demonstrating a strong correlation of the expression of VCAM1 with the IFNγ release (Figure 9E).

We conclude that CAR signaling is required for VCAM1 induction and is the strongest with both activation stimuli of CD3ζ and 4-1BB together.

2.3. Expression of the VCAM1 ligand VLA-4

For successful evaluation of the VCAM1 interaction of CAR T cells with target cells, we tested for the crucial expression of suitable ligands on the target cells. Therefore, we analyzed the surface expression of VLA-4, the major ligand of VCAM1 and CEA, the CAR targe antigen in the human keratinocyte cell line HaCaT and the pancreatic adenocarcinoma cell line BXPC-3.

VLA-4, is a heterodimer composed of the integrins CD29 (integrin β1) and CD49d (integrin α4). The BXPC-3 cell line showed high expression of CD29, whereas the expression of CD49d is low (Figure 10). BXPC-3 cells exhibited a high expression level of CEA, the CAR target antigen.

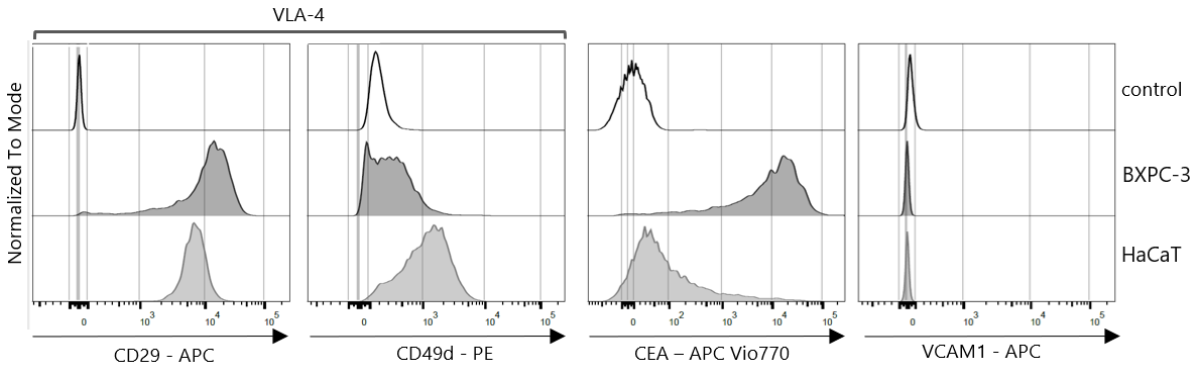

Figure 10: The VCAM1 ligand VLA-4 expression on HaCaT keratinocytes and on BXPC-3 tumor cells. *Cells were detached with incubation of 0.5 mM EDTA for 15 min. Expression of the CAR antigen CD66abce (CEA) and expression of CD29 and CD49d integrins was measured by flow cytometry, gated on living singulet cells. As control for CD29 and CD49d isotype staining on BXPC-3 cells was used and Hek293T cells as control for CEA and VCAM1 staining.*

HaCaT cells are described to, express both VLA-4 integrins[122,124]. The expression of high levels of both CD29 and CD49d on HaCaT cells was confirmed. CEA is expression was found to low levels on HaCaT cells. No VCAM1 expression was detected on BXPC-3 cells or on HaCaT cells. We conclude that HaCaT cells are an ideal target cell line to measure VCAM1 dependend binding properties, whereas BXPC-3 cells are ideal targets for anti-CEA CAR T cells in this context, to record the interaction of T cell expressed VCAM1 with tumor cell expressed VLA-4 without interference of tumor cell expressed VCAM1.

To gain information on the expression on the VCAM1 ligand expression in different T cell compartments, the expression of CD29 and CD49d was measured on T cells in co-culture with BXPC-3 tumor cells.

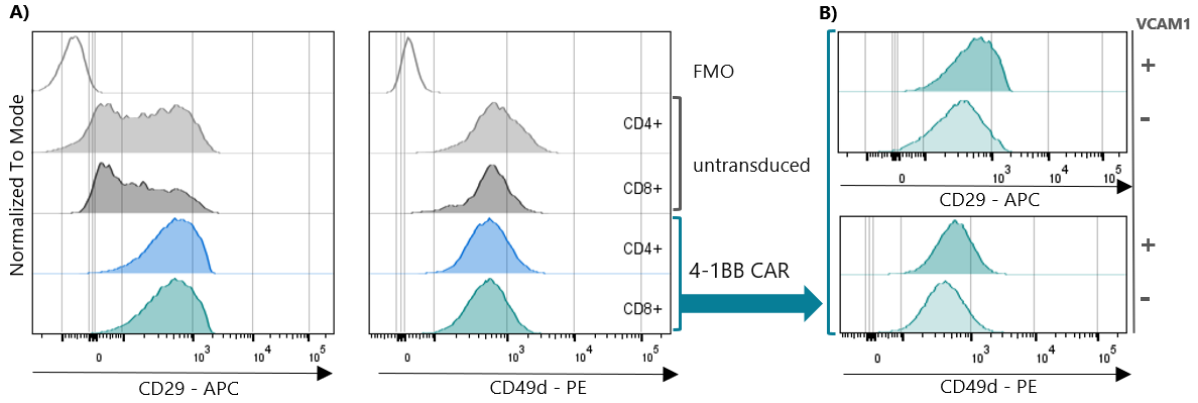

Figure 11: VLA-4 is expressed on CD4⁺ and CD8⁺ T cells independent of VCAM1 expression. *Expression on T cells was measured after 48 h of 0.1x10⁶ T cells in 2:1 co-culture with BXPC-3 tumor cells by flow cytometry,* ***A)*** *gated on CD4⁺ or CD8⁺ T cells,* ***B)*** *gated on CD8⁺ T cells with VCAM1⁺ or VCAM1⁻ fractions. Histograms are show for one representative donor. FMO = fluorescence minus one.*

In untransduced T cells CD4⁺ cells expressed higher levels of CD29 than CD8⁺ T cells (Figure 11A). Expression of CD29 increased in CAR T cells compared to untransduced T cells. The CD49d expression was the same in CAR⁺ and CAR⁻ cells. Both, CD4⁺ and CD8⁺ CAR T cells expressed CD29 and CD49d (Figure 11A&B) at the same level. The VLA-4 expression did not differ between VCAM1⁺ and VCAM1⁻ CAR T cells (Figure 11B).

Our findings reveal that both components of the VLA-4 heterodimer are present on CD4⁺ and CD8⁺ T cells, facilitating interactions also in between T cells through the VCAM1 axis.

2.4. VCAM1 knockdown and knockout in CAR T cells

2.4.1. shRNA mediated knockdown of VCAM1 in CAR T cells

To elucidate the role of VCAM1 in CAR T cell function, we used RNAi to differentially reduce expression levels of VCAM1. To that end we incorporated the targeting shRNA into the constructs, wearing the cDNA of the CAR (Figure 12A). The sequences that are transcribed to the shRNA are given in Table 12.

Table 12: shRNA sequences for knockdown of VCAM1 *and Kanamycin target as control. Sequences targeting exon 1-3 of VCAM1 were derived from the RNAi Consortium shRNA Library of BROAD Institute, and 1 nt was added to reach a length of 22 nt per shRNA.*

plasmid no.	target	source	sequence
#2210	Kanamycin	Zhao et al.; Cancer Cell 2015	ATCACCATGAGTGACGACGTGA
#2181	VCAM1 – Exon2	GPP - Broad institute	CCAGATAGATAGTCCACTGAAT
#2182	VCAM1 – Exon3	GPP - Broad institute	GCTGGAGATAGACTTACTGAAA
#2193	VCAM1 – Exon3	GPP - Broad institute	CGAGCTAAATTACACATTGATG

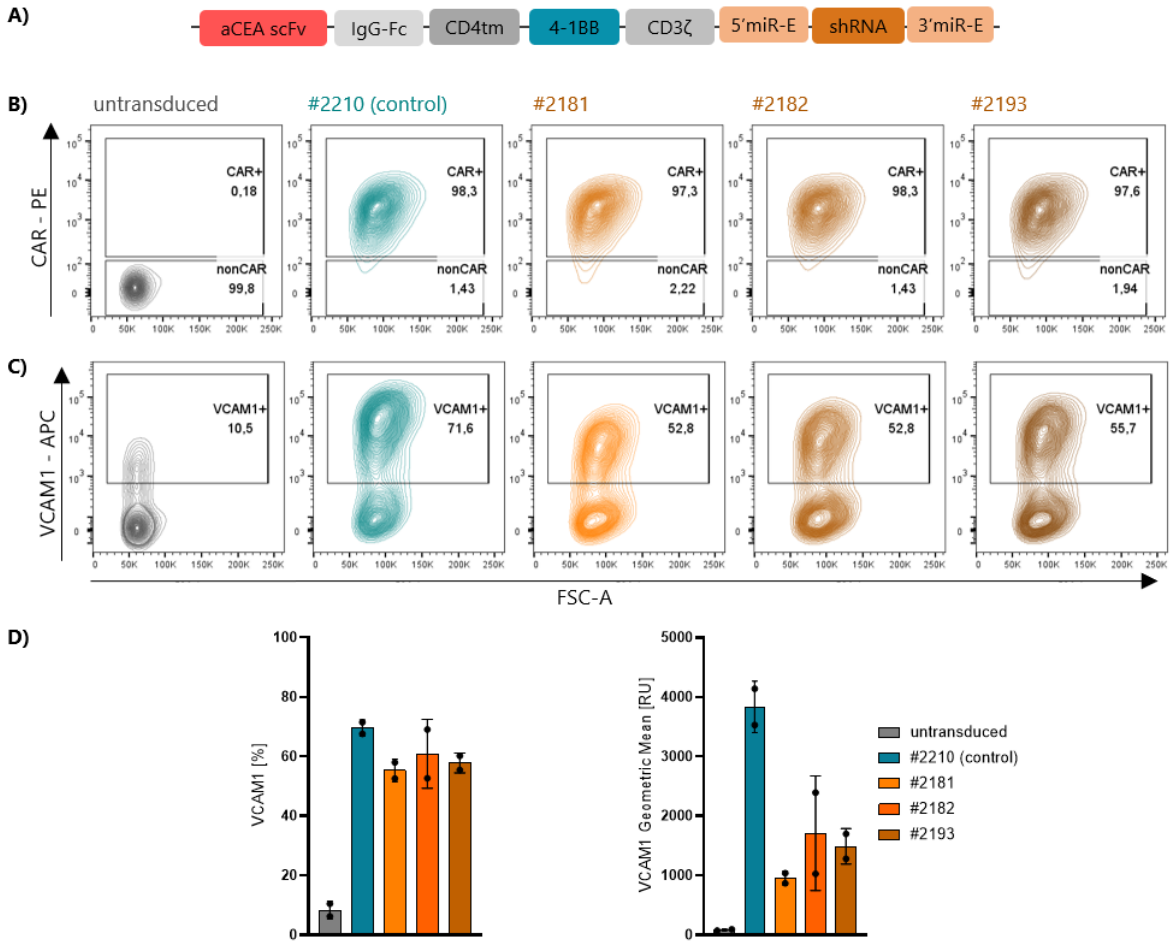

Figure 12: VCAM1 knockdown with specific shRNA. A) *Schematic structure of the construct with CAR and integrated shRNA.* ***B)-D)*** *Expression on T cells was measured by flow cytometry after 48 h in 2:1 co-culture of 0.1x10^6 T cells with antigen expressing BXPC-3 tumor cells.* ***B)*** *CAR expression on T cells and* ***C)*** *VCAM1 expression of CD8$^+$CAR$^+$ T cells of one representative donor are shown.* ***D)*** *Summary of two donors showing the mean and standard deviation of VCAM1 expression.*

The kanamycin shRNA[125] was used as control of irrelevant specificity (#2210). We tested three different shRNAs targeting VCAM1 (#2181, #2182 & #2193) in comparison to the control shRNA.

Since we observed maximal surface expression of VCAM1 after two days of stimulation with tumor cells (Figure 7) we chose this time point for measurement of VCAM1 and the respective knockdown (Figure 12B-D).

CARs of all constructs were expressed at similar levels on T cells (Figure 12B). Transduction with the VCAM1 targeting shRNA reduced the VCAM1 level comparted to the non-targeting control shRNA #2210 (Figure 12C&D). CAR T cell populations with VCAM1 targeting shRNA possess 10% less $VCAM1^+$ CAR T cells compared to the non-targeting control shRNA. VCAM1 specific shRNA strongly reduced the VCAM1 expression per cell with a reduction of the MFI to 39 – 75 %. The lowest VCAM1 expression was recorded for the construct #2181 which contains shRNA targeting exon two of VCAM1.

While the RNAi mediated VCAM1 knockdown reduced the levels of VCAM1 in CAR T cells the residual expression might impede the detection of VCAM1 dependent effect of CAR T cell function. For this reason, we continued with CRISPR/Cas9 mediated knockdown.

2.4.2. CRISPR/Cas9 mediated VCAM1 knockout in CAR T cells

In order to achieve a stronger reduction of VCAM1 expression we approached a complete knockout of VCAM1 by CRISPR/Cas9 gene editing of the anti-CEA CAR T cells (#908).

The CRISPR guide RNAs targeted exons one to three of VCAM1 (Table 13). Different combinations of two or three guide RNAs were tested for knockout efficiency (Figure 13A). VCAM1 and CAR expression was measured five days after CRISPR/Cas9 electroporation (Figure 13A-E). All tested guide RNA combinations reduced VCAM1 expression to a similar level. However the guide combination VCAM-C+F had the highest on- and off target score ratio according to the manufacturer (Table 13) and was therefore used in the following experiments, designated as "CRISPR-VCAM1".

Table 13: CRISPR guide RNAs for VCAM1 knockout and scrambled as control. *All sequences with on- and off target scores were derived from Integrated DNA Technologies (IDT), the sequence for the scrambled control stays with IDT.*

CRISPR guide	target	sequence	on target score	off target score
scrambled_1	none	-	-	-
VCAM1-C	VCAM1 – Exon 1	AGGATCACGACCATCTTCCC	99	62
VCAM1-D	VCAM1 – Exon 3	CTGATGTATACCCATTTGAC	61	61
VCAM1-F	VCAM1 – Exon 2	ATTCACAAGTTGCTGTGCAC	86	57

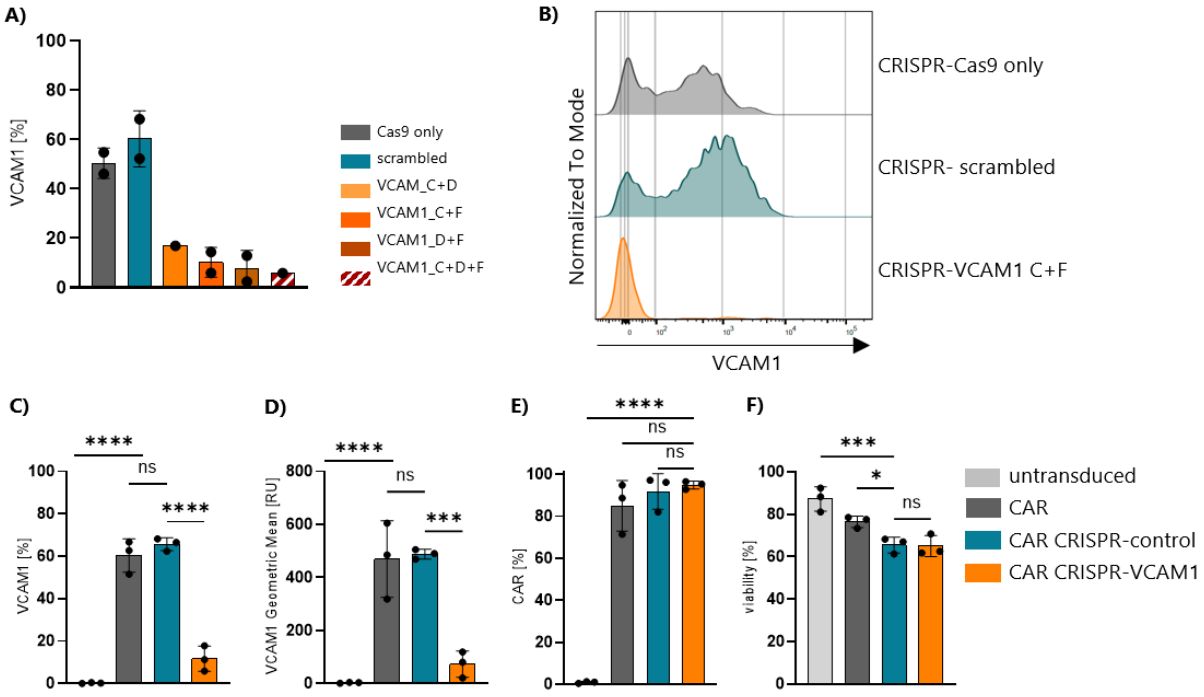

Figure 13: CRISPR mediated VCAM1 knockout in CAR T cells. *CRISPR/Cas9 knockout was performed after transduction and T cells expanded for 2d with 200 U/ml IL2.* ***A)-E)*** *Flow cytometry measurement of CD8⁺CAR⁺ T cells (CD8⁺non-CAR T cells for untransduced).* ***A)*** *VCAM1 expression after knockout with different guide RNA combinations. In the following only guide combination C+F is used for VCAM1 knockout.* ***B)*** *Exemplary histogram of VCAM1 expression after VCAM1 knockout or controls.* ***C)-D)*** *Mean and standard deviation of VCAM1 expression.* ***E)*** *Mean and standard deviation of CAR expression.* ***F)*** *Viability of T cells measured with the Vi-CELL cell counter. For statistics one-way ANOVA with Dunnett's multiple comparison test was calculated (*p<0.1 - ****p<0.0001, ns = not significant).*

VCAM1 expression was not affected in the CAR T cells that have been electroporated with Cas9 only, without addition of any RNA (Figure 13B). This shows that the electroporation process itself did not alter the VCAM1 expression. Five days after the VCAM1 knockout- process, 5-15 % of cells still expressed VCAM1, suggesting that those cells were not targeted in the CRISPR/Cas9 process.

The transduction of the #908 plasmid yielded 20-40 % CAR expression on T cells. With MACS sorting the CAR positive T cell were enriched to over 90 % and CAR expression remained stable after electroporation and CRISPR knockout of VCAM1 (Figure 13E).

Viability of the CAR T cells was reduced by the transduction process about 10 % and remained stable around 70% after the further procedure of the CRISPR mediated knockout (Figure 13F). CRISPR mediated knockout with the guide RNA combination VCAM1-C+VCAM1-F yielded a robust VCAM1 knockout keeping viable T cells with high CAR expression.

2.5. VCAM1 knockout reduces the activation and exhaustion phenotype in CD8⁺ CAR T cells

We tested the effect of VCAM1 knockout on the phenotype of CD8⁺ CAR T cells upon CAR mediated activation, in particular on the expression of surface markers for activation (Figure 14A) and exhaustion (Figure 14B).

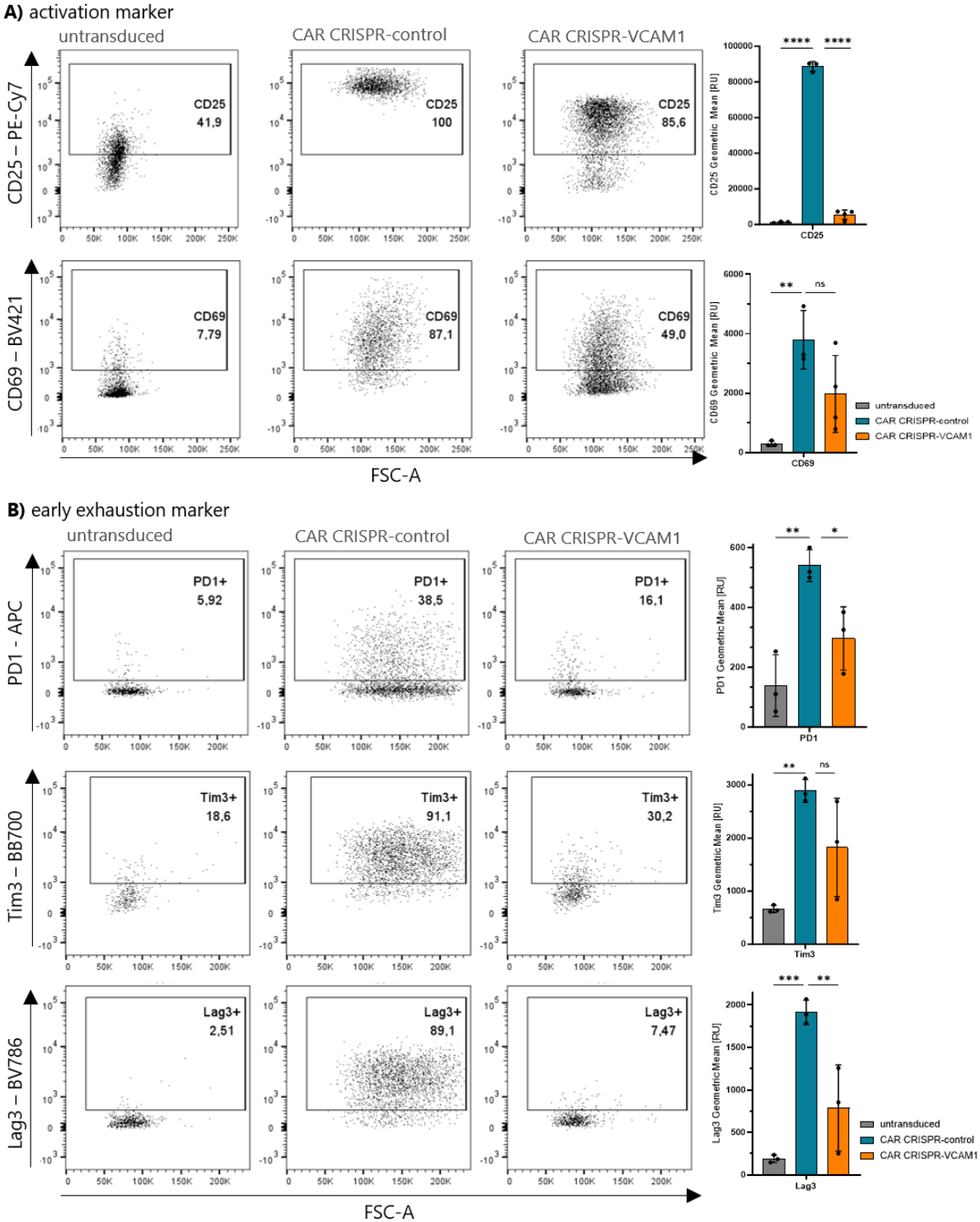

Figure 14: Activation and early exhaustion markers are increased in VCAM1⁺ CAR T cells. *Flow cytometry measurement of surface markers on 0.1x10⁶ T cells after 3 days of 2:1 co-culture with BXPC-3 tumor cells. Dot plots of one representative donor and mean with standard deviation for three independent donors are shown, for* ***A)*** *co-staining of activation markers and* ***B)*** *co-staining of exhaustion markers. Gated on CD8⁺ cells for untransduced T cells, on VCAM1⁺CD8⁺ T cells for CRISPR-control, on VCAM⁻CD8⁺ cells for CRISPR-VCAM1. For statistics one-way ANOVA with Dunnett's multiple comparison test was calculated (*p<0.1 - ****p<0.0001, ns = not significant.)*

For activation of CAR T cells we recorded CD25 and CD69 and compared expression levels between CAR T cells with control- and VCAM1 knockout. VCAM1 knockout resulted in a significant lower expression of CD25 and diminished levels of CD69 on surface after co-culture with BXPC-3 tumor cells (Figure 14A). Both markers increased strongly in CAR T cells compared to untransduced T cells under the same co-culture conditions.

CAR T cells expressing high levels of VCAM1, showed an increase in the forward scatter area in the flow cytometry analysis, which corresponds to an increase in cell size, indicating enhanced CAR T cell activation.

The early exhaustion markers PD1 (PDCD1; CD279), Tim3 (HAVCR2; CD366) and Lag3 (CD223) showed a strong increase in activated control CAR T cells compared to untransduced T cells (Figure 14B). Knockout of VCAM1 CAR T cells did not alter Tim3 expression in two of three donors. PD1 and Lag3 expression was significantly lower in CAR T cells lacking VCAM1 in all three donors compared to the VCAM1 positive CAR T cells.

2.6. VCAM1 is predominantly expressed by central memory CAR T cells

Since the VCAM1 knockout resulted in reduced activation and exhaustion phenotypes in CAR T cells, we aimed to identify the impact of VCAM1 knockout on compartments that sustain long-term persisting CAR T cells.

We tested the impact of the VCAM1 knockout on the composition of the memory CAR T cell compartments. The four subgroups of naive, effector, effector memory and central memory were distinguished by the two markers CCR7 and CD45RO[15,126,127].

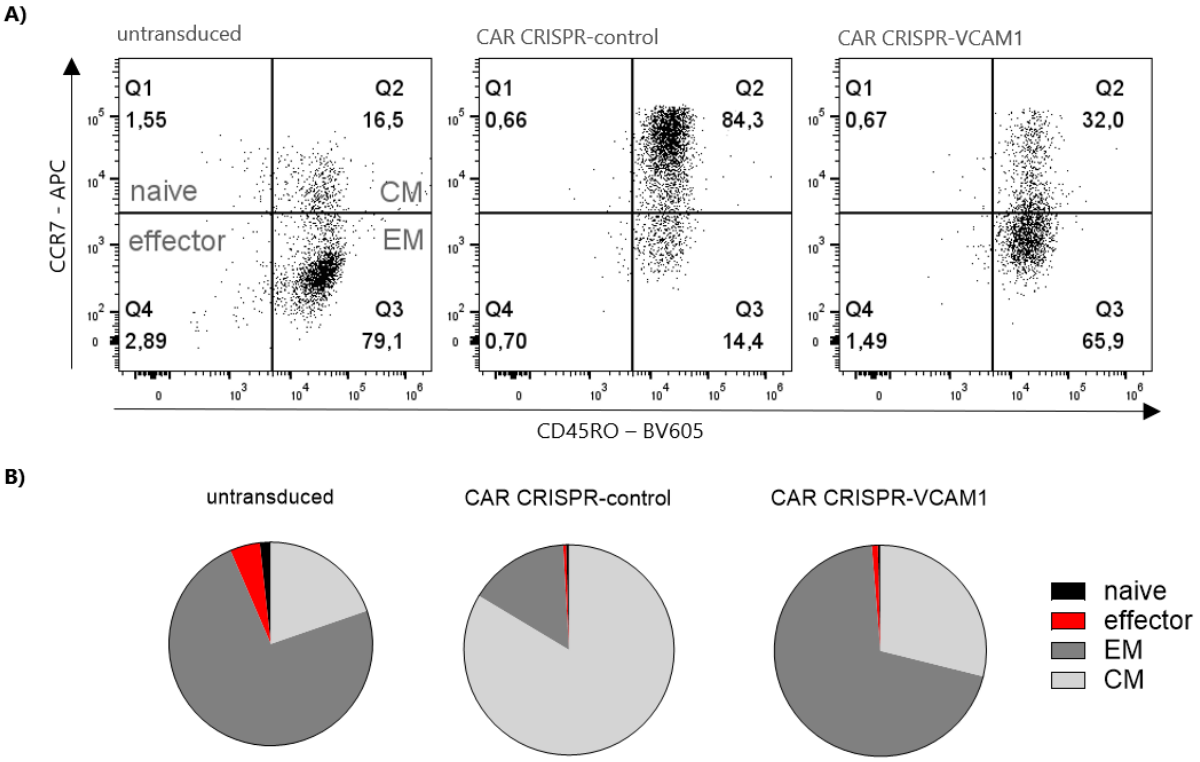

Figure 15: VCAM1 knockout reduced the number of CAR T cells in the central memory pool. *$CD8^+$ T cells were analyzed for CCR7 and CD45-RO expression by flow cytometry after knockout and expansion.* ***A)*** *Dot plots of one representative donor presenting the distribution of subsets of naïve T cells ($CCR7^+CD45RO^-$), effector T cells ($CCR7^-CD45RO^-$), central memory T cells (CM, $CCR7^+CD45RO^+$) and effector memory T cells (EM, $CCR7^-CD45RO^+$).* ***B)*** *Pie charts represent the median proportion of the subsets of two independent donors within the $CD8^+$ T cells.*

After seven days in culture VCAM1 knockout CAR T cells exhibited a drastic increase in the effector memory phenotype compared to the control CAR T cells (Figure 15). Over 80 % VCAM1 positive CAR T cells expressed both CCR7 and CD45RO, classifying them to the central memory phenotype. With knockout of VCAM1 the CAR T cells mainly reduced the expression of CCR7. Less than 2% of $CD8^+$ T cells of all groups showed a naïve phenotype. Untransduced T cells exhibited the phenotype of effector memory cells to over 70%. High CD45RO expression was measured for untransduced T cells as well as for CAR T cells with and without VCAM1.
We found that VCAM1 knockout in CAR T cells leads to an enrichment of the effector memory pool, maintaining them in a state akin to that of untransduced T cells.

2.7. CAR T cell degranulation is decreased upon VCAM1 knockout

So far, we could establish, that VCAM1 expression results in pronounced exhaustion and a reduced effector memory phenotype. However, the major criterion for CAR T cell functionality is the degranulation and cytokine secretion capacity, critical for inducing cytotoxicity against cancer cells.

The degranulation of lytic granules, as indicated by the surface marker CD107a (LAMP-1) was reduced in VCAM1 knockout CAR T cells after co-culture with BXPC-3 tumor cells, compared to the CRISPR control (Figure 16A).

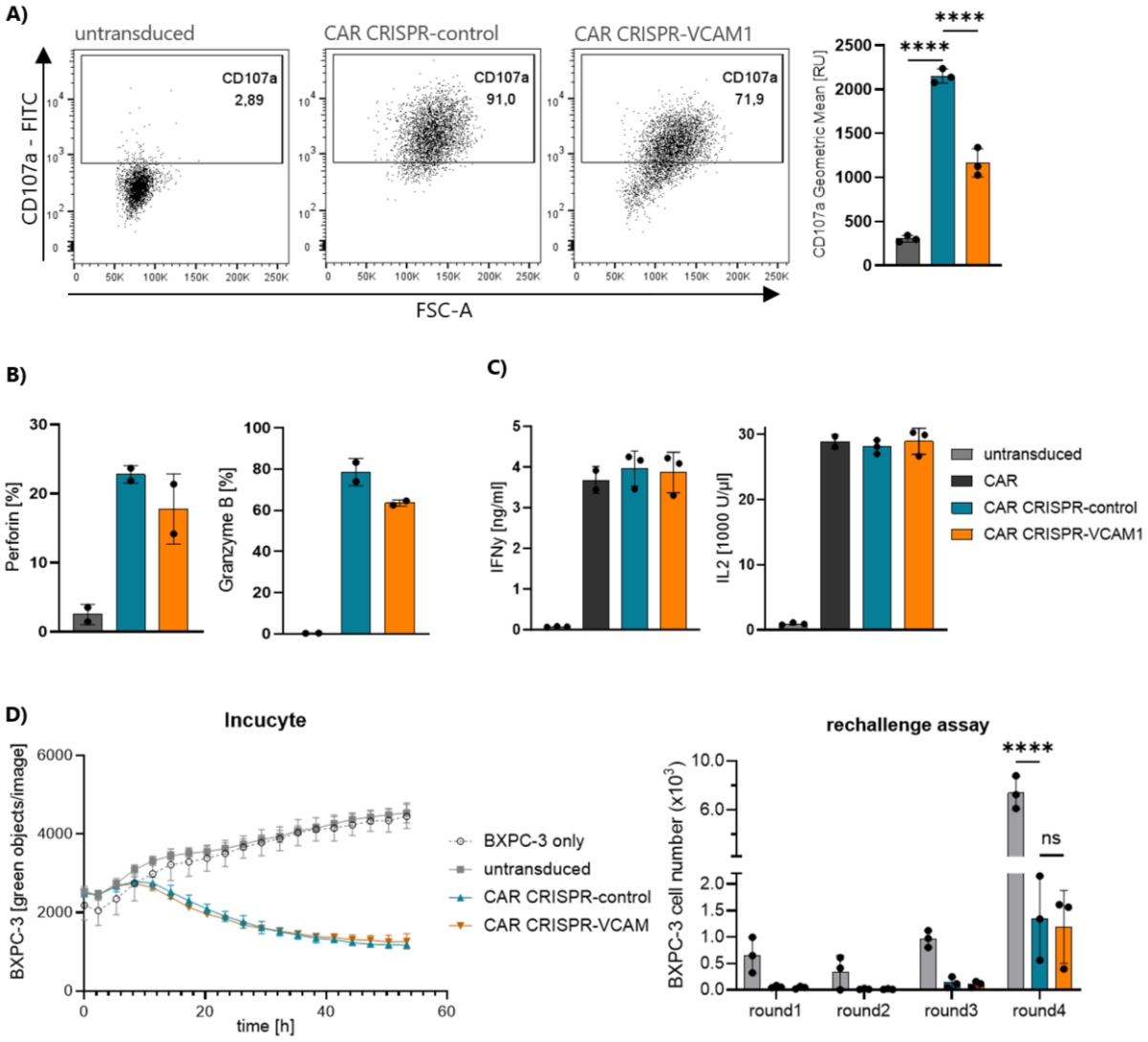

Figure 16: VCAM1 knockout decreased degranulation but not the cytotoxic capacity on of CAR T cells on BXPC-3 tumor cells. *For **A) & B)** 0.1x10⁶ T cells were co-cultivated 2:1 BXPC-3 tumor cells for 3 days. **A)** On the day of measurement by flow cytometry, Monensin, Brefeldin and CD107a antibody were added to the culture and incubated for 5h, then surface staining was performed. **B)** T cells were stained with extracellular markers & live dead dye before fixation and intracellular staining for perforin and granzyme. Pan CD8⁺ cells are shown for untransduced T cells, VCAM1⁺CD8⁺ cells are show for CRISPR-control, VCAM⁻CD8⁺ cells are shown for CRISPRR-VCAM1, **C)** After 48h co-culture the supernatants were analyzed for IFNγ and IL2 analyzed by ELISA. **D)** 0.05x10⁶ T cells were co-cultivated 1:1 with BXPC-3-GFP⁺ cells for 48h, green fluorescence was recorded in the Incucyte. **E)** For the rechallenge assay 0.1x10⁶ T cells were co-cultured 1:1 with BXPC-3-GFP⁺ tumor cells for 3-4 days per round, 10% of the whole co-culture was recorded with cell-counting beads by flow cytometry, the remaining co-culture was seeded on fresh 0.1x10⁶ BXPC-3 cells for another round. **A)** One-way ANOVA **E)** Two-way ANOVA, with Dunnett's multiple comparison test was calculated. (*p<0.1 - ****p<0.0001, ns = not significant).*

CAR T cells increased intracellular levels of perforin and granzyme upon co-culture with BXPC -3 tumor cells, compared to the untransduced T cells (Figure 16B). CAR T cells with VCAM1 knockout showed no robust difference in the perforin level compared to the VCAM1 positive CAR T cells. The granzyme B expression level was reduced by over 10% in the CAR T cells lacking VCAM1.

IFNγ and IL2 release of T cells increased upon CAR mediated T cell stimulation. No difference in the amount of secreted cytokines by the CAR T cells with and without VCAM1 knockout was measured (Figure 16C). Untransduced T cells did not secrete relevant amounts of either of the cytokines.

To compare the killing capacity of CAR T cells with VCAM1 knockout to controls, we tracked the GPF expressing BXPC-3 tumor cells in co-culture with CAR T cells and the tumor cell count was tracked over time, using the Incucyte ZOOM live-cell imager (Figure 16D). CAR T cell populations with VCAM1 knockout showed equally effective anti-tumor cytotoxicity as the control CAR T cells.

As our previous results suggested that VCAM1 knockout results in decreased activation and exhaustion, we speculated that VCAM1 expressed by CAR T cells can alter the long-term performance of CAR T cells. Therefore, we repeatedly exposed CAR T cells to CEA^+ tumor cells and compared the anti-tumor effector function of CAR T cells with and without VCAM1 knockout. During the initial three rounds, CAR T cells both with and without VCAM1 knockout equally efficiently eliminated all tumor cells. At the end of the fourth round, as the T cell viability declines, their capacity to control the tumor growth diminishes correspondingly.

At this juncture, no difference in tumor-killing efficacy was observed between VCAM1 knockout CAR T cells and the $VCAM1^+$ CRISPR-control population, despite a reduction of CD107a and intracellular perforin and granzyme B levels were measured.

2.8. VCAM1 co-localizes with the CAR in the T cell - tumor cell contact area.

To better understand the role of VCAM1 in CAR-mediated tumor cell binding we next performed live cell imaging of both the CAR and VCAM1.

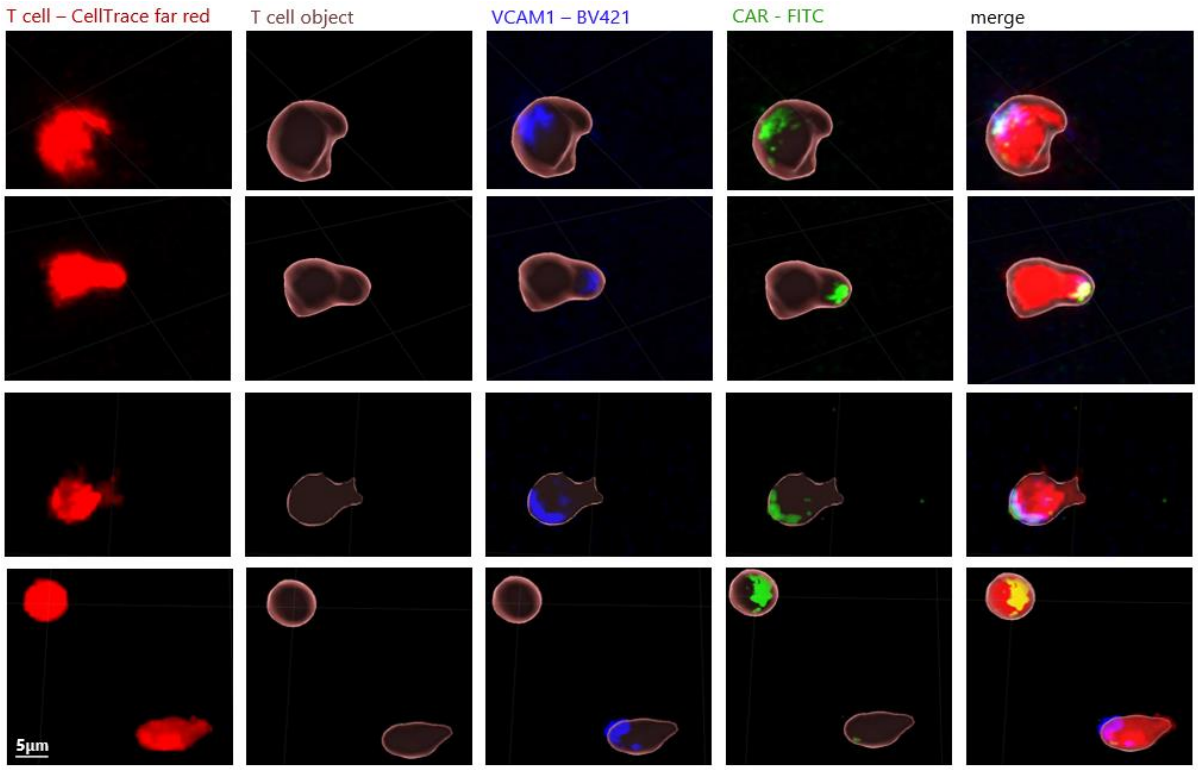

Figure 17: Co-localization of CAR and VCAM1. *CAR T cells were intracellular stained with CellTrace Far Red and subsequentially for VCAM1 and the CAR on surface, 0.04x10^6 T cells were seeded 1:5 on BXPC-3 tumor cells. Measurement was done at the STELLARIS 8 confocal microscope overnight. Each row shows one representative cell. 1126 cells of three independent donors were analyzed. 20.4% were double positive (CAR$^+$VCAM1$^+$) 29.5% were CAR$^+$ 2.4% VCAM$^+$. CellTrace Far Red signal (first column) was used for object generation of T cells with the Imaris 9.9.1 software (second column). Recording of single channels and the overlay (merge) are shown. BXPC-3 cells were recorded in the brightfield channel only and are excluded from the fluorescence visualization.*

In co-culture of anti-CEA CAR T cells with BXPC-3 tumor cells, VCAM1 and CAR co-localized on the same spot on the respective cell (Figure 17). In line with our flow cytometry results (Figure **8**), not all T cells that showed CAR signal also showed co-staining with VCAM1.

CAR and VCAM1 polarized on the same side of the T cell surface, in presence and absence of BXPC-3 tumor cells.

Time course imaging showed CAR T cells in contact to the CEA positive BXPC-3 tumor cells, with VCAM1 being localized in the contact region. Consecutive captures from these events revealed sustained contact of the T cells to BXPC-3 cells with VCAM1 in the contact region during the entire contact time (Figure 17).

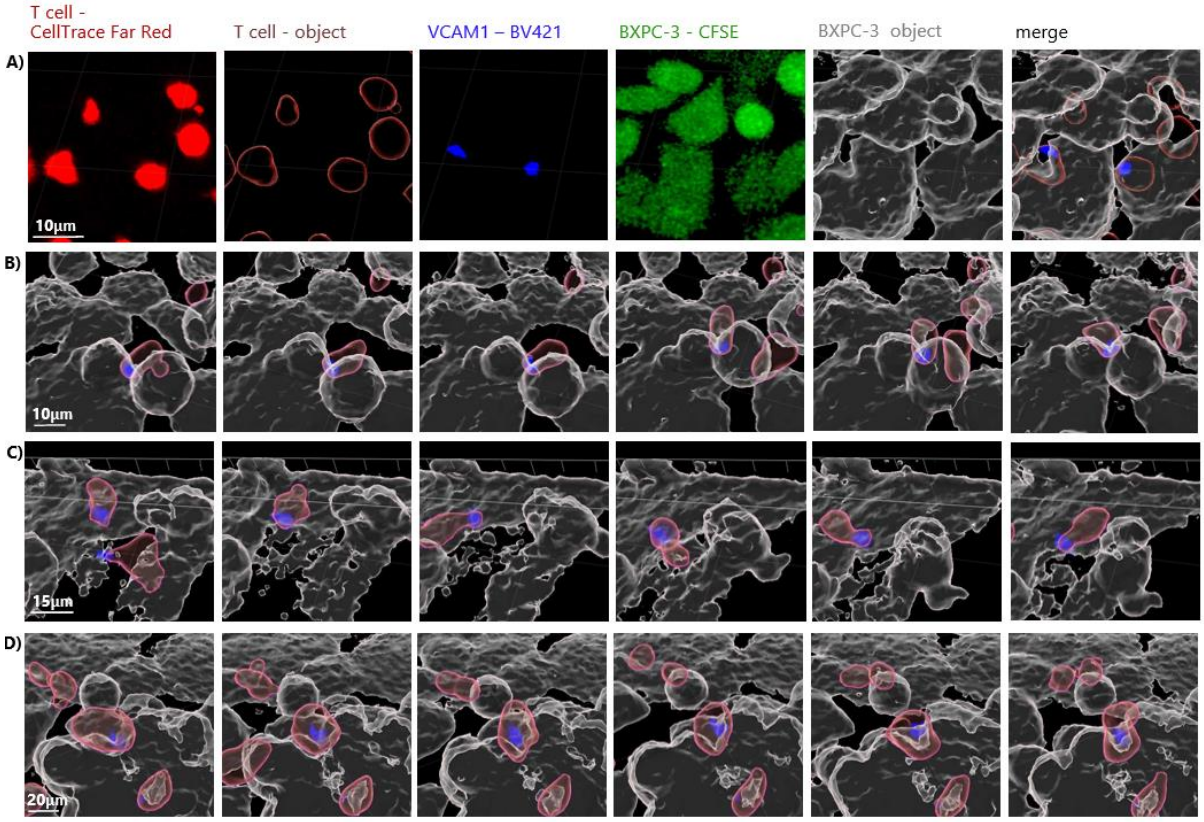

Figure 18: VCAM1 localized on T cells in the tumor cell contact region. *CAR T cells were intracellular stained with CellTrace Far Red and subsequentially for VCAM1 on surface and 0.1x10^6 T cells seeded 1:2 on CFSE labeled BXPC-3 tumor cells. Life cell imaging was performed over night at the stellaris 8 microscope.* ***A)*** *Example of object generation, for T cell objects based on the CellTrace Far Red signal, for BXPC-3 objects based on the CFSE signal with the Imaris 9.9.1 software. Images of six consecutive frames (1s per frame) of one region of interest for each* ***B)-D)*** *are shown.*

The findings of both, co-localization of VCAM1 with CAR on the same spot on CAR T cells and the sustained presence of VCAM1 in the contact region to BXPC-3 tumor cells strongly supported our assumption of relevance for VCAM1 in the interaction of CAR T cells with their target tumor cells.

2.9. Avidity of CAR T cells to target cells is reduced upon VCAM1 knockout

We have shown, that VCAM1 clusters with the CAR in the T cell – tumor cell contact area. Therefore, we hypothesized that VCAM1 is predominantly required for cell attachment, similar to its role in epithelial cells.

To test this hypothesis we measured the avidity of the anti-CEA CAR T cells with and without VCAM1 to target cells with the zMovi. This device applies acoustic waves to exert increasing force on the connection between CAR T cells and a monolayer of target cells and records the detachment of the effector cells from the monolayer.

As target cell monolayer we used the CEA^{low} VLA-4^{+} epithelial cell line HaCaT (Figure 19A) and the CEA^{high}VLA-4^{+} tumor cell line BXPC-3 (Figure 19B), both lacking VCAM1 expression. As expected, the overall avidity of CAR T cells to BXPC-3 cells was higher than to HaCaT cells, as the former expresses higher levels of CEA, the CAR antigen.

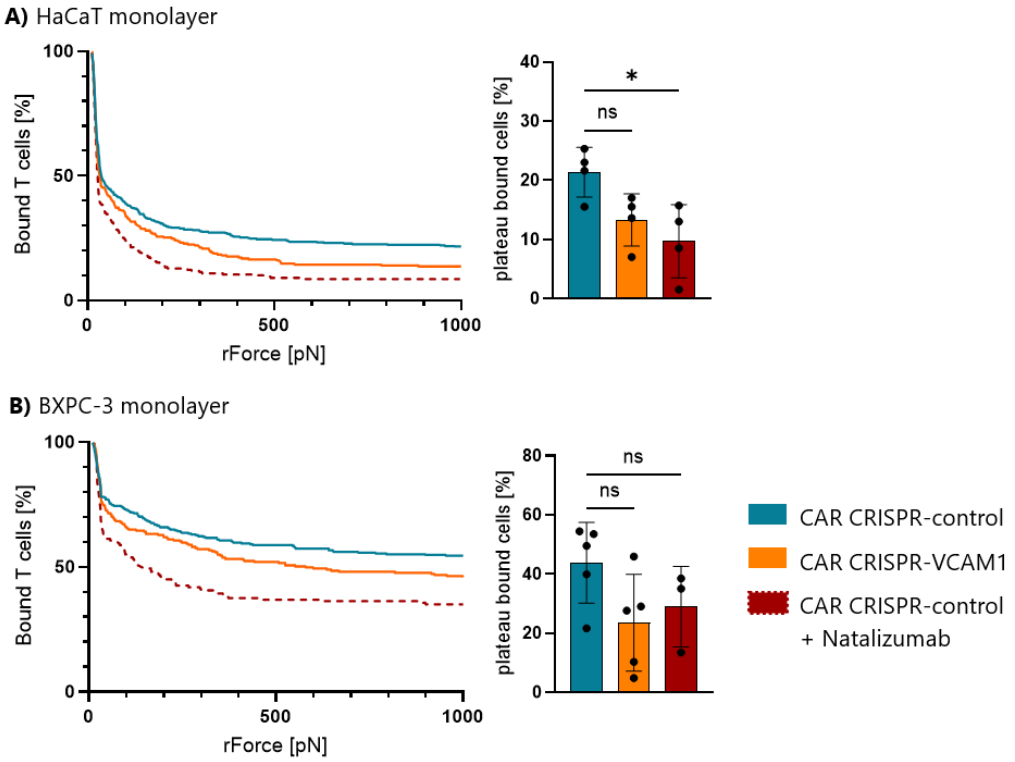

Figure 19: Avidity of CAR T cells: A) *to monolayer of CEA^{low} VLA-4^{high} HaCaT cells and* ***B)*** *to CEA^{high} VLA-4^{low} BXPC-3 cells was measured after 5min pre-incubation on the zMovi. As control the VLA-4 inhibitor Natalizumab was preincubated at 30 mg/ml for 5 min and then CAR CRISPR-control T cells were added. Mean and standard deviation are shown. For statistics one-way ANOVA with Dunnett's multiple comparison test was calculated (*p<0.1, ns = not significant).*

VCAM1 knockout reduced the avidity of CAR T cells to both, CEA^{low} HaCaT cells and CEA^{high} BXPC-3.

To interfere with the VLA-4 interaction we took advantage of blocking with the antibody Natalizumab, that binds to the α4-integrin (CD49d) and thereby prevents VCAM1 – VLA-4 interaction. The presence of Natalizumab reduced CAR T cell avidity to both HaCaT and BXPC-3 target cells, confirming the conclusion based on of the VCAM1 knockout data, that VCAM1 on CAR T cells increases the binding strength to the CAR target cells BXPC-3 and HaCaT.

3. Discussion

CAR T cell therapy has proven to be very successful in the treatment of hematologic cancers. When targeting solid organ malignancies, the feasibility for successful cure is facing many obstacles. Embedded in a restrictive tumor microenvironment and with upregulation of inhibitory immune checkpoint molecules and chemokines and intratumor clonal diversity of solid tumor entities, many escape mechanisms hinder effective tumor clearance with current CAR products[34,128–131]. The hostile tumor environment with massive immune repression requires modification of CAR T cells in order to improve resistance and prolonged activation. Supporting CAR T cell function with addition of checkpoint molecules blockade has the potential to improve CAR T cell efficacy in solid tumors[4,104]. First in human studies have proven safety of CRISPR engineered anti-cancer T cell products[57,132], opening a more versatile toolbox for additional fine tuning of CAR T cells.

Targeting carcinoembryonic antigen (CEA) with CAR T cell therapy is relevant since high level of CEA are associated with poor cancer prognosis[133] and CEA is aberrantly expressed in various cancer types such as lung[134]-, breast[135,136]-, colorectal- and pancreatic cancers[137,138]. The latter possess a challenging microenvironment characterized by a dense stroma[37], which allows tumor resection in only 15-20% of all cases[38,39] and impedes T cell infiltration. CEA was reported as a safe target for CAR T cells in gastrointestinal cancers[40,139].

The different integrin dimers α4β7, αMβ2, α9β1, and αDβ2 are reported as interaction partners for VCAM1[140–144]. The best studied dimer, VLA-4, is composed of CD49d (integrin α4) and CD29 (integrin β1).

To address whether the expression levels of VCAM1 and VLA-4 differ between healthy and diseased tissue we correlated RNA expression of healthy pancreatic tissue samples of the GTEx portal and RNA expression of pancreatic adenocarcinoma (PAAD) of the TCGA data base expression with the GEPIA 2[145] correlation analysis tool (Figure 20). Expression levels of VCAM1 were found to be higher in PAAD than in healthy pancreatic tissue. Expression of CD29 and CD49d showed a moderate correlation to VCAM1 in both conditions. Interestingly expression data for PAAD showed elevated levels of both CD29 and CD49d compared to healthy pancreas, supporting the hypothesis that T cell binding of tumor tissue can be mediated by VCAM1.

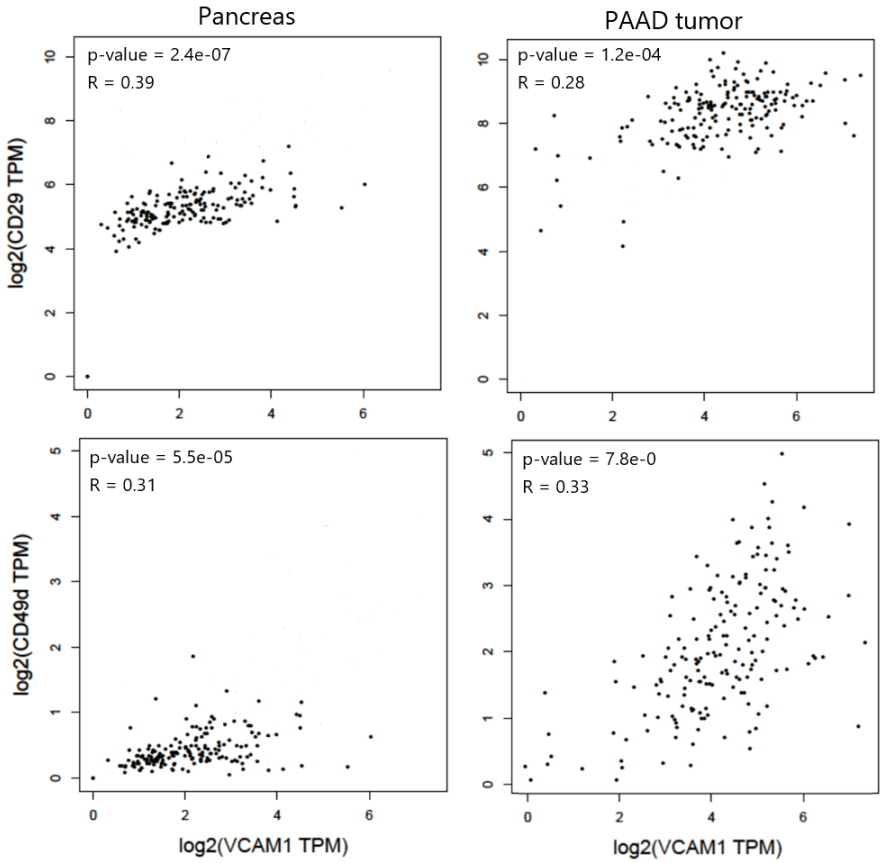

***Figure 20: Differential expression of VLA-4 in healthy and diseased pancreas**. For healthy pancreatic tissue 167 samples of the GTEx portal and for pancreatic adenocarcinoma (PAAD) 179 samples of the TCGA database were compared for their expression of CD29 and CD49d using the GEPIA 2 correlation analysis tool.*

To gain insights into T cell mechanisms, tumor infiltrating T cells (TILs) provide a valuable tool since those cells obviously penetrated and persisted within the tumor tissue. Chromatin accessibility of VCAM1 was found by Riegel et al.[110] to be upregulated in terminal exhausted clusters of TILs in various tumor entities by ATAC-seq. There are barely any reports of VCAM1 being expressed by T cells and to our knowledge there was no report of VCAM1 expression by CAR T cells to date. Taking the observation of upregulated gene activity of VCAM1 in exhausted TILs into the context of CAR redirected T cell therapy, we asked whether VCAM1 expression by CAR T cells may contribute to anti-tumor capacities.

After stimulation of anti-CEA CAR T cells with CAR dependent and CAR independent stimulation, VCAM1 was found to be expressed only on $CD8^+$ CAR T cells, barely on $CD4^+$ and very low in untransduced T cells VCAM1. As the ATAC-seq of TILs showed increased chromatin accessibility of VCAM1, we expected a higher induction also in untransduced T cells upon activation by CD3/CD28 and PMA/Iono. However CAR T cells are known to be faster activated than untransduced T cells[146,147]. Further, the in vitro conditions can not resemble the more complex and much longer persistence times that TILs experience in a patient.

Expression of VCAM1 was found to cohere to the CAR MFI, an interesting finding, as Greenman and Reiter et al. could show a strong correlation between CAR expression levels and avidity[114], which might be explained by CAR expression level dependent upregulation of adhesion molecules like VCAM1.
When stimulating T cells with CARs possessing different costimulatory molecules, a stronger induction of VCAM1 in 4-1BB than in CD28 was observed. An unexpected finding as CD28 is reported to induce overall stronger and faster CAR T cell activation[148]. However the different co-stimulatory moieties are known to induce different metabolic programs and differentiate to phenotypic lineages[15,149]. CAR T cells with CD28 co-stimulation favor the proliferation of $CD4^+$ cells[18] while CAR T cells with 4-1BB co-stimulation primarily foster proliferation and memory formation of $CD8^+$ cells [150,151]. 4-1BB promotes stronger activation of NFκB than CD28[152] further modulating the promotor region of VCAM1 that contains functional NFκB tandem domains.

With removal of either CD3ζ or 4-1BB domain from the CAR the expression of VCAM1 on T cells was reduced. Removal of both, the CD3ζ and the 4-1BB domain abolished the VCAM1 expression entirely, what underlines the high dependency of VCAM1 to the CAR signaling. Upon activation of CAR T cells there follows a release of high levels of IFNγ[153,154]. Reduced secretion of IFNγ correlated to the VCAM1 expression, further outlining the influence of the CAR T cell activation on VCAM1 expression. The extracellular IgG CH2-CH3 hinge domain can mediate clustering[155–157], and facilitate recruitment of downstream signaling molecules as ZAP70[158]. The aggregation of proteins like VCAM1 can be influenced by the hinge and transmembrane domain. Hence the construct #2602 was built with exchange of the IgG and transmembrane domain and VCAM1 expression was affected but not reduced as strong as with removal of the signaling domains. Apart from cluster formation and reduced internalization also increased translocation of VCAM1 from intracellular storage or transcriptomic enhancement and increased production of the protein can enhance the expression of VCAM1 on the T cell surface.

VCAM1 blockade by antibody treatment is not desirable for T cell therapy modulation, as strong side effects by the blockade of VCAM1 on endothelium and other tissues can be expected. For CAR T cell therapy, VCAM1 blockade by antibodies could additionally reduce the infiltration to the tumor site because the extravasation from the blood vessels will be inhibited with systemic VCAM1 blockade. The knockdown or knockout of VCAM1 on CAR T cells provides a efficient, targeted solution and can be achieved with integration of shRNAs to the CAR construct or CRISPR/Cas9 mediated knockout.
As the anti-CEA CAR T cells with 4-1BB co-stimulatory domain (#908) showed a higher VCAM1 expression as the CD28 co-stimulatory counterpart (#607) the former was chosen as base for knockdown or knockout of VCAM1.

Plasmids containing one of three different VCAM1-targeting shRNAs were compared to the irrelevant control shRNA. There are two isoforms of human VCAM1, containing either six or seven Ig-like domains[83]. All three guide RNAs target exon two or three of VCAM1 which are present in both isoforms and yielded a reduction of VCAM1 expression. With shRNA, knockdown efficiency is limited by the ratio of transcribed mRNA to transcribed shRNA. With increased transcription of VCAM1, the mRNA will be incompletely degraded by the shRNA and reach the translation process. At peak of activation the CAR T cells with integrated shRNA showed a four-fold lower expression of VCAM1 than the control CAR T cells, indicating a high knockdown efficiency however with remaining residual expression. The conformity of VCAM1 knockdown by all three shRNA sequences substantiates correct targeting, as off-target effects are more likely to generate different outcomes. To further enhance VCAM1 knockdown efficiencies, two or three shRNA sequences could be combined in one plasmid. However, transduction efficiencies correlate with plasmid size and we experienced a lower CAR MFI when using larger plasmids. As the CAR MFI also correlates with VCAM1 expression as discussed before, we avoided increasing the plasmid size with implementation of further shRNA sequences.
With CRISPR/Cas9 a complete knockout of VCAM1 was achieved, preserving high CAR expression levels and thus serving as a better model to study differences to VCAM1 expressing CAR T cells.

Epigenetic mechanisms regulate T cell differentiation and response[159], the corresponding cell state leads to up and down regulation of surface molecules. CAR T cells with VCAM1 knockout show a strong reduction of the activation markers CD25 and CD69 and early exhaustion markers like PD1, Tim3 and Lag3 on surface, compared to the control population. Activation and exhaustion correlate with each other. It has to be taken into account that the short-term observation in cell culture (3-4 weeks) can significantly differ from the long-term circulation of T cells in vivo which can last from months to years[33,160]. Despite these differences, our data support the correlation of VCAM1 expression, and the upregulation of exhaustion markers as seen in the ATAC-seq of TILs.
Different groups elaborated that CD45Ro expression on Lymphocytes predicts a favorable clinical outcome in solid tumors[161–163]. CD45Ro expression is not dampened in CAR T cell populations with VCAM1 knockout compared to CAR T cell control. Whereas the expression of CCR7 is strongly reduced with knockout of VCAM1 in $CD8^+$ CAR T cells, shifting the population towards the effector memory type[164]. CCR7 is crucial for sensing chemotaxis and for the entry of circulating lymphocytes to lymphatic tissue[165,166], with reduction of CCR7 expression the CAR T cells rather circulate in the peripheral lymphoid tissues and gain the potential to start rapid effector function[126]. Additional expression of CD28 is needed substantiate the central memory phenotype of VCAM1 expressing CAR T cells.

Analysis of cytokine levels of the VCAM1 knockout and control CAR T cells did not reveal discernible differences. In the study a mixture of $CD4^+$ and $CD8^+$ CAR T cells were utilized, noting that $CD4^+$ T cells do not express VCAM1. For the cytokine measurement the supernatant from the combined cell population was analyzed and may mask specific variations in the $CD8^+$ subpopulation where the CRISPR knockout could induce significant changes in the VCAM1 expression. Further, we dealt with a dynamic upregulation of VCAM1 but differences in the cytokine secretion at different time points were not captured by the ELISA where the accumulated cytokines after 48h were measured in the supernatant.

The upregulation of CD107a (LAMP1) on surface of T cells indicates the fusion of lysosomes with the cell membrane[167]. In $CD8^+$ T cells a high CD107a expression indicates higher rates of release of granzymes and perforin. With knockout of VCAM1 less CD107 was found to be expressed on surface of $CD8^+$ CAR T cells. In line also the detected intracellular levels of perforin and granzyme B were lower in VCAM1 knockout T cells compared to the control population. For the latter different explanations are possible as granzyme B and perforin are intracellular stored in lysosomal vesicles, either a high secretion or incomplete new synthesis can lead to reduced intracellular levels of both. With additionally reduced levels of CD107a reduced secretion and dampened production of the lytic molecules is assumed.

As the phenotype analysis has shown reduced activation and reduced release of cytotoxic granules in CAR T cells with VCAM1 knockout, also a diminished ability for tumor cell control in the knockout group was expected. However, the cytotoxic activity of CAR T cells with VCAM1 knockout, measured by tracing the count of GFP labeled BXPC-3 tumor cells in co-culture, was non-inferior compared to the control group. The time course analysis covered the peak of VCAM1 expression after 48 h with the biggest differences of VCAM1 expression between the knockout and control group. However, beginning cytotoxic activity was observed to set in after 11 h already, thus VCAM1 independent engagement with the tumor cells has taken place before.

Gene activity of IRF3 is enhanced in terminal exhausted clusters (Figure 4F) likewise to VCAM1. We have recently seen that reduction of IRF4 increases cytotoxic performance on low antigen expressing cells in the long run[65]. Similar effects were expected for VCAM1 but in also in repetitive stimulation of VCAM1 knockout CAR T cells no differences were observed compared to the control. In both cytotoxicity assay the whole $CD4^+$ $CD8^+$ T cell pool contributed to the outcome and in the analysis of the CRISPR knockout group ~5 % of $CD8^+$ CAR T cells were detected with remaining VCAM1 expression which are also present in the co-culture, contributing to the killing efficiency. Overall we see a strong influence of the VCAM1 knockout on activation and exhaustion markers on CAR T cells, nevertheless the cytotoxic function remained stable under these conditions.

In vitro we detected fast upregulation of VCAM1 whereas in the ATAC seq screen, VCAM1 gene activity was increased in the terminal exhausted TILs, indicating a difference in kinetics between

the in vitro and in vivo setting. The activity mediating downstream effects of VCAM1 can be concealed by strong baseline activation of in vitro CAR T cell populations whereas in the terminal exhausted TILs high degree of dysfunction is reached.

In live-cell microscopic analysis VCAM1 molecules clustered together with the CAR on surface of T cells and maintained presence in the contact area to tumor cells. This gives strong evidence that VCAM1 plays a role in tumor cell adhesion. Overall, CAR and VCAM1 positive cell frequency counted in microscopic overview was lower than measured by flow cytometry but TCR complexes are known to be downregulated through internalization upon antigen encounter[168,169] and a similar effect was discovered for CAR molecules[170]. Under live-cell imaging conditions the internalization of CAR molecules could be more pronounced than for flow cytometry analysis, as the cells are analyzed in co-culture and in presence of antigen for live-cell imaging. Giving the co-localization of VCAM1 and CAR on the surface of CAR T cells and the reinforced avidity of VCAM1 expressing CAR T cells, an integration and stabilization of VCAM1 the immunological CAR synapse is likely.

VCAM1 negative CAR T cells show reduced avidity to HaCaT and BXPC-3 cells compared to VCAM1 positive CAR T cells. The reduced avidity is a possible explanation for the reduced activation phenotype, observed in the VCAM1 knockout CAR T cells. Greenman et al.[114] described increasing avidity with higher number of CAR molecules on surface, this effect could be explained by the concurrent increase of VCAM1 co-expression.
Recently ICAM1 knockout in $CD8^+$ T cells was reported to increase T cell viability and expansion, assumingly by reducing T cell binding and homotypic clustering[116]. Further they could show that TILs with low ICAM1 levels persisted longer. The structural similarity of ICAM1 and VCAM1 suggests a similar effect of both. The longer persistence of $ICAM1^{low}$ TILs goes in line with our findings of low expression of VCAM1 in less exhausted TIL clusters.
Tuning the avidity of (CAR) T cells was reported to provide optimal anti-tumor activity[113,171,172] with reduced on-target off-tumor effects[173,174]. Tuning the avidity does not necessarily mean to pursue an increase in binding strength. Increased scFv affinity above a certain threshold does not increase but sometimes impair anti-tumor performance[175,176], partly because of reduced serial killing potential[177,178]. Also high avidity T cell products with severe off-target side effects have been reported[179–181]. Fine tuning of the CAR T cell avidity has the potential to increase safety and efficacy in anti-tumor treatment and can be achieved with modulation of the VCAM1 expression. We showed that reduction of VCAM1 surface expression on CAR T cells by CRISPR mediated knockout is feasible, without harming CAR expression or viability of T cells.

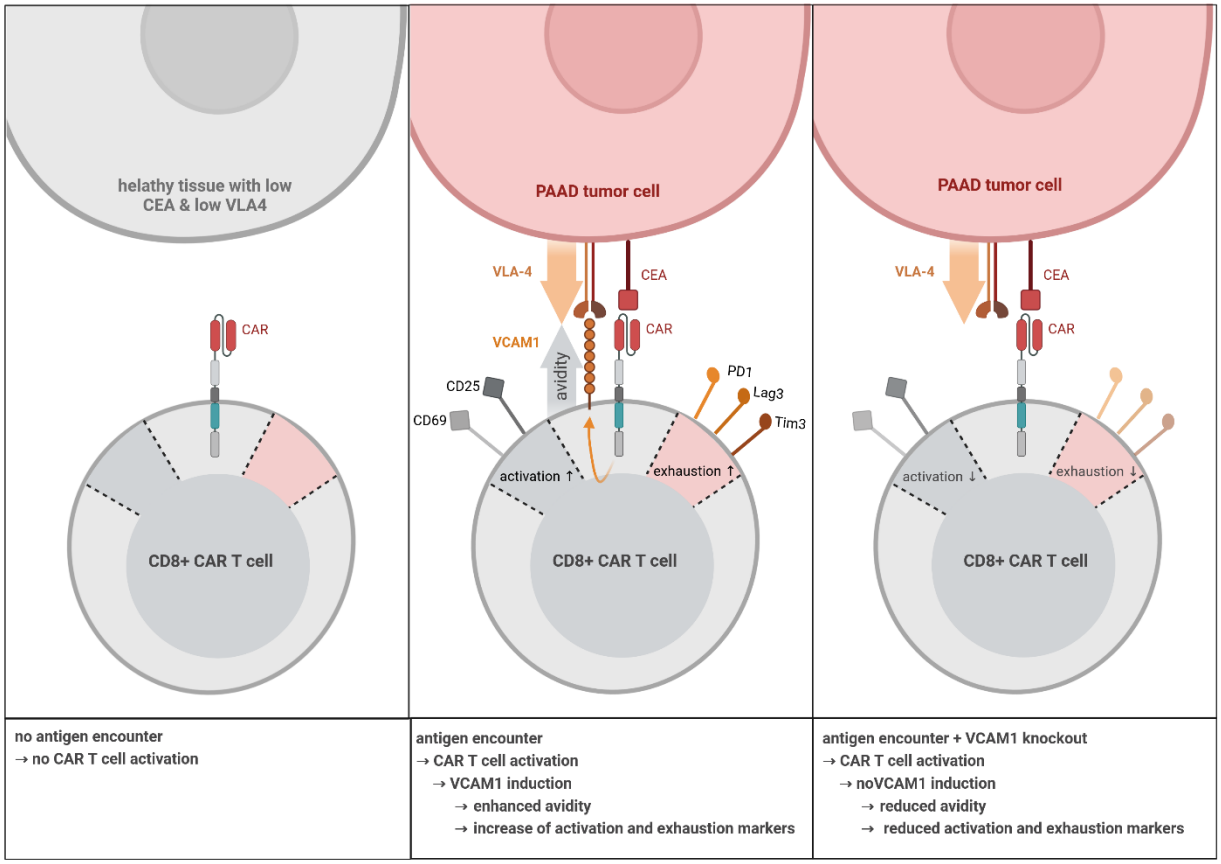

Figure 21: The non canonical role of VCAM1 - on CD8⁺ CAR T cell in contact to cancer cells. *The effect of VCAM1 in activated CD8⁺ anti-CEA CAR T cells. Upon antigen encounter the T cell receives activating stimuli via the CAR. The initial activation leads to recruitment of VCAM1 to the cell surface. With VCAM1 the avidity to the target cell is increased what leads to enhanced expression of activation and early exhaustion markers on the CD8⁺ CAR T cell. With knockout of VCAM1 the avidity to the CEA⁺ tumor cell is reduced; less activation and early exhaustion markers are expressed.*

In its canonical role, VCAM1 induces leucocyte rolling, by expression on activated endothelial cells. VCAM1 expression by CD8⁺ T cells could act vice versa to enhance the adherence of T cells to the endothelium but we found CAR T cells, inducing the expression of VCAM1 only after activation, suggesting that only after antigen encounter at the tumor site, VCAM1 on CD8⁺ CAR T cells will come into action. With our findings we describe a new role of VCAM1 (summarized in Figure 21), expressed by CD8⁺ CAR T cells, mediating avidity to tumor cells and inducing CAR T cell activation and exhaustion.

4. References

1. Siegel, R.L., Miller, K.D., Wagle, N.S., and Jemal, A. (2023). Cancer statistics, 2023. CA. Cancer J. Clin. *73*, 17–48. https://doi.org/10.3322/caac.21763.

2. Dabas, P., and Danda, A. (2023). Revolutionizing cancer treatment: a comprehensive review of CAR-T cell therapy. Med. Oncol. *40*, 275. https://doi.org/10.1007/s12032-023-02146-y.

3. Sung, H., Ferlay, J., Siegel, R.L., Laversanne, M., Soerjomataram, I., Jemal, A., and Bray, F. (2021). Global Cancer Statistics 2020: GLOBOCAN Estimates of Incidence and Mortality Worldwide for 36 Cancers in 185 Countries. CA. Cancer J. Clin. *71*, 209–249. https://doi.org/10.3322/caac.21660.

4. Grosser, R., Cherkassky, L., Chintala, N., and Adusumilli, P.S. (2019). Combination Immunotherapy with CAR T Cells and Checkpoint Blockade for the Treatment of Solid Tumors. Cancer Cell *36*, 471–482. https://doi.org/10.1016/j.ccell.2019.09.006.

5. Zhao, Y., Deng, J., Rao, S., Guo, S., Shen, J., Du, F., Wu, X., Chen, Y., Li, M., Chen, M., et al. (2022). Tumor Infiltrating Lymphocyte (TIL) Therapy for Solid Tumor Treatment: Progressions and Challenges. Cancers *14*, 4160. https://doi.org/10.3390/cancers14174160.

6. Eshhar, Z., Gross, G., Waks, T., Lustgarten, J., Bach, N., Ratner, A., Treisman, J., and Schindler, D.G. (1995). T-Bodies: Chimeric T-Cell Receptors with Antibody-Type Specificity. Methods *8*, 133–142. https://doi.org/10.1006/meth.1995.9993.

7. Srivastava, S., and Riddell, S.R. (2015). Engineering CAR-T cells: Design concepts. Trends Immunol. *36*, 494–502. https://doi.org/10.1016/j.it.2015.06.004.

8. Jayaraman, J., Mellody, M.P., Hou, A.J., Desai, R.P., Fung, A.W., Pham, A.H.T., Chen, Y.Y., and Zhao, W. (2020). CAR-T design: Elements and their synergistic function. EBioMedicine *58*, 102931. https://doi.org/10.1016/j.ebiom.2020.102931.

9. Mo, F., Duan, S., Jiang, X., Yang, X., Hou, X., Shi, W., Carlos, C.J.J., Liu, A., Yin, S., Wang, W., et al. (2021). Nanobody-based chimeric antigen receptor T cells designed by CRISPR/Cas9 technology for solid tumor immunotherapy. Signal Transduct. Target. Ther. *6*, 1–12. https://doi.org/10.1038/s41392-021-00462-1.

10. Li, D., Wang, R., Liang, T., Ren, H., Park, C., Tai, C.-H., Ni, W., Zhou, J., Mackay, S., Edmondson, E., et al. (2023). Camel nanobody-based B7-H3 CAR-T cells show high efficacy against large solid tumours. Nat. Commun. *14*, 5920. https://doi.org/10.1038/s41467-023-41631-w.

11. Patasic, L., Seifried, J., Bezler, V., Kaljanac, M., Schneider, I.C., Schmitz, H., Tondera, C., Hartmann, J., Hombach, A., Buchholz, C.J., et al. (2020). Designed Ankyrin Repeat Protein (DARPin) to target chimeric antigen receptor (CAR)-redirected T cells towards CD4+ T cells to reduce the latent HIV+ cell reservoir. Med. Microbiol. Immunol. (Berl.) *209*, 681–691. https://doi.org/10.1007/s00430-020-00692-0.

12. Hombach, A., Wieczarkowiecz, A., Marquardt, T., Heuser, C., Usai, L., Pohl, C., Seliger, B., and Abken, H. (2001). Tumor-Specific T Cell Activation by Recombinant Immunoreceptors: CD3ζ Signaling and CD28 Costimulation Are Simultaneously Required for Efficient IL-2

Secretion and Can Be Integrated Into One Combined CD28/CD3ζ Signaling Receptor Molecule. J. Immunol. *167*, 6123–6131. https://doi.org/10.4049/jimmunol.167.11.6123.

13. Murphy, K., and Weaver, C. (2018). Antigenerkennung durch B-Zell- und T-Zell-Rezeptoren. In Janeway Immunologie, K. Murphy and C. Weaver, eds. (Springer), pp. 177–220. https://doi.org/10.1007/978-3-662-56004-4_4.

14. Mezősi-Csaplár, M., Szöőr, Á., and Vereb, G. (2023). CD28 and 41BB Costimulatory Domains Alone or in Combination Differentially Influence Cell Surface Dynamics and Organization of Chimeric Antigen Receptors and Early Activation of CAR T Cells. Cancers *15*, 3081. https://doi.org/10.3390/cancers15123081.

15. Kawalekar, O.U., O'Connor, R.S., Fraietta, J.A., Guo, L., McGettigan, S.E., Posey, A.D., Patel, P.R., Guedan, S., Scholler, J., Keith, B., et al. (2016). Distinct Signaling of Coreceptors Regulates Specific Metabolism Pathways and Impacts Memory Development in CAR T Cells. Immunity *44*, 380–390. https://doi.org/10.1016/j.immuni.2016.01.021.

16. Cappell, K.M., and Kochenderfer, J.N. (2021). A comparison of chimeric antigen receptors containing CD28 versus 4-1BB costimulatory domains. Nat. Rev. Clin. Oncol. *18*, 715–727. https://doi.org/10.1038/s41571-021-00530-z.

17. Goodman, D.B., Azimi, C.S., Kearns, K., Talbot, A., Garakani, K., Garcia, J., Patel, N., Hwang, B., Lee, D., Park, E., et al. (2022). Pooled screening of CAR T cells identifies diverse immune signaling domains for next-generation immunotherapies. Sci. Transl. Med. *14*, eabm1463. https://doi.org/10.1126/scitranslmed.abm1463.

18. Weinkove, R., George, P., Dasyam, N., and McLellan, A.D. (2019). Selecting costimulatory domains for chimeric antigen receptors: functional and clinical considerations. Clin. Transl. Immunol. *8*, e1049. https://doi.org/10.1002/cti2.1049.

19. Chmielewski, M., and Abken, H. (2015). TRUCKs: the fourth generation of CARs. Expert Opin. Biol. Ther. *15*, 1145–1154. https://doi.org/10.1517/14712598.2015.1046430.

20. Park, J.H., Rivière, I., Gonen, M., Wang, X., Sénéchal, B., Curran, K.J., Sauter, C., Wang, Y., Santomasso, B., Mead, E., et al. (2018). Long-Term Follow-up of CD19 CAR Therapy in Acute Lymphoblastic Leukemia. N. Engl. J. Med. *378*, 449–459. https://doi.org/10.1056/NEJMoa1709919.

21. Li, L., Li, Q., Yan, Z.-X., Sheng, L.-S., Fu, D., Xu, P., Wang, L., and Zhao, W.-L. (2022). Transgenic expression of IL-7 regulates CAR-T cell metabolism and enhances in vivo persistence against tumor cells. Sci. Rep. *12*, 12506. https://doi.org/10.1038/s41598-022-16616-2.

22. Krenciute, G., Prinzing, B.L., Yi, Z., Wu, M.-F., Liu, H., Dotti, G., Balyasnikova, I.V., and Gottschalk, S. (2017). Transgenic Expression of IL15 Improves Antiglioma Activity of IL13Rα2-CAR T Cells but Results in Antigen Loss Variants. Cancer Immunol. Res. *5*, 571–581. https://doi.org/10.1158/2326-6066.CIR-16-0376.

23. Pang, N., Shi, J., Qin, L., Chen, A., Tang, Y., Yang, H., Huang, Y., Wu, Q., Li, X., He, B., et al. (2021). IL-7 and CCL19-secreting CAR-T cell therapy for tumors with positive glypican-3 or

mesothelin. J. Hematol. Oncol.J Hematol Oncol *14*, 118. https://doi.org/10.1186/s13045-021-01128-9.

24. Agliardi, G., Liuzzi, A.R., Hotblack, A., De Feo, D., Núñez, N., Stowe, C.L., Friebel, E., Nannini, F., Rindlisbacher, L., Roberts, T.A., et al. (2021). Intratumoral IL-12 delivery empowers CAR-T cell immunotherapy in a pre-clinical model of glioblastoma. Nat. Commun. *12*, 444. https://doi.org/10.1038/s41467-020-20599-x.

25. Chmielewski, M., and Abken, H. (2012). CAR T cells transform to trucks: chimeric antigen receptor-redirected T cells engineered to deliver inducible IL-12 modulate the tumour stroma to combat cancer. Cancer Immunol. Immunother. CII *61*, 1269–1277. https://doi.org/10.1007/s00262-012-1202-z.

26. Choi, B.D., Yu, X., Castano, A.P., Bouffard, A.A., Schmidts, A., Larson, R.C., Bailey, S.R., Boroughs, A.C., Frigault, M.J., Leick, M.B., et al. (2019). CAR-T cells secreting BiTEs circumvent antigen escape without detectable toxicity. Nat. Biotechnol. *37*, 1049–1058. https://doi.org/10.1038/s41587-019-0192-1.

27. Chen, J., Zhu, T., Jiang, G., Zeng, Q., Li, Z., and Huang, X. (2023). Target delivery of a PD-1-TREM2 scFv by CAR-T cells enhances anti-tumor efficacy in colorectal cancer. Mol. Cancer *22*, 131. https://doi.org/10.1186/s12943-023-01830-x.

28. Rafiq, S., Yeku, O.O., Jackson, H.J., Purdon, T.J., van Leeuwen, D.G., Drakes, D.J., Song, M., Miele, M.M., Li, Z., Wang, P., et al. (2018). Targeted delivery of a PD-1-blocking scFv by CAR-T cells enhances anti-tumor efficacy in vivo. Nat. Biotechnol. *36*, 847–856. https://doi.org/10.1038/nbt.4195.

29. Bourbon, E., Ghesquières, H., and Bachy, E. (2021). CAR-T cells, from principle to clinical applications. Bull. Cancer (Paris) *108*, S4–S17. https://doi.org/10.1016/j.bulcan.2021.02.017.

30. Cappell, K.M., and Kochenderfer, J.N. (2023). Long-term outcomes following CAR T cell therapy: what we know so far. Nat. Rev. Clin. Oncol. *20*, 359–371. https://doi.org/10.1038/s41571-023-00754-1.

31. Maude, S.L., Frey, N., Shaw, P.A., Aplenc, R., Barrett, D.M., Bunin, N.J., Chew, A., Gonzalez, V.E., Zheng, Z., Lacey, S.F., et al. (2014). Chimeric antigen receptor T cells for sustained remissions in leukemia. N. Engl. J. Med. *371*, 1507–1517. https://doi.org/10.1056/NEJMoa1407222.

32. Neelapu, S.S., Locke, F.L., Bartlett, N.L., Lekakis, L.J., Miklos, D.B., Jacobson, C.A., Braunschweig, I., Oluwole, O.O., Siddiqi, T., Lin, Y., et al. (2017). Axicabtagene Ciloleucel CAR T-Cell Therapy in Refractory Large B-Cell Lymphoma. N. Engl. J. Med. *377*, 2531–2544. https://doi.org/10.1056/NEJMoa1707447.

33. Melenhorst, J.J., Chen, G.M., Wang, M., Porter, D.L., Chen, C., Collins, M.A., Gao, P., Bandyopadhyay, S., Sun, H., Zhao, Z., et al. (2022). Decade-long leukaemia remissions with persistence of CD4+ CAR T cells. Nature *602*, 503–509. https://doi.org/10.1038/s41586-021-04390-6.

34. Watanabe, K., Kuramitsu, S., Posey, A.D., and June, C.H. (2018). Expanding the Therapeutic Window for CAR T Cell Therapy in Solid Tumors: The Knowns and Unknowns of CAR T Cell Biology. Front. Immunol. *9*.

35. Hong, M., Clubb, J.D., and Chen, Y.Y. (2020). Engineering CAR-T Cells for Next-Generation Cancer Therapy. Cancer Cell *38*, 473–488. https://doi.org/10.1016/j.ccell.2020.07.005.

36. Marofi, F., Motavalli, R., Safonov, V.A., Thangavelu, L., Yumashev, A.V., Alexander, M., Shomali, N., Chartrand, M.S., Pathak, Y., Jarahian, M., et al. (2021). CAR T cells in solid tumors: challenges and opportunities. Stem Cell Res. Ther. *12*, 81. https://doi.org/10.1186/s13287-020-02128-1.

37. Ryan, D.P., Hong, T.S., and Bardeesy, N. (2014). Pancreatic Adenocarcinoma. N. Engl. J. Med. *371*, 1039–1049. https://doi.org/10.1056/NEJMra1404198.

38. Vauthey, J.-N., and Dixon, E. (2009). AHPBA/SSO/SSAT Consensus Conference on Resectable and Borderline Resectable Pancreatic Cancer: Rationale and Overview of the Conference. Ann. Surg. Oncol. *16*, 1725–1726. https://doi.org/10.1245/s10434-009-0409-5.

39. Konstantinidis, I.T., Warshaw, A.L., Allen, J.N., Blaszkowsky, L.S., Castillo, C.F.-D., Deshpande, V., Hong, T.S., Kwak, E.L., Lauwers, G.Y., Ryan, D.P., et al. (2013). Pancreatic ductal adenocarcinoma: is there a survival difference for R1 resections versus locally advanced unresectable tumors? What is a "true" R0 resection? Ann. Surg. *257*, 731–736. https://doi.org/10.1097/SLA.0b013e318263da2f.

40. Zhang, C., Wang, Z., Yang, Z., Wang, M., Li, S., Li, Y., Zhang, R., Xiong, Z., Wei, Z., Shen, J., et al. (2017). Phase I Escalating-Dose Trial of CAR-T Therapy Targeting CEA+ Metastatic Colorectal Cancers. Mol. Ther. *25*, 1248–1258. https://doi.org/10.1016/j.ymthe.2017.03.010.

41. Specht, J.M., Lee, S., Turtle, C., Berger, C., Veatch, J., Gooley, T., Mullane, E., Chaney, C., Riddell, S., and Maloney, D.G. (2018). Phase I study of immunotherapy for advanced ROR1+ malignancies with autologous ROR1-specific chimeric antigen receptor-modified (CAR)-T cells. J. Clin. Oncol. *36*, TPS79–TPS79. https://doi.org/10.1200/JCO.2018.36.5_suppl.TPS79.

42. Feng, K., Guo, Y., Dai, H., Wang, Y., Li, X., Jia, H., and Han, W. (2016). Chimeric antigen receptor-modified T cells for the immunotherapy of patients with EGFR-expressing advanced relapsed/refractory non-small cell lung cancer. Sci. China Life Sci. *59*, 468–479. https://doi.org/10.1007/s11427-016-5023-8.

43. Del Bufalo, F., De Angelis, B., Caruana, I., Del Baldo, G., De Ioris, M.A., Serra, A., Mastronuzzi, A., Cefalo, M.G., Pagliara, D., Amicucci, M., et al. (2023). GD2-CART01 for Relapsed or Refractory High-Risk Neuroblastoma. N. Engl. J. Med. *388*, 1284–1295. https://doi.org/10.1056/NEJMoa2210859.

44. Brown, C.E., Alizadeh, D., Starr, R., Weng, L., Wagner, J.R., Naranjo, A., Ostberg, J.R., Blanchard, M.S., Kilpatrick, J., Simpson, J., et al. (2016). Regression of Glioblastoma after Chimeric Antigen Receptor T-Cell Therapy. N. Engl. J. Med. *375*, 2561–2569. https://doi.org/10.1056/NEJMoa1610497.

45. Maggs, L., Cattaneo, G., Dal, A.E., Moghaddam, A.S., and Ferrone, S. (2021). CAR T Cell-Based Immunotherapy for the Treatment of Glioblastoma. Front. Neurosci. *15*.

46. Brown, C.E., Hibbard, J.C., Alizadeh, D., Blanchard, M.S., Natri, H.M., Wang, D., Ostberg, J.R., Aguilar, B., Wagner, J.R., Paul, J.A., et al. (2024). Locoregional delivery of IL-13Rα2-targeting CAR-T cells in recurrent high-grade glioma: a phase 1 trial. Nat. Med. https://doi.org/10.1038/s41591-024-02875-1.

47. Choi, B.D., Gerstner, E.R., Frigault, M.J., Leick, M.B., Mount, C.W., Balaj, L., Nikiforow, S., Carter, B.S., Curry, W.T., Gallagher, K., et al. (2024). Intraventricular CARv3-TEAM-E T Cells in Recurrent Glioblastoma. N. Engl. J. Med. *0*, null. https://doi.org/10.1056/NEJMoa2314390.

48. O'Rourke, D.M., Nasrallah, M.P., Desai, A., Melenhorst, J.J., Mansfield, K., Morrissette, J.J.D., Martinez-Lage, M., Brem, S., Maloney, E., Shen, A., et al. (2017). A single dose of peripherally infused EGFRvIII-directed CAR T cells mediates antigen loss and induces adaptive resistance in patients with recurrent glioblastoma. Sci. Transl. Med. *9*, eaaa0984. https://doi.org/10.1126/scitranslmed.aaa0984.

49. Rafiq, S., Hackett, C.S., and Brentjens, R.J. (2020). Engineering strategies to overcome the current roadblocks in CAR T cell therapy. Nat. Rev. Clin. Oncol. *17*, 147–167. https://doi.org/10.1038/s41571-019-0297-y.

50. Cherkassky, L., Morello, A., Villena-Vargas, J., Feng, Y., Dimitrov, D.S., Jones, D.R., Sadelain, M., and Adusumilli, P.S. (2016). Human CAR T cells with cell-intrinsic PD-1 checkpoint blockade resist tumor-mediated inhibition. J. Clin. Invest. *126*, 3130–3144. https://doi.org/10.1172/JCI83092.

51. Srivastava, S., Furlan, S.N., Jaeger-Ruckstuhl, C.A., Sarvothama, M., Berger, C., Smythe, K.S., Garrison, S.M., Specht, J.M., Lee, S.M., Amezquita, R.A., et al. (2021). Immunogenic Chemotherapy Enhances Recruitment of CAR-T Cells to Lung Tumors and Improves Antitumor Efficacy when Combined with Checkpoint Blockade. Cancer Cell *39*, 193-208.e10. https://doi.org/10.1016/j.ccell.2020.11.005.

52. Rossetti, R., Brand, H., Lima, S.C.G., Furtado, I.P., Silveira, R.M., Fantacini, D.M.C., Covas, D.T., and de Souza, L.E.B. (2022). Combination of genetically engineered T cells and immune checkpoint blockade for the treatment of cancer. Immunother. Adv. *2*, ltac005. https://doi.org/10.1093/immadv/ltac005.

53. Cao, X., Jin, X., Zhang, X., Utsav, P., Zhang, Y., Guo, R., Lu, W., and Zhao, M. (2023). Small-Molecule Compounds Boost CAR-T Cell Therapy in Hematological Malignancies. Curr. Treat. Options Oncol. *24*, 184–211. https://doi.org/10.1007/s11864-023-01049-4.

54. Svoboda, J., Gerson, J.N., Landsburg, D.J., Chong, E.A., Barta, S.K., Dwivedy Nasta, S., Ruella, M., Hexner, E.O., Marshall, A., Leskowitz, R., et al. (2022). Interleukin-18 Secreting Autologous Anti-CD19 CAR T-Cells (huCART19-IL18) in Patients with Non-Hodgkin Lymphomas Relapsed or Refractory to Prior CAR T-Cell Therapy. Blood *140*, 4612–4614. https://doi.org/10.1182/blood-2022-162393.

55. Hamieh, M., Mansilla-Soto, J., Rivière, I., and Sadelain, M. (2023). Programming CAR T Cell Tumor Recognition: Tuned Antigen Sensing and Logic Gating. Cancer Discov. *13*, 829–843. https://doi.org/10.1158/2159-8290.CD-23-0101.

56. Tousley, A.M., Rotiroti, M.C., Labanieh, L., Rysavy, L.W., Kim, W.-J., Lareau, C., Sotillo, E., Weber, E.W., Rietberg, S.P., Dalton, G.N., et al. (2023). Co-opting signalling molecules enables logic-gated control of CAR T cells. Nature *615*, 507–516. https://doi.org/10.1038/s41586-023-05778-2.

57. Stadtmauer, E.A., Fraietta, J.A., Davis, M.M., Cohen, A.D., Weber, K.L., Lancaster, E., Mangan, P.A., Kulikovskaya, I., Gupta, M., Chen, F., et al. (2020). CRISPR-engineered T cells in patients with refractory cancer. Science *367*, eaba7365. https://doi.org/10.1126/science.aba7365.

58. Zhang, J., Hu, Y., Yang, J., Li, W., Zhang, M., Wang, Q., Zhang, L., Wei, G., Tian, Y., Zhao, K., et al. (2022). Non-viral, specifically targeted CAR-T cells achieve high safety and efficacy in B-NHL. Nature *609*, 369–374. https://doi.org/10.1038/s41586-022-05140-y.

59. Caribou's first CRISPR CAR-T impresses (2022). Nat. Biotechnol. *40*, 807–807. https://doi.org/10.1038/s41587-022-01371-6.

60. Shi, L., Meng, T., Zhao, Z., Han, J., Zhang, W., Gao, F., and Cai, J. (2017). CRISPR knock out CTLA-4 enhances the anti-tumor activity of cytotoxic T lymphocytes. Gene *636*, 36–41. https://doi.org/10.1016/j.gene.2017.09.010.

61. Dimitri, A., Herbst, F., and Fraietta, J.A. (2022). Engineering the next-generation of CAR T-cells with CRISPR-Cas9 gene editing. Mol. Cancer *21*, 78. https://doi.org/10.1186/s12943-022-01559-z.

62. Xu, X., and Qi, L.S. (2019). A CRISPR–dCas Toolbox for Genetic Engineering and Synthetic Biology. J. Mol. Biol. *431*, 34–47. https://doi.org/10.1016/j.jmb.2018.06.037.

63. Zhou, J., Yu, J., Wang, Y., Wang, H., Wang, J., Wang, Y., Yu, L., and Yan, Z. (2021). ShRNA-mediated silencing of PD-1 augments the efficacy of chimeric antigen receptor T cells on subcutaneous prostate and leukemia xenograft. Biomed. Pharmacother. *137*, 111339. https://doi.org/10.1016/j.biopha.2021.111339.

64. Reichenbach, P., Giordano Attianese, G.M.P., Ouchen, K., Cribioli, E., Triboulet, M., Ash, S., Saillard, M., Vuillefroy de Silly, R., Coukos, G., and Irving, M. (2023). A lentiviral vector for the production of T cells with an inducible transgene and a constitutively expressed tumour-targeting receptor. Nat. Biomed. Eng. *7*, 1063–1080. https://doi.org/10.1038/s41551-023-01013-5.

65. Harrer, D.C., Bezler, V., Hartley, J., Herr, W., and Abken, H. (2023). IRF4 downregulation improves sensitivity and endurance of CAR T cell functional capacities. Front. Immunol. *14*, 1185618. https://doi.org/10.3389/fimmu.2023.1185618.

66. Monks, C.R.F., Freiberg, B.A., Kupfer, H., Sciaky, N., and Kupfer, A. (1998). Three-dimensional segregation of supramolecular activation clusters in T cells. Nature *395*, 82–86. https://doi.org/10.1038/25764.

67. Roda-Navarro, P., and Álvarez-Vallina, L. (2020). Understanding the Spatial Topology of Artificial Immunological Synapses Assembled in T Cell-Redirecting Strategies: A Major Issue in Cancer Immunotherapy. Front. Cell Dev. Biol. *7*.

68. Huppa, J.B., and Davis, M.M. (2003). T-cell-antigen recognition and the immunological synapse. Nat. Rev. Immunol. *3*, 973–983. https://doi.org/10.1038/nri1245.

69. Friedl, P., den Boer, A.T., and Gunzer, M. (2005). Tuning immune responses: diversity and adaptation of the immunological synapse. Nat. Rev. Immunol. *5*, 532–545. https://doi.org/10.1038/nri1647.

70. Hogg, N., Patzak, I., and Willenbrock, F. (2011). The insider's guide to leukocyte integrin signalling and function. Nat. Rev. Immunol. *11*, 416–426. https://doi.org/10.1038/nri2986.

71. Gérard, A., Cope, A.P., Kemper, C., Alon, R., and Köchl, R. (2021). LFA-1 in T cell priming, differentiation, and effector functions. Trends Immunol. *42*, 706–722. https://doi.org/10.1016/j.it.2021.06.004.

72. Mittelbrunn, M., Molina, A., Escribese, M.M., Yáñez-Mó, M., Escudero, E., Ursa, Á., Tejedor, R., Mampaso, F., and Sánchez-Madrid, F. (2004). VLA-4 integrin concentrates at the peripheral supramolecular activation complex of the immune synapse and drives T helper 1 responses. Proc. Natl. Acad. Sci. *101*, 11058–11063. https://doi.org/10.1073/pnas.0307927101.

73. Huse, M. (2012). Microtubule-organizing center polarity and the immunological synapse: protein kinase C and beyond. Front. Immunol. *3*.

74. Hogg, N., Laschinger, M., Giles, K., and McDowall, A. (2003). T-cell integrins: more than just sticking points. J. Cell Sci. *116*, 4695–4705. https://doi.org/10.1242/jcs.00876.

75. Johnson, K.G., Bromley, S.K., Dustin, M.L., and Thomas, M.L. (2000). A supramolecular basis for CD45 tyrosine phosphatase regulation in sustained T cell activation. Proc. Natl. Acad. Sci. *97*, 10138–10143. https://doi.org/10.1073/pnas.97.18.10138.

76. Allenspach, E.J., Cullinan, P., Tong, J., Tang, Q., Tesciuba, A.G., Cannon, J.L., Takahashi, S.M., Morgan, R., Burkhardt, J.K., and Sperling, A.I. (2001). ERM-Dependent Movement of CD43 Defines a Novel Protein Complex Distal to the Immunological Synapse. Immunity *15*, 739–750. https://doi.org/10.1016/S1074-7613(01)00224-2.

77. Barden, M., Holzinger, A., Velas, L., Mezősi-Csaplár, M., Szöőr, Á., Vereb, G., Schütz, G.J., Hombach, A.A., and Abken, H. (2023). CAR and TCR form individual signaling synapses and do not cross-activate, however, can co-operate in T cell activation. Front. Immunol. *14*.

78. Muller, Y.D., Nguyen, D.P., Ferreira, L.M.R., Ho, P., Raffin, C., Valencia, R.V.B., Congrave-Wilson, Z., Roth, T.L., Eyquem, J., Van Gool, F., et al. (2021). The CD28-Transmembrane Domain Mediates Chimeric Antigen Receptor Heterodimerization With CD28. Front. Immunol. *12*, 639818. https://doi.org/10.3389/fimmu.2021.639818.

79. Park, S., Shevlin, E., Vedvyas, Y., Zaman, M., Park, S., Hsu, Y.-M.S., Min, I.M., and Jin, M.M. (2017). Micromolar affinity CAR T cells to ICAM-1 achieves rapid tumor elimination while avoiding systemic toxicity. Sci. Rep. *7*, 14366. https://doi.org/10.1038/s41598-017-14749-3.

80. Harjunpää, H., Llort Asens, M., Guenther, C., and Fagerholm, S.C. (2019). Cell Adhesion Molecules and Their Roles and Regulation in the Immune and Tumor Microenvironment. Front. Immunol. *10*.

81. Abram, C.L., and Lowell, C.A. (2009). The Ins and Outs of Leukocyte Integrin Signaling. Annu. Rev. Immunol. *27*, 339–362. https://doi.org/10.1146/annurev.immunol.021908.132554.

82. Mantovani, A., and Dejana, E. (1998). Endothelium. In Encyclopedia of Immunology (Second Edition), P. J. Delves, ed. (Elsevier), pp. 802–806. https://doi.org/10.1006/rwei.1999.0212.

83. Cybulsky, M.I., Fries, J.W., Williams, A.J., Sultan, P., Eddy, R., Byers, M., Shows, T., Gimbrone, M.A., and Collins, T. (1991). Gene structure, chromosomal location, and basis for alternative mRNA splicing of the human VCAM1 gene. Proc. Natl. Acad. Sci. *88*, 7859–7863. https://doi.org/10.1073/pnas.88.17.7859.

84. Activated endothelium binds lymphocytes through a novel binding site in the alternately spliced domain of vascular cell adhesion molecule-1 (1992). J. Exp. Med. *176*, 99–107.

85. Vonderheide, R.H., and Springer, T.A. (1992). Lymphocyte adhesion through very late antigen 4: evidence for a novel binding site in the alternatively spliced domain of vascular cell adhesion molecule 1 and an additional alpha 4 integrin counter-receptor on stimulated endothelium. J. Exp. Med. *175*, 1433–1442. https://doi.org/10.1084/jem.175.6.1433.

86. Osborn, L., Hession, C., Tizard, R., Vassallo, C., Luhowskyj, S., Chi-Rosso, G., and Lobb, R. (1989). Direct expression cloning of vascular cell adhesion molecule 1, a cytokine-induced endothelial protein that binds to lymphocytes. Cell *59*, 1203–1211. https://doi.org/10.1016/0092-8674(89)90775-7.

87. Sharma, R., Sharma, R., Khaket, T.P., Dutta, C., Chakraborty, B., and Mukherjee, T.K. (2017). Breast cancer metastasis: Putative therapeutic role of vascular cell adhesion molecule-1. Cell. Oncol. *40*, 199–208. https://doi.org/10.1007/s13402-017-0324-x.

88. Kong, D.-H., Kim, Y.K., Kim, M.R., Jang, J.H., and Lee, S. (2018). Emerging Roles of Vascular Cell Adhesion Molecule-1 (VCAM-1) in Immunological Disorders and Cancer. Int. J. Mol. Sci. *19*, 1057. https://doi.org/10.3390/ijms19041057.

89. Pinho, S., Wei, Q., Maryanovich, M., Zhang, D., Balandrán, J.C., Pierce, H., Nakahara, F., Di Staulo, A., Bartholdy, B.A., Xu, J., et al. (2022). VCAM1 confers innate immune tolerance on haematopoietic and leukaemic stem cells. Nat. Cell Biol. *24*, 290–298. https://doi.org/10.1038/s41556-022-00849-4.

90. Diaz, L.S., Foster, H., Stone, M.R., Fujimura, S., Relman, D.A., and Levy, J.A. (2005). VCAM-1 Expression on CD8+ Cells Correlates with Enhanced Anti-HIV Suppressing Activity. J. Immunol. *174*, 1574–1579. https://doi.org/10.4049/jimmunol.174.3.1574.

91. Gurtner, G.C., Davis, V., Li, H., McCoy, M.J., Sharpe, A., and Cybulsky, M.I. (1995). Targeted disruption of the murine VCAM1 gene: essential role of VCAM-1 in chorioallantoic fusion and placentation. Genes Dev. *9*, 1–14. https://doi.org/10.1101/gad.9.1.1.

92. Barreiro, O., Yáñez-Mó, M., Serrador, J.M., Montoya, M.C., Vicente-Manzanares, M., Tejedor, R., Furthmayr, H., and Sánchez-Madrid, F. (2002). Dynamic interaction of VCAM-1

and ICAM-1 with moesin and ezrin in a novel endothelial docking structure for adherent leukocytes. J. Cell Biol. *157*, 1233–1245. https://doi.org/10.1083/jcb.200112126.

93. Marchese, M.E., Berdnikovs, S., and Cook-Mills, J.M. (2012). Distinct Sites within the Vascular Cell Adhesion Molecule-1 (VCAM-1) Cytoplasmic Domain Regulate VCAM-1 Activation of Calcium Fluxes versus Rac1 during Leukocyte Transendothelial Migration. Biochemistry *51*, 8235–8246. https://doi.org/10.1021/bi300925r.

94. Deem, T.L., and Cook-Mills, J.M. (2004). Vascular cell adhesion molecule 1 (VCAM-1) activation of endothelial cell matrix metalloproteinases: role of reactive oxygen species. Blood *104*, 2385–2393. https://doi.org/10.1182/blood-2004-02-0665.

95. blood-brain-barrier-immune-cell-transmigration-vcam-1-cd106-signaling-pathways-rnd-systems.png (AVIF-Grafik, 770 × 927 Pixel) - Skaliert (78%) https://resources.rndsystems.com/images/Pathways/full-pathway-image/blood-brain-barrier-immune-cell-transmigration-vcam-1-cd106-signaling-pathways-rnd-systems.png.

96. Deem, T.L., Abdala-Valencia, H., and Cook-Mills, J.M. (2007). VCAM-1 Activation of Endothelial Cell Protein Tyrosine Phosphatase 1B1. J. Immunol. *178*, 3865–3873. https://doi.org/10.4049/jimmunol.178.6.3865.

97. Blank, C.U., Haining, W.N., Held, W., Hogan, P.G., Kallies, A., Lugli, E., Lynn, R.C., Philip, M., Rao, A., Restifo, N.P., et al. (2019). Defining "T cell exhaustion." Nat. Rev. Immunol. *19*, 665–674. https://doi.org/10.1038/s41577-019-0221-9.

98. Delgoffe, G.M., Xu, C., Mackall, C.L., Green, M.R., Gottschalk, S., Speiser, D.E., Zehn, D., and Beavis, P.A. (2021). The role of exhaustion in CAR T cell therapy. Cancer Cell *39*, 885–888. https://doi.org/10.1016/j.ccell.2021.06.012.

99. Dolina, J.S., Van Braeckel-Budimir, N., Thomas, G.D., and Salek-Ardakani, S. (2021). CD8+ T Cell Exhaustion in Cancer. Front. Immunol. *12*.

100. Role of TCF-1 in differentiation, exhaustion, and memory of CD8+ T cells: A review https://doi.org/10.1096/fj.202002566R.

101. Wherry, E.J., and Kurachi, M. (2015). Molecular and cellular insights into T cell exhaustion. Nat. Rev. Immunol. *15*, 486–499. https://doi.org/10.1038/nri3862.

102. Khan, O., Giles, J.R., McDonald, S., Manne, S., Ngiow, S.F., Patel, K.P., Werner, M.T., Huang, A.C., Alexander, K.A., Wu, J.E., et al. (2019). TOX transcriptionally and epigenetically programs CD8+ T cell exhaustion. Nature *571*, 211–218. https://doi.org/10.1038/s41586-019-1325-x.

103. He, X., and Xu, C. (2020). Immune checkpoint signaling and cancer immunotherapy. Cell Res. *30*, 660–669. https://doi.org/10.1038/s41422-020-0343-4.

104. Hosseinkhani, N., Derakhshani, A., Kooshkaki, O., Abdoli Shadbad, M., Hajiasgharzadeh, K., Baghbanzadeh, A., Safarpour, H., Mokhtarzadeh, A., Brunetti, O., Yue, S.C., et al. (2020). Immune Checkpoints and CAR-T Cells: The Pioneers in Future Cancer Therapies? Int. J. Mol. Sci. *21*, 8305. https://doi.org/10.3390/ijms21218305.

105. Kozłowski, M., Borzyszkowska, D., and Cymbaluk-Płoska, A. (2022). The Role of TIM-3 and LAG-3 in the Microenvironment and Immunotherapy of Ovarian Cancer. Biomedicines *10*, 2826. https://doi.org/10.3390/biomedicines10112826.

106. Chamoto, K., Yaguchi, T., Tajima, M., and Honjo, T. (2023). Insights from a 30-year journey: function, regulation and therapeutic modulation of PD1. Nat. Rev. Immunol. *23*, 682–695. https://doi.org/10.1038/s41577-023-00867-9.

107. Sun, Q., Hong, Z., Zhang, C., Wang, L., Han, Z., and Ma, D. (2023). Immune checkpoint therapy for solid tumours: clinical dilemmas and future trends. Signal Transduct. Target. Ther. *8*, 1–26. https://doi.org/10.1038/s41392-023-01522-4.

108. Klebanoff, C.A., Gattinoni, L., Torabi-Parizi, P., Kerstann, K., Cardones, A.R., Finkelstein, S.E., Palmer, D.C., Antony, P.A., Hwang, S.T., Rosenberg, S.A., et al. (2005). Central memory self/tumor-reactive CD8+ T cells confer superior antitumor immunity compared with effector memory T cells. Proc. Natl. Acad. Sci. U. S. A. *102*, 9571–9576. https://doi.org/10.1073/pnas.0503726102.

109. Jung, I.-Y., Noguera-Ortega, E., Bartoszek, R., Collins, S.M., Williams, E., Davis, M., Jadlowsky, J.K., Plesa, G., Siegel, D.L., Chew, A., et al. (2023). Tissue-resident memory CAR T cells with stem-like characteristics display enhanced efficacy against solid and liquid tumors. Cell Rep. Med. *4*. https://doi.org/10.1016/j.xcrm.2023.101053.

110. Riegel, D., Romero-Fernández, E., Simon, M., Adenugba, A.R., Singer, K., Mayr, R., Weber, F., Kleemann, M., Imbusch, C.D., Kreutz, M., et al. (2023). Integrated single-cell profiling dissects cell-state-specific enhancer landscapes of human tumor-infiltrating CD8+ T cells. Mol. Cell *83*, 622-636.e10. https://doi.org/10.1016/j.molcel.2022.12.029.

111. Chang, J.T., Wherry, E.J., and Goldrath, A.W. (2014). Molecular regulation of effector and memory T cell differentiation. Nat. Immunol. *15*, 1104–1115. https://doi.org/10.1038/ni.3031.

112. Lugli, E., Galletti, G., Boi, S.K., and Youngblood, B.A. (2020). Stem, Effector, and Hybrid States of Memory CD8+ T Cells. Trends Immunol. *41*, 17–28. https://doi.org/10.1016/j.it.2019.11.004.

113. Larson, R.C., Kann, M.C., Bailey, S.R., Haradhvala, N.J., Llopis, P.M., Bouffard, A.A., Scarfó, I., Leick, M.B., Grauwet, K., Berger, T.R., et al. (2022). CAR T cell killing requires the IFNγR pathway in solid but not liquid tumours. Nature *604*, 563–570. https://doi.org/10.1038/s41586-022-04585-5.

114. Greenman, R., Pizem, Y., Haus-Cohen, M., Goor, A., Horev, G., Denkberg, G., Sinik, K., Elbaz, Y., Bronner, V., Levin, A.G., et al. (2021). Shaping Functional Avidity of CAR T Cells: Affinity, Avidity, and Antigen Density That Regulate Response. Mol. Cancer Ther. *20*, 872–884. https://doi.org/10.1158/1535-7163.MCT-19-1109.

115. Philip, M., Fairchild, L., Sun, L., Horste, E.L., Camara, S., Shakiba, M., Scott, A.C., Viale, A., Lauer, P., Merghoub, T., et al. (2017). Chromatin states define tumour-specific T cell dysfunction and reprogramming. Nature *545*, 452–456. https://doi.org/10.1038/nature22367.

116. Lin, C.-P., Levy, P.L., Alflen, A., Apriamashvili, G., Ligtenberg, M.A., Vredevoogd, D.W., Bleijerveld, O.B., Alkan, F., Malka, Y., Hoekman, L., et al. (2024). Multimodal stimulation screens reveal unique and shared genes limiting T cell fitness. Cancer Cell. https://doi.org/10.1016/j.ccell.2024.02.016.

117. Fellmann, C., Hoffmann, T., Sridhar, V., Hopfgartner, B., Muhar, M., Roth, M., Lai, D.Y., Barbosa, I.A.M., Kwon, J.S., Guan, Y., et al. (2013). An Optimized microRNA Backbone for Effective Single-Copy RNAi. Cell Rep. *5*, 1704–1713. https://doi.org/10.1016/j.celrep.2013.11.020.

118. Choi, J.-G., Bharaj, P., Abraham, S., Ma, H., Yi, G., Ye, C., Dang, Y., Manjunath, N., Wu, H., and Shankar, P. (2015). Multiplexing Seven miRNA-Based shRNAs to Suppress HIV Replication. Mol. Ther. *23*, 310–320. https://doi.org/10.1038/mt.2014.205.

119. Weijtens, M., Willemsen, R., Hart, E., and Bolhuis, R. (1998). A retroviral vector system 'STITCH' in combination with an optimized single chain antibody chimeric receptor gene structure allows efficient gene transduction and expression in human T lymphocytes. Gene Ther. *5*, 1195–1203. https://doi.org/10.1038/sj.gt.3300696.

120. Hombach, A.A., and Abken, H. (2011). Costimulation by chimeric antigen receptors revisited the T cell antitumor response benefits from combined CD28-OX40 signalling. Int. J. Cancer *129*, 2935–2944. https://doi.org/10.1002/ijc.25960.

121. Tan, M.H., Nowak, N.J., Loor, R., Ochi, H., Sandberg, A.A., Lopez, C., Pickren, J.W., Berjian, R., Douglass, H.O., and Chu, T.M. (1986). Characterization of a New Primary Human Pancreatic Tumor Line. Cancer Invest. *4*, 15–23. https://doi.org/10.3109/07357908609039823.

122. Boukamp, P., Petrussevska, R.T., Breitkreutz, D., Hornung, J., Markham, A., and Fusenig, N.E. (1988). Normal keratinization in a spontaneously immortalized aneuploid human keratinocyte cell line. J. Cell Biol. *106*, 761–771. https://doi.org/10.1083/jcb.106.3.761.

123. DuBridge, R.B., Tang, P., Hsia, H.C., Leong, P.M., Miller, J.H., and Calos, M.P. (1987). Analysis of mutation in human cells by using an Epstein-Barr virus shuttle system. Mol. Cell. Biol. *7*, 379–387. https://doi.org/10.1128/mcb.7.1.379-387.1987.

124. Zhu, C., Liu, J., He, B., Qu, X., and Peng, D. (2019). The role of human immortal skin keratinocytes-acellular dermal matrix scaffold in skin repair and regeneration. J. Cell. Biochem. *120*, 12182–12191. https://doi.org/10.1002/jcb.28588.

125. Zhao, Z., Condomines, M., van der Stegen, S.J.C., Perna, F., Kloss, C.C., Gunset, G., Plotkin, J., and Sadelain, M. (2015). Structural Design of Engineered Costimulation Determines Tumor Rejection Kinetics and Persistence of CAR T Cells. Cancer Cell *28*, 415–428. https://doi.org/10.1016/j.ccell.2015.09.004.

126. Mahnke, Y.D., Brodie, T.M., Sallusto, F., Roederer, M., and Lugli, E. (2013). The who's who of T-cell differentiation: Human memory T-cell subsets. Eur. J. Immunol. *43*, 2797–2809. https://doi.org/10.1002/eji.201343751.

127. Bardhan, K., Aksoylar, H.-I., Le Bourgeois, T., Strauss, L., Weaver, J.D., Delcuze, B., Charest, A., Patsoukis, N., and Boussiotis, V.A. (2019). Phosphorylation of PD-1-Y248 is a marker of

PD-1-mediated inhibitory function in human T cells. Sci. Rep. *9*, 17252. https://doi.org/10.1038/s41598-019-53463-0.

128. Patel, U., Abernathy, J., Savani, B.N., Oluwole, O., Sengsayadeth, S., and Dholaria, B. (2022). CAR T cell therapy in solid tumors: A review of current clinical trials. eJHaem *3*, 24–31. https://doi.org/10.1002/jha2.356.

129. Boccalatte, F., Mina, R., Aroldi, A., Leone, S., Suryadevara, C.M., Placantonakis, D.G., and Bruno, B. (2022). Advances and Hurdles in CAR T Cell Immune Therapy for Solid Tumors. Cancers *14*, 5108. https://doi.org/10.3390/cancers14205108.

130. Yan, T., Zhu, L., and Chen, J. (2023). Current advances and challenges in CAR T-Cell therapy for solid tumors: tumor-associated antigens and the tumor microenvironment. Exp. Hematol. Oncol. *12*, 14. https://doi.org/10.1186/s40164-023-00373-7.

131. Guzman, G., Reed, M.R., Bielamowicz, K., Koss, B., and Rodriguez, A. (2023). CAR-T Therapies in Solid Tumors: Opportunities and Challenges. Curr. Oncol. Rep. *25*, 479–489. https://doi.org/10.1007/s11912-023-01380-x.

132. Ottaviano, G., Georgiadis, C., Gkazi, S.A., Syed, F., Zhan, H., Etuk, A., Preece, R., Chu, J., Kubat, A., Adams, S., et al. (2022). Phase 1 clinical trial of CRISPR-engineered CAR19 universal T cells for treatment of children with refractory B cell leukemia. Sci. Transl. Med. *14*, eabq3010. https://doi.org/10.1126/scitranslmed.abq3010.

133. Wu, Y., Jiang, M., Qin, Y., Lin, F., and Lai, M. (2018). Single and combined use of neutrophil–lymphocyte ratio, platelet–lymphocyte ratio and carcinoembryonic antigen in diagnosing gastric cancer. Clin. Chim. Acta *481*, 20–24. https://doi.org/10.1016/j.cca.2018.02.027.

134. Grunnet, M., and Sorensen, J.B. (2012). Carcinoembryonic antigen (CEA) as tumor marker in lung cancer. Lung Cancer *76*, 138–143. https://doi.org/10.1016/j.lungcan.2011.11.012.

135. Tang, S., Zhou, F., Sun, Y., Wei, L., Zhu, S., Yang, R., Huang, Y., and Yang, J. (2016). CEA in breast ductal secretions as a promising biomarker for the diagnosis of breast cancer: a systematic review and meta-analysis. Breast Cancer *23*, 813–819. https://doi.org/10.1007/s12282-016-0680-9.

136. Khushk, M., Khan, A., Rehman, A., Sheraz, S., Tunio, Y.M., Rehman, K., Rehman, D., Ahmed, M., Abbas, K., and Khan, M.E. (2021). The Role of Tumor Markers: Carcinoembryonic Antigen and Cancer Antigen 15-3 in Patients With Breast Cancer. Cureus *13*, e16298. https://doi.org/10.7759/cureus.16298.

137. Hall, C., Clarke, L., Pal, A., Buchwald, P., Eglinton, T., Wakeman, C., and Frizelle, F. (2019). A Review of the Role of Carcinoembryonic Antigen in Clinical Practice. Ann. Coloproctology *35*, 294–305. https://doi.org/10.3393/ac.2019.11.13.

138. Aldilaijan, A.F., Kim, Y.I., Kim, C.W., Yoon, Y.S., Park, I.J., Lim, S.-B., Kim, J., Ro, J.-S., and Kim, J.C. (2023). Clinical implication of tissue carcinoembryonic antigen expression in association with serum carcinoembryonic antigen in colorectal cancer. Sci. Rep. *13*, 7616. https://doi.org/10.1038/s41598-023-34855-9.

139. Holzinger, A., and Abken, H. (2017). CAR T cells targeting solid tumors: carcinoembryonic antigen (CEA) proves to be a safe target. Cancer Immunol. Immunother. CII *66*, 1505–1507. https://doi.org/10.1007/s00262-017-2045-4.

140. Walsh, G.M., Symon, F.A., Lazarovils, A.L., and Wardlaw, A.J. (1996). Integrin alpha 4 beta 7 mediates human eosinophil interaction with MAdCAM-1, VCAM-1 and fibronectin. Immunology *89*, 112–119. https://doi.org/10.1046/j.1365-2567.1996.d01-713.x.

141. Costa, M.F.S., Bornstein, V.U., Candéa, A.L., Henriques-Pons, A., Henriques, M.G., and Penido, C. (2012). CCL25 induces $\alpha_4\beta_7$ integrin-dependent migration of IL-17$^+$ γδ T lymphocytes during an allergic reaction. Eur. J. Immunol. *42*, 1250–1260. https://doi.org/10.1002/eji.201142021.

142. Barthel, S.R., Annis, D.S., Mosher, D.F., and Johansson, M.W. (2006). Differential engagement of modules 1 and 4 of vascular cell adhesion molecule-1 (CD106) by integrins alpha4beta1 (CD49d/29) and alphaMbeta2 (CD11b/18) of eosinophils. J. Biol. Chem. *281*, 32175–32187. https://doi.org/10.1074/jbc.M600943200.

143. Grayson, M.H., Van der Vieren, M., Sterbinsky, S.A., Michael Gallatin, W., Hoffman, P.A., Staunton, D.E., and Bochner, B.S. (1998). alphadbeta2 integrin is expressed on human eosinophils and functions as an alternative ligand for vascular cell adhesion molecule 1 (VCAM-1). J. Exp. Med. *188*, 2187–2191. https://doi.org/10.1084/jem.188.11.2187.

144. Schlesinger, M., and Bendas, G. (2015). Vascular cell adhesion molecule-1 (VCAM-1)-An increasing insight into its role in tumorigenicity and metastasis: VCAM-1 in tumorigenicity. Int. J. Cancer *136*, 2504–2514. https://doi.org/10.1002/ijc.28927.

145. Tang, Z., Kang, B., Li, C., Chen, T., and Zhang, Z. (2019). GEPIA2: an enhanced web server for large-scale expression profiling and interactive analysis. Nucleic Acids Res. *47*, W556–W560. https://doi.org/10.1093/nar/gkz430.

146. Li, R., Ma, C., Cai, H., and Chen, W. (2020). The CAR T-Cell Mechanoimmunology at a Glance. Adv. Sci. *7*, 2002628. https://doi.org/10.1002/advs.202002628.

147. Yun, K., Siegler, E.L., and Kenderian, S.S. (2023). Who wins the combat, CAR or TCR? Leukemia *37*, 1953–1962. https://doi.org/10.1038/s41375-023-01976-z.

148. Salter, A.I., Ivey, R.G., Kennedy, J.J., Voillet, V., Rajan, A., Alderman, E.J., Voytovich, U.J., Lin, C., Sommermeyer, D., Liu, L., et al. (2018). Phosphoproteomic analysis of chimeric antigen receptor signaling reveals kinetic and quantitative differences that affect cell function. Sci. Signal. *11*, eaat6753. https://doi.org/10.1126/scisignal.aat6753.

149. Abken, H. (2016). Costimulation Engages the Gear in Driving CARs. Immunity *44*, 214–216. https://doi.org/10.1016/j.immuni.2016.02.001.

150. Singh, R., Kim, Y.-H., Lee, S.-J., Eom, H.-S., and Choi, B.K. (2024). 4-1BB immunotherapy: advances and hurdles. Exp. Mol. Med. *56*, 32–39. https://doi.org/10.1038/s12276-023-01136-4.

151. Sabbagh, L., Pulle, G., Liu, Y., Tsitsikov, E.N., and Watts, T.H. (2008). ERK-Dependent Bim Modulation Downstream of the 4-1BB-TRAF1 Signaling Axis Is a Critical Mediator of CD8 T

Cell Survival In Vivo1. J. Immunol. *180*, 8093–8101. https://doi.org/10.4049/jimmunol.180.12.8093.

152. Linhares, A.D.S., Sharma, S., Steinberger, P., and Leitner, J. (2024). Transcriptional reprogramming via signaling domains of CD2, CD28, and 4-1BB. iScience *27*. https://doi.org/10.1016/j.isci.2024.109267.

153. Manni, S., Del Bufalo, F., Merli, P., Silvestris, D.A., Guercio, M., Caruso, S., Reddel, S., Iaffaldano, L., Pezzella, M., Di Cecca, S., et al. (2023). Neutralizing IFNγ improves safety without compromising efficacy of CAR-T cell therapy in B-cell malignancies. Nat. Commun. *14*, 3423. https://doi.org/10.1038/s41467-023-38723-y.

154. Bailey, S.R., Vatsa, S., Larson, R.C., Bouffard, A.A., Scarfò, I., Kann, M.C., Berger, T.R., Leick, M.B., Wehrli, M., Schmidts, A., et al. (2022). Blockade or Deletion of IFNγ Reduces Macrophage Activation without Compromising CAR T-cell Function in Hematologic Malignancies. Blood Cancer Discov. *3*, 136–153. https://doi.org/10.1158/2643-3230.BCD-21-0181.

155. Nezlin, R., and Ghetie, V. (2004). Interactions of Immunoglobulins Outside the Antigen-Combining Site. In Advances in Immunology (Academic Press), pp. 155–215. https://doi.org/10.1016/S0065-2776(04)82004-2.

156. Li, W., Prabakaran, P., Chen, W., Zhu, Z., Feng, Y., and Dimitrov, D.S. (2016). Antibody Aggregation: Insights from Sequence and Structure. Antibodies *5*, 19. https://doi.org/10.3390/antib5030019.

157. Wang, Y., Gao, Y., Niu, C., Wang, B., Zhao, S., Roex, G., Qian, J., Qie, J., Chen, L., Yi, C., et al. (2022). Chimeric antigen receptor clustering via cysteines enhances T-cell efficacy against tumor. Cancer Immunol. Immunother. *71*, 2801–2814. https://doi.org/10.1007/s00262-022-03195-4.

158. Majzner, R.G., Rietberg, S.P., Sotillo, E., Dong, R., Vachharajani, V.T., Labanieh, L., Myklebust, J.H., Kadapakkam, M., Weber, E.W., Tousley, A.M., et al. (2020). Tuning the Antigen Density Requirement for CAR T-cell Activity. Cancer Discov. *10*, 702–723. https://doi.org/10.1158/2159-8290.CD-19-0945.

159. Schmidl, C., Delacher, M., Huehn, J., and Feuerer, M. (2018). Epigenetic mechanisms regulating T-cell responses. J. Allergy Clin. Immunol. *142*, 728–743. https://doi.org/10.1016/j.jaci.2018.07.014.

160. Macallan, D.C., Busch, R., and Asquith, B. (2019). Current estimates of T cell kinetics in humans. Curr. Opin. Syst. Biol. *18*, 77–86. https://doi.org/10.1016/j.coisb.2019.10.002.

161. Hu, G., and Wang, S. (2017). Tumor-infiltrating CD45RO+ Memory T Lymphocytes Predict Favorable Clinical Outcome in Solid Tumors. Sci. Rep. *7*, 10376. https://doi.org/10.1038/s41598-017-11122-2.

162. Wu, K., Zheng, X., Yao, Z., Zheng, Z., Huang, W., Mu, X., Sun, F., Liu, Z., and Zheng, J. (2021). Accumulation of CD45RO+CD8+ T cells is a diagnostic and prognostic biomarker for clear cell renal cell carcinoma. Aging *13*, 14304–14321. https://doi.org/10.18632/aging.203045.

163. Sun, X., Zhai, J., Sun, B., Parra, E.R., Jiang, M., Ma, W., Wang, J., Kang, A.M., Kannan, K., Pandurengan, R., et al. (2022). Effector memory cytotoxic CD3+/CD8+/CD45RO+ T cells are predictive of good survival and a lower risk of recurrence in triple-negative breast cancer. Mod. Pathol. *35*, 601–608. https://doi.org/10.1038/s41379-021-00973-w.

164. Buggert, M., Price, D.A., Mackay, L.K., and Betts, M.R. (2023). Human circulating and tissue-resident memory CD8+ T cells. Nat. Immunol. *24*, 1076–1086. https://doi.org/10.1038/s41590-023-01538-6.

165. Förster, R., Davalos-Misslitz, A.C., and Rot, A. (2008). CCR7 and its ligands: balancing immunity and tolerance. Nat. Rev. Immunol. *8*, 362–371. https://doi.org/10.1038/nri2297.

166. Bill, C.A., Allen, C.M., and Vines, C.M. (2022). C-C Chemokine Receptor 7 in Cancer. Cells *11*, 656. https://doi.org/10.3390/cells11040656.

167. Betts, M.R., Brenchley, J.M., Price, D.A., De Rosa, S.C., Douek, D.C., Roederer, M., and Koup, R.A. (2003). Sensitive and viable identification of antigen-specific CD8+ T cells by a flow cytometric assay for degranulation. J. Immunol. Methods *281*, 65–78. https://doi.org/10.1016/S0022-1759(03)00265-5.

168. Cai, Z., Kishimoto, H., Brunmark, A., Jackson, M.R., Peterson, P.A., and Sprent, J. (1997). Requirements for Peptide-induced T Cell Receptor Downregulation on Naive CD8+ T Cells. J. Exp. Med. *185*, 641–652. https://doi.org/10.1084/jem.185.4.641.

169. Huang, J.-F., Yang, Y., Sepulveda, H., Shi, W., Hwang, I., Peterson, P.A., Jackson, M.R., Sprent, J., and Cai, Z. (1999). TCR-Mediated Internalization of Peptide-MHC Complexes Acquired by T Cells. Science *286*, 952–954. https://doi.org/10.1126/science.286.5441.952.

170. Li, W., Qiu, S., Chen, J., Jiang, S., Chen, W., Jiang, J., Wang, F., Si, W., Shu, Y., Wei, P., et al. (2020). Chimeric Antigen Receptor Designed to Prevent Ubiquitination and Downregulation Showed Durable Antitumor Efficacy. Immunity *53*, 456-470.e6. https://doi.org/10.1016/j.immuni.2020.07.011.

171. Schmidt, J., Chiffelle, J., Perez, M.A.S., Magnin, M., Bobisse, S., Arnaud, M., Genolet, R., Cesbron, J., Barras, D., Navarro Rodrigo, B., et al. (2023). Neoantigen-specific CD8 T cells with high structural avidity preferentially reside in and eliminate tumors. Nat. Commun. *14*, 3188. https://doi.org/10.1038/s41467-023-38946-z.

172. Leick, M.B., Silva, H., Scarfò, I., Larson, R., Choi, B.D., Bouffard, A.A., Gallagher, K., Schmidts, A., Bailey, S.R., Kann, M.C., et al. (2022). Non-cleavable hinge enhances avidity and expansion of CAR-T cells for acute myeloid leukemia. Cancer Cell *40*, 494-508.e5. https://doi.org/10.1016/j.ccell.2022.04.001.

173. Ma, P., Ren, P., Zhang, C., Tang, J., Yu, Z., Zhu, X., Fan, K., Li, G., Zhu, W., Sang, W., et al. (2021). Avidity-Based Selection of Tissue-Specific CAR-T Cells from a Combinatorial Cellular Library of CARs. Adv. Sci. *8*, 2003091. https://doi.org/10.1002/advs.202003091.

174. Drent, E., Themeli, M., Poels, R., de Jong-Korlaar, R., Yuan, H., de Bruijn, J., Martens, A.C.M., Zweegman, S., van de Donk, N.W.C.J., Groen, R.W.J., et al. (2017). A Rational Strategy for Reducing On-Target Off-Tumor Effects of CD38-Chimeric Antigen Receptors by Affinity

Optimization. Mol. Ther. J. Am. Soc. Gene Ther. *25*, 1946–1958. https://doi.org/10.1016/j.ymthe.2017.04.024.

175. Chmielewski, M., Hombach, A., Heuser, C., Adams, G.P., and Abken, H. (2004). T Cell Activation by Antibody-Like Immunoreceptors: Increase in Affinity of the Single-Chain Fragment Domain above Threshold Does Not Increase T Cell Activation against Antigen-Positive Target Cells but Decreases Selectivity1. J. Immunol. *173*, 7647–7653. https://doi.org/10.4049/jimmunol.173.12.7647.

176. He, C., Mansilla-Soto, J., Khanra, N., Hamieh, M., Bustos, V., Paquette, A.J., Garcia Angus, A., Shore, D.M., Rice, W.J., Khelashvili, G., et al. (2023). CD19 CAR antigen engagement mechanisms and affinity tuning. Sci. Immunol. *8*, eadf1426. https://doi.org/10.1126/sciimmunol.adf1426.

177. Davenport, A.J., Jenkins, M.R., Cross, R.S., Yong, C.S., Prince, H.M., Ritchie, D.S., Trapani, J.A., Kershaw, M.H., Darcy, P.K., and Neeson, P.J. (2015). CAR-T Cells Inflict Sequential Killing of Multiple Tumor Target Cells. Cancer Immunol. Res. *3*, 483–494. https://doi.org/10.1158/2326-6066.CIR-15-0048.

178. Benmebarek, M.-R., Karches, C.H., Cadilha, B.L., Lesch, S., Endres, S., and Kobold, S. (2019). Killing Mechanisms of Chimeric Antigen Receptor (CAR) T Cells. Int. J. Mol. Sci. *20*, 1283. https://doi.org/10.3390/ijms20061283.

179. Parkhurst, M.R., Yang, J.C., Langan, R.C., Dudley, M.E., Nathan, D.-A.N., Feldman, S.A., Davis, J.L., Morgan, R.A., Merino, M.J., Sherry, R.M., et al. (2011). T cells targeting carcinoembryonic antigen can mediate regression of metastatic colorectal cancer but induce severe transient colitis. Mol. Ther. J. Am. Soc. Gene Ther. *19*, 620–626. https://doi.org/10.1038/mt.2010.272.

180. Linette, G.P., Stadtmauer, E.A., Maus, M.V., Rapoport, A.P., Levine, B.L., Emery, L., Litzky, L., Bagg, A., Carreno, B.M., Cimino, P.J., et al. (2013). Cardiovascular toxicity and titin cross-reactivity of affinity-enhanced T cells in myeloma and melanoma. Blood *122*, 863–871. https://doi.org/10.1182/blood-2013-03-490565.

181. Cameron, B.J., Gerry, A.B., Dukes, J., Harper, J.V., Kannan, V., Bianchi, F.C., Grand, F., Brewer, J.E., Gupta, M., Plesa, G., et al. (2013). Identification of a Titin-derived HLA-A1-presented peptide as a cross-reactive target for engineered MAGE A3-directed T cells. Sci. Transl. Med. *5*, 197ra103. https://doi.org/10.1126/scitranslmed.3006034.

182. Lao, J., Oikawa, A., Bromley, J.R., McInerney, P., Suttangkakul, A., Smith-Moritz, A.M., Plahar, H., Chiu, T.-Y., González Fernández-Niño, S.M., Ebert, B., et al. (2014). The plant glycosyltransferase clone collection for functional genomics. Plant J. Cell Mol. Biol. *79*, 517–529. https://doi.org/10.1111/tpj.12577.

5. Appendix

5.1. List of Abbreviations

4-1BB (CD137)	Tumor necrosis factor receptor superfamily member *9* (TNFRSF9)
AICD	Activation induced cell death
ATAC-seq	Assay for transposase-accessible chromatin sequencing
CAR	Chimeric antigen receptor
Cas9	CRISPR associated protein 9
CCR7 (CD197)	C-chemokine receptor type 7
CD	Cluster of differentiation (CD3, CD4, CD8, CD28, CD45Ro)
cDNA	Coding DNA
CEA	Carcinoembryonic antigen
CM	Central memory
CRISPR	Clustered regulatory interspaced palindromic repeats
crRNA	CRISPR RNA
ELISA	Enzyme-linked immuosorbant assay
EM	Effector memory
ERM	Ezrin-radixin-moesin family
FMO	Fluorescence minus one
FSC-A	Forward scatter - area
HSC	Hematopoietic stem cell
IgG	Immune globulin G
Lag3 (CD223)	Lymphocyte-activation gene 3
MFI	Mean fluorescence intensity
mRNA	Messenger RNA
nt	Nucleotide
PAAD	Pancreatic adenocarcinoma
PBMC	Peripheral blood mononuclear cell
PD1 (CD279)	Programmed cell death protein 1
PKCα	Protein kinase C alpha
pN	Pico Newton
PTB1B	Protein tyrosine phosphatase 1B
Rac1	Ras-related C3 botulinum toxin substrate 1
RU	Relative unit
ROS	Reactive oxygen species
scFv	Single chain variable fragment
shRNA	Short hairpin RNA
TCR	T cell receptor
TIL	Tumor infiltration cell
TIL	Tumor infiltrating lymphocyte
Tim3 (CD366, HAVCR2)	T cell immunoglobulin and mucin-domain containing-3
TM	Trans-membrane
TME	Tumor microenvironment
TPM	Transcripts per million
tracrRNA	Trans-activating CRISPR RNA
Treg	Regulatory T cell
TRUCK	T cells redirected for antigen-unrestricted cytokine-initiated killing
VCAM1 (CD106)	Vascular adhesion molecule 1

5.2. List of Figures

Figure 1: The Chimeric Antigen Receptor building blocks 2

Figure 2: The immunological CAR synapse. 4

Figure 3: The canonical role of VCAM1. 6

Figure 4: Single-cell ATAC-seq identifies VCAM1 gene activity in terminal exhaustion clusters of primary human CD8+ TILs. 9

Figure 5: Timeline of the CAR T cell production and VCAM1 modification process. 23

Figure 6: Gating strategy for flow cytometry data. 26

Figure 7: CAR T cells but not untransduced T cells express VCAM1 upon stimulation. 30

Figure 8: 4-1BB CAR induced stronger VCAM1 expression in CD8+ T cells than the CD28 CAR. 31

Figure 9: VCAM1 expression is depended on intracellular CAR signaling domains......32

Figure 10: The VCAM1 ligand VLA-4 expression on HaCaT keratinocytes and on BXPC-3 tumor cells......34

Figure 11: Figure 12: VCAM1 knockdown with specific shRNA.VLA-4 is expressed on CD4+ and CD8+ T cells independent o VCAM1 expression. 35

Figure 12: VCAM1 knockdown with specific shRNA. 36

Figure 13: CRISPR mediated VCAM1 knockout in CAR T cells. 38

Figure 14: Activation and early exhaustion markers are increased in VCAM1^{+} CAR T cells...40

Figure 15: VCAM1 knockout reduced the number of CAR T cells in the central memory pool. 42

Figure 16: VCAM1 knockout decreased degranulation but not the cytotoxic capacity on of CAR T cells on BXPC-3 tumor cells. 43

Figure 17: Co-localization of CAR and VCAM1......45

Figure 18: VCAM1 localized in T cells towards the tumor cell contact region. 46

Figure 19: Avidity of CAR T cells:.....47

Figure 20: Differential expression of VLA-4 in healthy and diseased pancreas......49

Figure 21: The non canonical role of VCAM1 - on CD8+ CAR T cell in contact to cancer cells. 54

5.3. List of Tables

Table 1: Chemicals and reagents 12

Table 2: Kits used for bacterial work, DNA extreaction, CRISPR/Cas9 and FACS. 13

Table 3: Buffers and solutions used for bacterial work, cell culture and ELISA. 13

Table 4: PCR reagents for mutagenesis, Gibson assembly and sequencing. 13

Table 5: Primers used for mutagenesis, Gibson assembly and sequecing. 14

Table 6: Plasmids that were used for retroviral CAR transduction. 15

Table 7: crRNAs and tracrRNA used for CRISPR/Cas9,. 16

Table 8: Media and supplements used for cell culture. 16

Table 9: Cell lines 16

Table 10: Antibodies used for cell culture, ELISA, FACS, MACS, microscopy and zMovi. 17

Table 11: Software used for data generation, visualization and analysis. 18

Table 12: shRNA sequences for knockdown of VCAM1 and Kanamycin target as control 36

Table 13: CRISPR guide RNAs for VCAM1 knockout and scrambled as control. 38

5.4. VCAM1 exons and target sites

Exons of VCAM1 and the binding sites for CRISPR guide RNAs is shown.

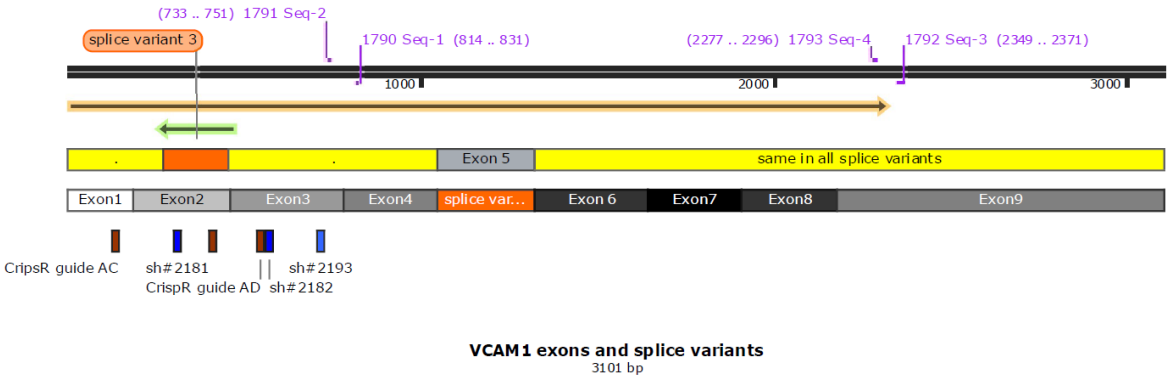

VCAM1 exons and splice variants
3101 bp

5.5. Genomic sequences of CAR constructs

All shown CAR sequences were inserted to the pBullet vector backbone[182] for amplification and transduction. DNA sequence, annotation and unique 6-cutter restriction sites are shown.

5.5.1. #2181 pBullet_Lk_BW431/26scFv_IgG1Fc-CD4TM_41BB_CD3ζ _mir30_shVCAM1-exon2

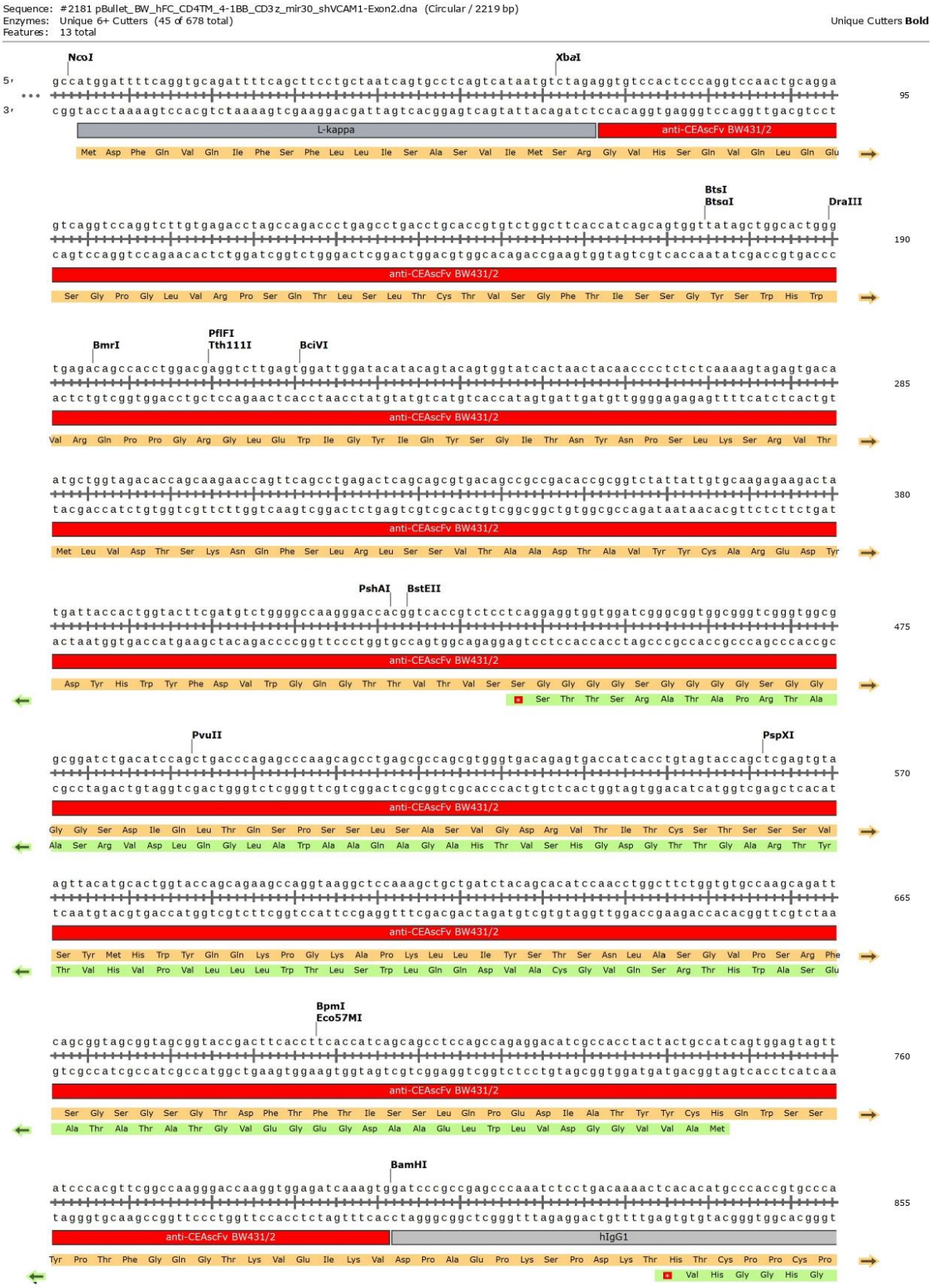

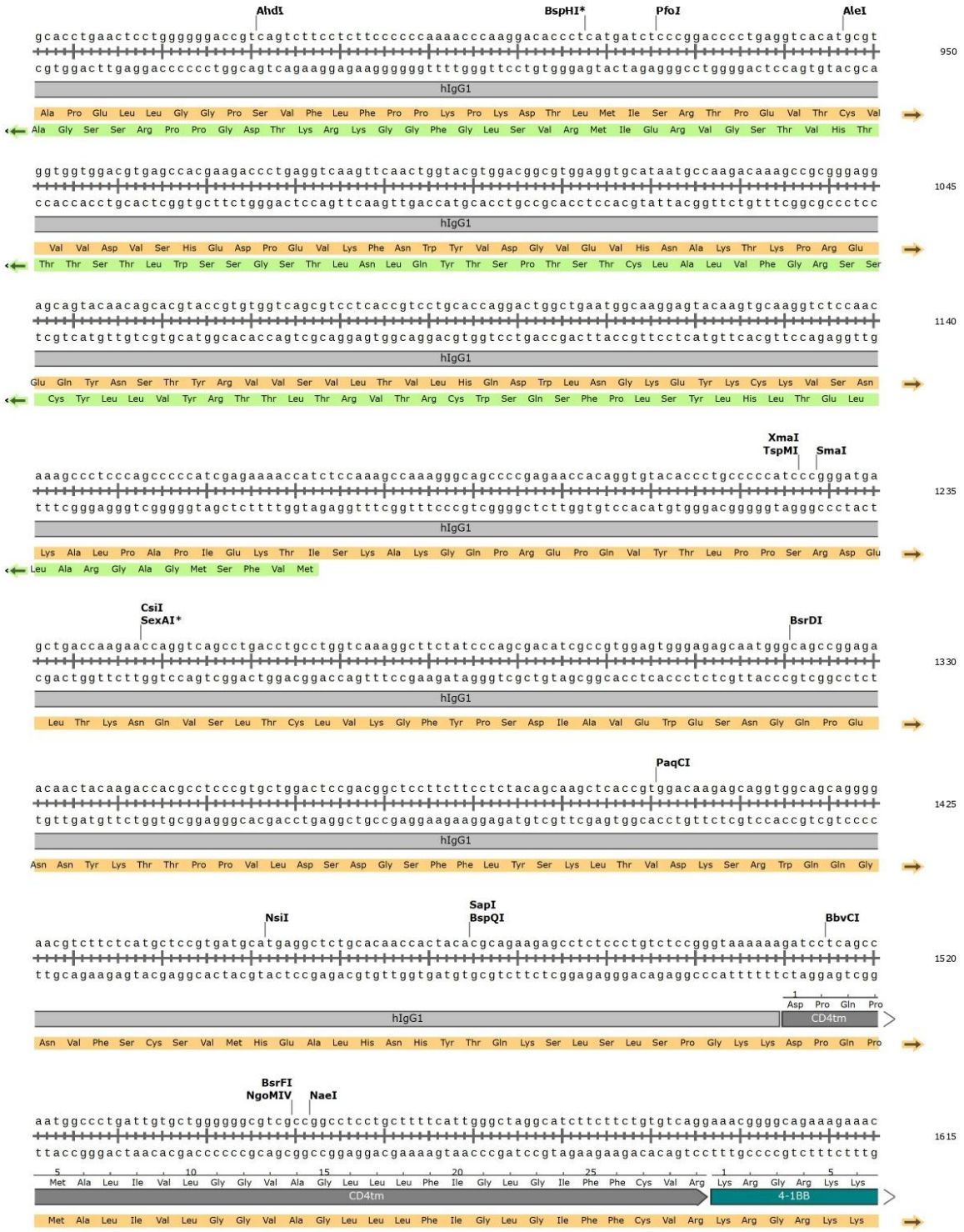
AhdI
BspHI*
PfoI
AleI
950
hIgG1
1045
1140
XmaI
TspMI
SmaI
1235
CsiI
SexAI*
BsrDI
1330
PaqCI
1425
NsiI
SapI
BspQI
BbvCI
1520
CD4tm
BsrFI
NgoMIV
NaeI
1615
4-1BB

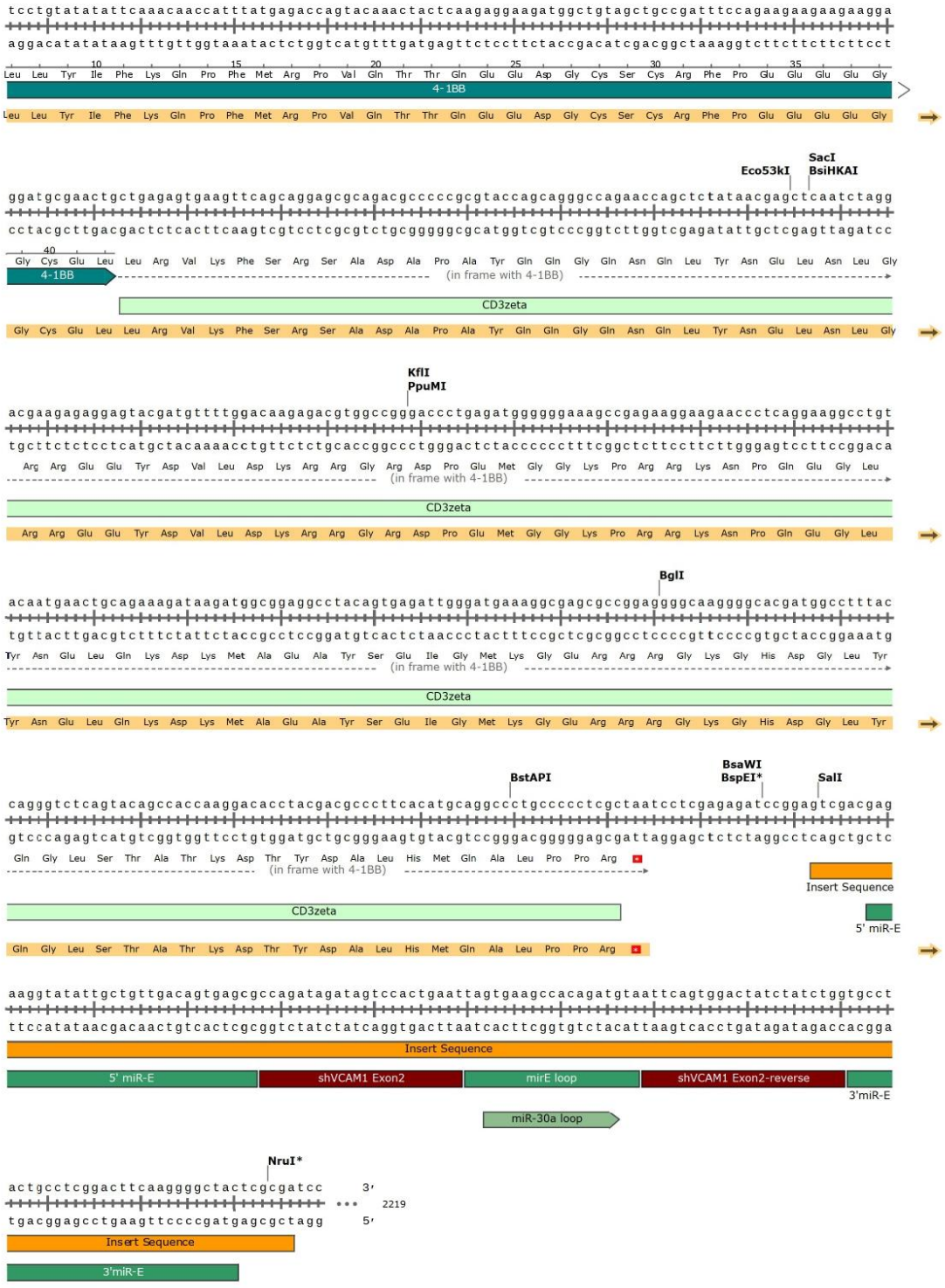
1710
1805
1900
1995
2090
2185
Eco53kI
SacI
BsiHKAI
KflI
PpuMI
BglI
BstAPI
BsaWI
BspEI*
SalI
NruI*
4-1BB
(in frame with 4-1BB)
CD3zeta
Insert Sequence
5' miR-E
shVCAM1 Exon2
mirE loop
shVCAM1 Exon2-reverse
3'miR-E
miR-30a loop
2219

5.5.2. #2182 pBullet_Lk_BW431/26scFv_IgG1Fc-CD4TM_41BB_CD3ζ_mir30_shVCAM1-exon3-early


XmaI
TspMI
SmaI
CsiI
ScxAI*
BsrDI
hIgG1
PaqCI
NsiI
SapI
BspQI
hIgG1
BbvCI
BsrFI
NgoMIV
NaeI
hIgG1
CD4tm
4-1BB
4-1BB
(in frame with 4-1BB)
CD3zeta
SacI
BsiHKAI
Eco53kI
KflI
PpuMI
(in frame with 4-1BB)
CD3zeta
BglI
(in frame with 4-1BB)
CD3zeta
BsaWI
BspEI*
BstAPI
SalI
BsrBI
(in frame with 4-1BB)
Insert Sequence
CD3zeta
5' miR-E
shVCAM1 Exone early
mirE loop
shVCAM1 Exone early
miR-30a loop
NruI*
Insert Sequence
3'miR-E
shVCAM1 Exone early

5.5.3. #2193 pBullet_Lk_BW431/26scFv_IgG1Fc-CD4TM_41BB_CD3ζ _mir30_shVCAM1-exon3-late

Sequence: #2193 pBullet_BW_hFC_CD4TM_4-1BB_CD3z_mir30_shVCAM1-Exon3-late.dna (Circular / 2218 bp)
Enzymes: Unique 6+ Cutters (48 of 678 total)
Features: 13 total

Unique Cutters **Bold**

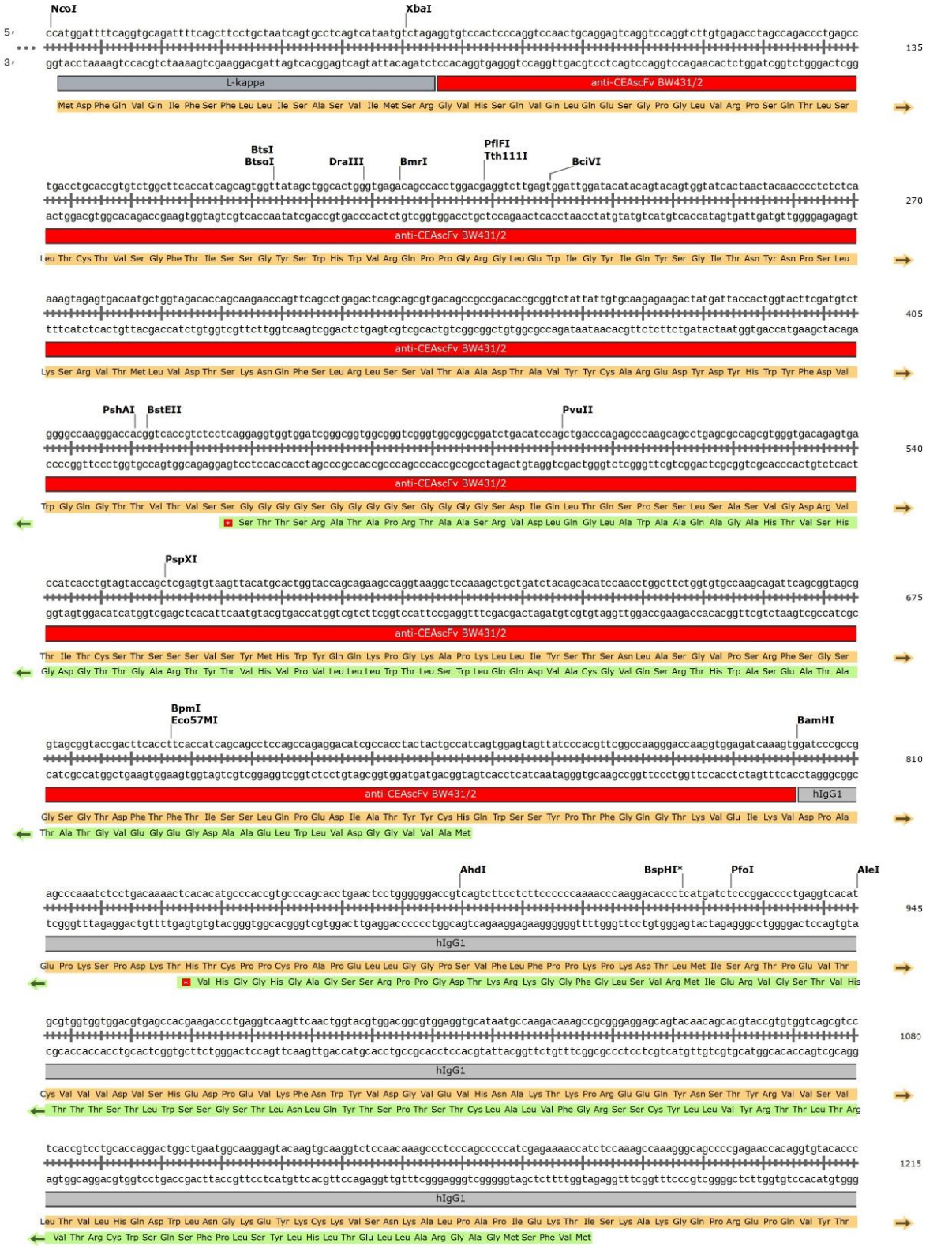


XmaI
TspMI
SmaI
CsiI
ScxAI*
BsrDI
hIgG1
PaqCI
NsiI
SapI
BspQI
hIgG1
BbvCI
BsrFI
NgoMIV
NaeI
hIgG1
CD4tm
4-1BB
4-1BB
(in frame with 4-1BB)
CD3zeta
SacI
BsiHKAI
Eco53kI
KflI
PpuMI
(in frame with 4-1BB)
CD3zeta
BglI
(in frame with 4-1BB)
CD3zeta
BsaWI
BspEI*
BstAPI
SalI
BsaBI
(in frame with 4-1BB)
Insert Sequence
CD3zeta
5' miR-E
broad institut sh - exo...
mirE loop
broad institut sh - exon3 late -reverse
miR-30a loop
BssSI
BssSαI
NruI*
Insert Sequence
broad institut sh -...
3'miR-E

5.5.4. #2210 pBullet_Lk_BW431/26scFv_IgG1Fc-CD4TM_41BB_CD3ζ _mir30_shKanamycin

Sequence: #2210 pBullet_BW_hFC_CD4TM_4-1BB_CD3z_mir30_shKanamycin.dna (Circular / 2218 bp)
Enzymes: Unique 6+ Cutters (45 of 678 total)
Features: 13 total

Unique Cutters **Bold**

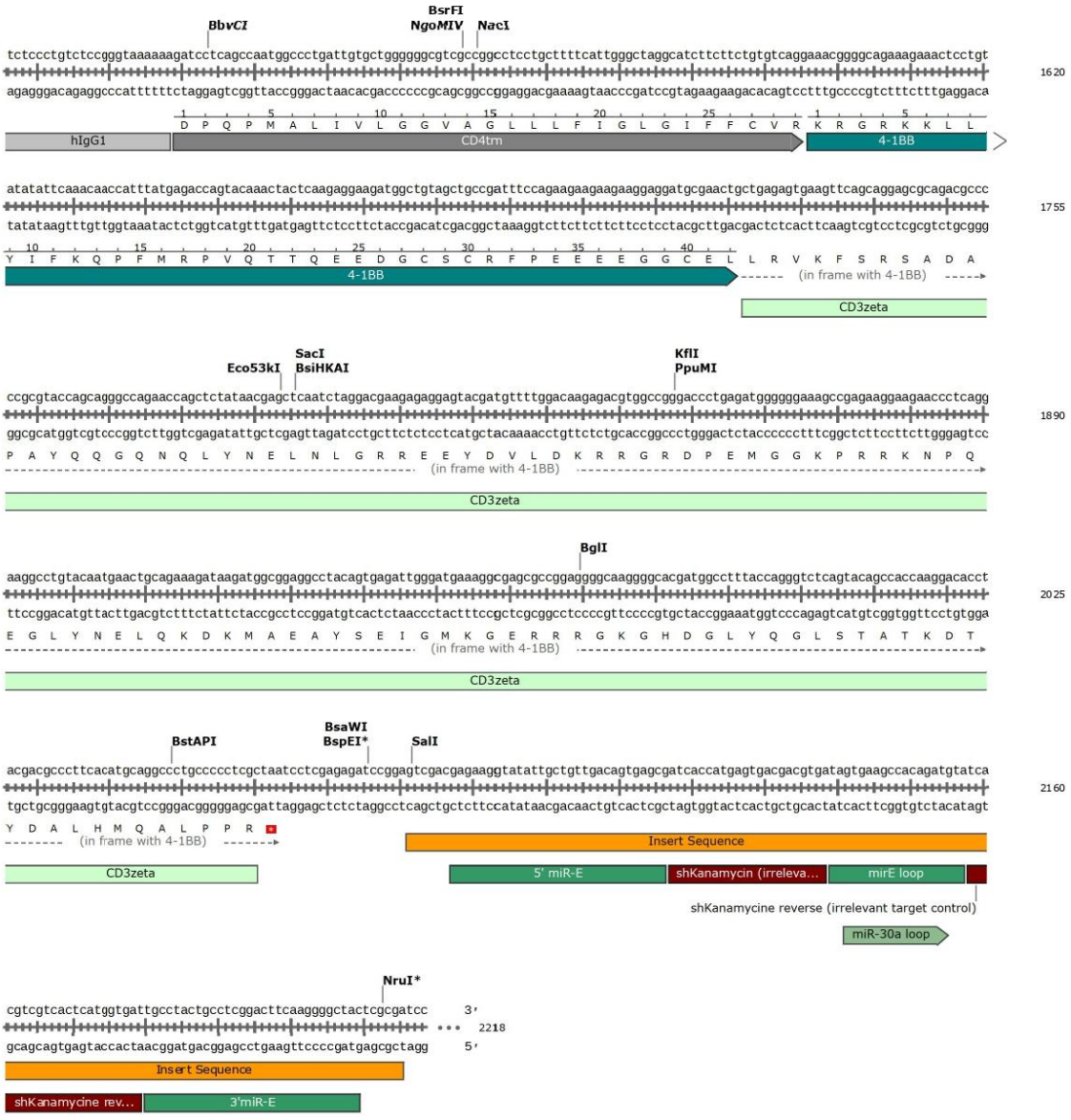
BbvCI
BsrFI
NgoMIV
NacI
tctccctgtctccgggtaaaaaagatcctcagccaatggccctgattgtgctgggggcgtcgccggcctcctgcttttcattgggctaggcatcttcttctgtgtcaggaaacggggcagaaagaaactcctgt
agagggacagaggcccatttttctaggagtcggttaccgggactaacacgacccccgcagcggccggaggacgaaaagtaacccgatccgtagaagaagacacagtcctttgccccgtctttctttgaggaca
1620
D P Q P M A L I V L G G V A G L L L F I G L G I F F C V R K R G R K K L L
hIgG1
CD4tm
4-1BB
atatattcaaacaaccatttatgagaccagtacaaactactcaagaggaagatggctgtagctgccgatttccagaagaagaagaaggaggatgcgaactgctgagagtgaagttcagcaggagcgcagacgccc
tatataagtttgttggtaaatactctggtcatgtttgatgagttctccttctaccgacatcgacggctaaaggtcttcttcttcttcctcctacgcttgacgactctcacttcaagtcgtcctcgcgtctgcggg
1755
Y I F K Q P F M R P V Q T T Q E E D G C S C R F P E E E E G G C E L L R V K F S R S A D A
4-1BB
(in frame with 4-1BB)
CD3zeta
SacI
Eco53kI
BsiHKAI
KflI
PpuMI
ccgcgtaccagcagggccagaaccagctctataacgagctcaatctaggacgaagagaggagtacgatgttttggacaagagacgtggccgggaccctgagatgggggaaagccgagaaggaagaaccctcagg
ggcgcatggtcgtcccggtcttggtcgagatattgctcgagttagatcctgcttctctcctcatgctacaaaacctgttctctgcaccggccctgggactctacccccctttcggctcttccttcttgggagtcc
1890
P A Y Q Q G Q N Q L Y N E L N L G R R E E Y D V L D K R R G R D P E M G G K P R R K N P Q
(in frame with 4-1BB)
CD3zeta
BglI
aaggcctgtacaatgaactgcagaaagataagatggcggaggcctacagtgagattgggatgaaaggcgagcgccggaggggcaaggggcacgatggcctttaccagggtctcagtacagccaccaaggacacct
ttccggacatgttacttgacgtctttctattctaccgcctccggatgtcactctaaccctactttccgctcgcggcctccccgttccccgtgctaccggaaatggtcccagagtcatgtcggtggttcctgtgga
2025
E G L Y N E L Q K D K M A E A Y S E I G M K G E R R G K G H D G L Y Q G L S T A T K D T
(in frame with 4-1BB)
CD3zeta
BstAPI
BsaWI
BspEI*
SalI
acgacgcccttcacatgcaggccctgccccctcgctaatcctcgagagatccggagtcgacgagaaggtatattgctgttgacagtgagcgatcaccatgagtgacgacgtgatagtgaagccacagatgtatca
tgctgcgggaagtgtacgtccgggacgggggagcgattaggagctctctaggcctcagctgctcttccatataacgacaactgtcactcgctagtggtactcactgctgcactatcacttcggtgtctacatagt
2160
Y D A L H M Q A L P P R
(in frame with 4-1BB)
Insert Sequence
CD3zeta
5' miR-E
shKanamycin (irreleva...
mirE loop
shKanamycine reverse (irrelevant target control)
miR-30a loop
NruI*
cgtcgtcactcatggtgattgcctactgcctcggacttcaaggggctactcgcgatcc 3'
gcagcagtgagtaccactaacggatgacggagcctgaagttccccgatgagcgctagg 5'
2218
Insert Sequence
shKanamycine rev...
3'miR-E

5.5.5. #2602 pBullet_Lk-BW431/26scFv_CD8hinge-CD8TM_41BB_CD3ζ

Sequence: #2602 pBullet_Lk_BW431 26scFv_CD8hinge_CD8TM_41BB_CD3z.dna (Circular / 1504 bp)
Enzymes: Unique 6+ Cutters (39 of 678 total)
Features: 8 total

Unique Cutters **Bold**

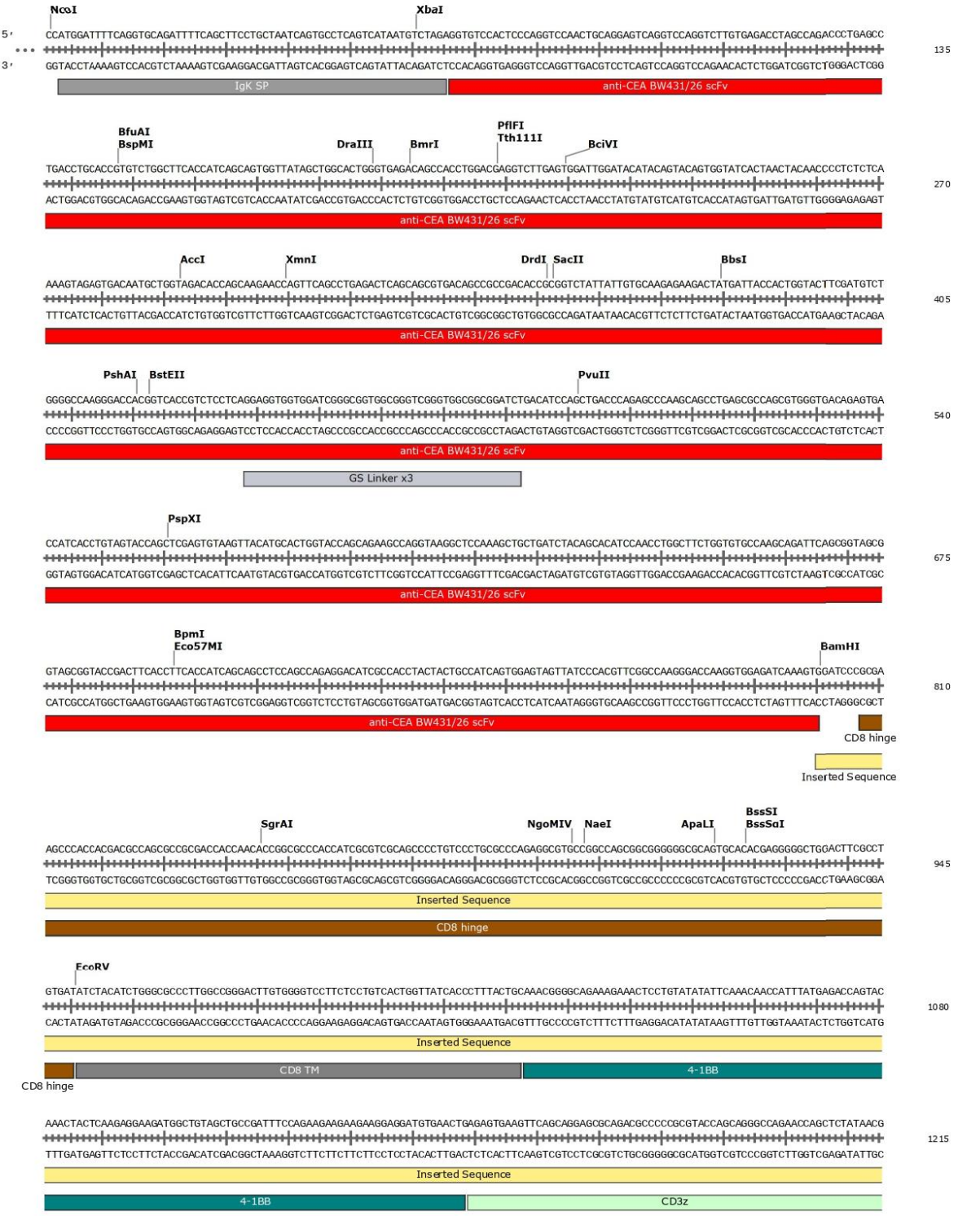

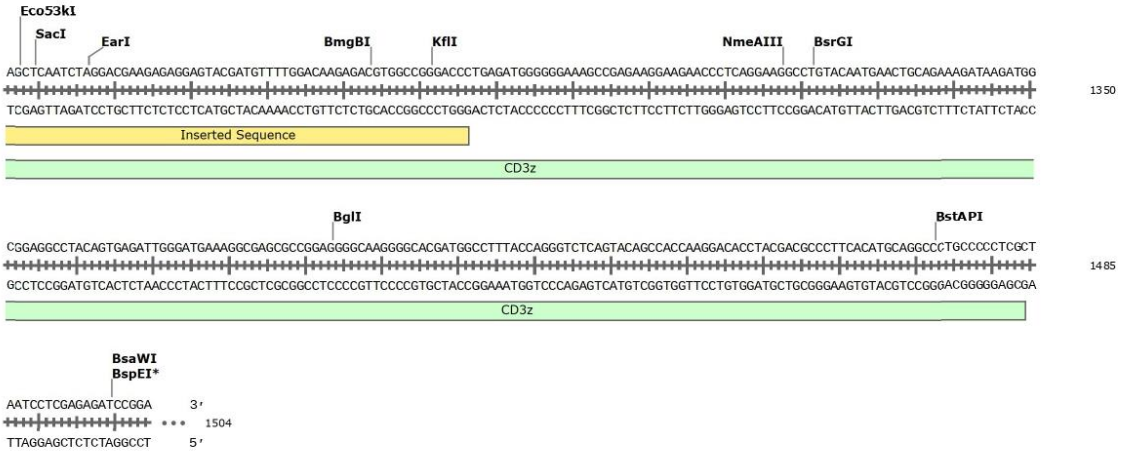
Eco53kI
SacI
EarI
BmgBI
KflI
NmeAIII
BsrGI
AGCTCAATCTAGGACGAAGAGAGGAGTACGATGTTTTGGACAAGAGACGTGGCCGGGACCCTGAGATGGGGGGAAAGCCGAGAAGGAAGAACCCTCAGGAAGGCCTGTACAATGAACTGCAGAAAGATAAGATGG
1350
TCGAGTTAGATCCTGCTTCTCTCCTCATGCTACAAAACCTGTTCTCTGCACCGGCCCTGGGACTCTACCCCCCTTTCGGCTCTTCCTTCTTGGGAGTCCTTCCGGACATGTTACTTGACGTCTTTCTATTCTACC
Inserted Sequence
CD3z
BglI
BstAPI
CGGAGGCCTACAGTGAGATTGGGATGAAAGGCGAGCGCCGGAGGGGCAAGGGGCACGATGGCCTTTACCAGGGTCTCAGTACAGCCACCAAGGACACCTACGACGCCCTTCACATGCAGGCCCTGCCCCCTCGCT
1485
GCCTCCGGATGTCACTCTAACCCTACTTTCCGCTCGCGGCCTCCCCGTTCCCCGTGCTACCGGAAATGGTCCCAGAGTCATGTCGGTGGTTCCTGTGGATGCTGCGGGAAGTGTACGTCCGGGACGGGGGAGCGA
CD3z
BsaWI
BspEI*
AATCCTCGAGAGATCCGGA 3′
1504
TTAGGAGCTCTCTAGGCCT 5′

5.5.6. #2737 pBullet_Lk_BW431/26scFv_IgG1Fc-CD4TM_41BB

Sequence: #2737 pBullet-Lk-BW431-26-scFv-hIgG1Fc-CD4-41BB (no CD3z).dna (Circular / 2064 bp)
Features: 8 total


human IgG1
CD4tm
4-1BB(ic)
CD3zeta(ic)

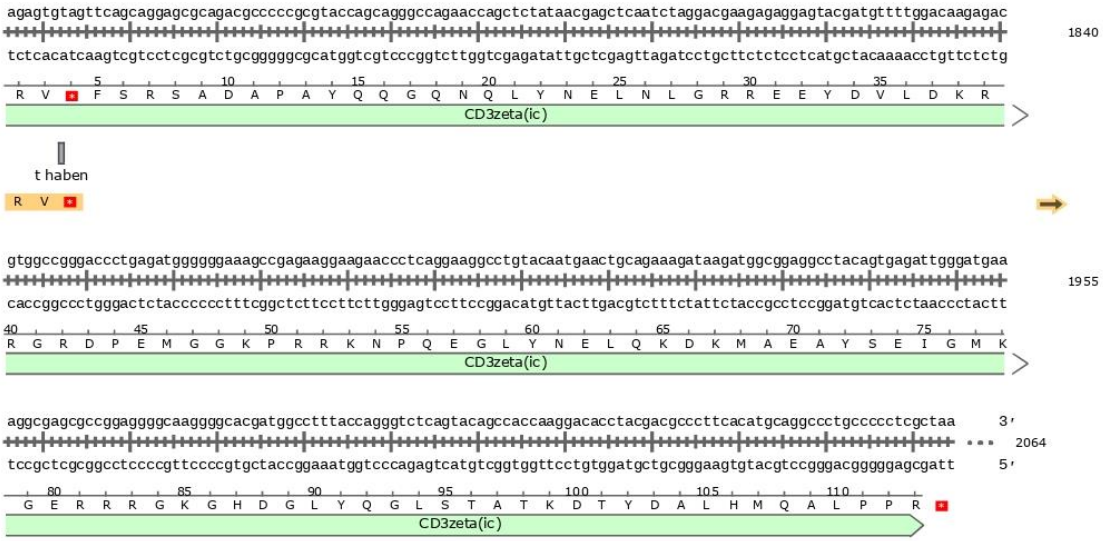
agagtgtagttcagcaggagcgcagacgccccgcgtaccagcagggccagaaccagctctataacgagctcaatctaggacgaagagaggagtacgatgttttggacaagagac
1840
tctcacatcaagtcgtcctcgcgtctgcgggggcgcatggtcgtcccggtcttggtcgagatattgctcgagttagatcctgcttctctcctcatgctacaaaacctgttctctg
R V F S R S A D A P A Y Q Q G Q N Q L Y N E L N L G R R E E Y D V L D K R
CD3zeta(ic)
t haben
R V
gtggccgggaccctgagatgggggaaagccgagaaggaagaaccctcaggaaggcctgtacaatgaactgcagaaagataagatggcggaggcctacagtgagattgggatgaa
1955
caccggccctgggactctacccccctttcggctcttccttcttgggagtccttccggacatgttacttgacgtctttctattctaccgcctccggatgtcactctaaccctactt
R G R D P E M G G K P R R K N P Q E G L Y N E L Q K D K M A E A Y S E I G M K
CD3zeta(ic)
aggcgagcgccggaggggcaaggggcacgatggcctttaccagggtctcagtacagccaccaaggacacctacgacgcccttcacatgcaggccctgccccctcgctaa
3′
2064
tccgctcgcggcctccccgttccccgtgctaccggaaatggtcccagagtcatgtcggtggttcctgtggatgctgcgggaagtgtacgtccgggacgggggagcgatt
5′
G E R R R G K G H D G L Y Q G L S T A T K D T Y D A L H M Q A L P P R
CD3zeta(ic)

5.5.7. #2738 pBullet_Lk_BW431/26scFv_IgG1Fc-CD4TM_CD3 ζ

Sequence: #2738 pBullet-Lk-BW431-26-scFv-hIgG1Fc-CD4-CD3zeta (no costim).dna (Circular / 1947 bp)
Enzymes: Unique Cutters (49 of 678 total)
Features: 5 total

Unique Cutters **Bold**

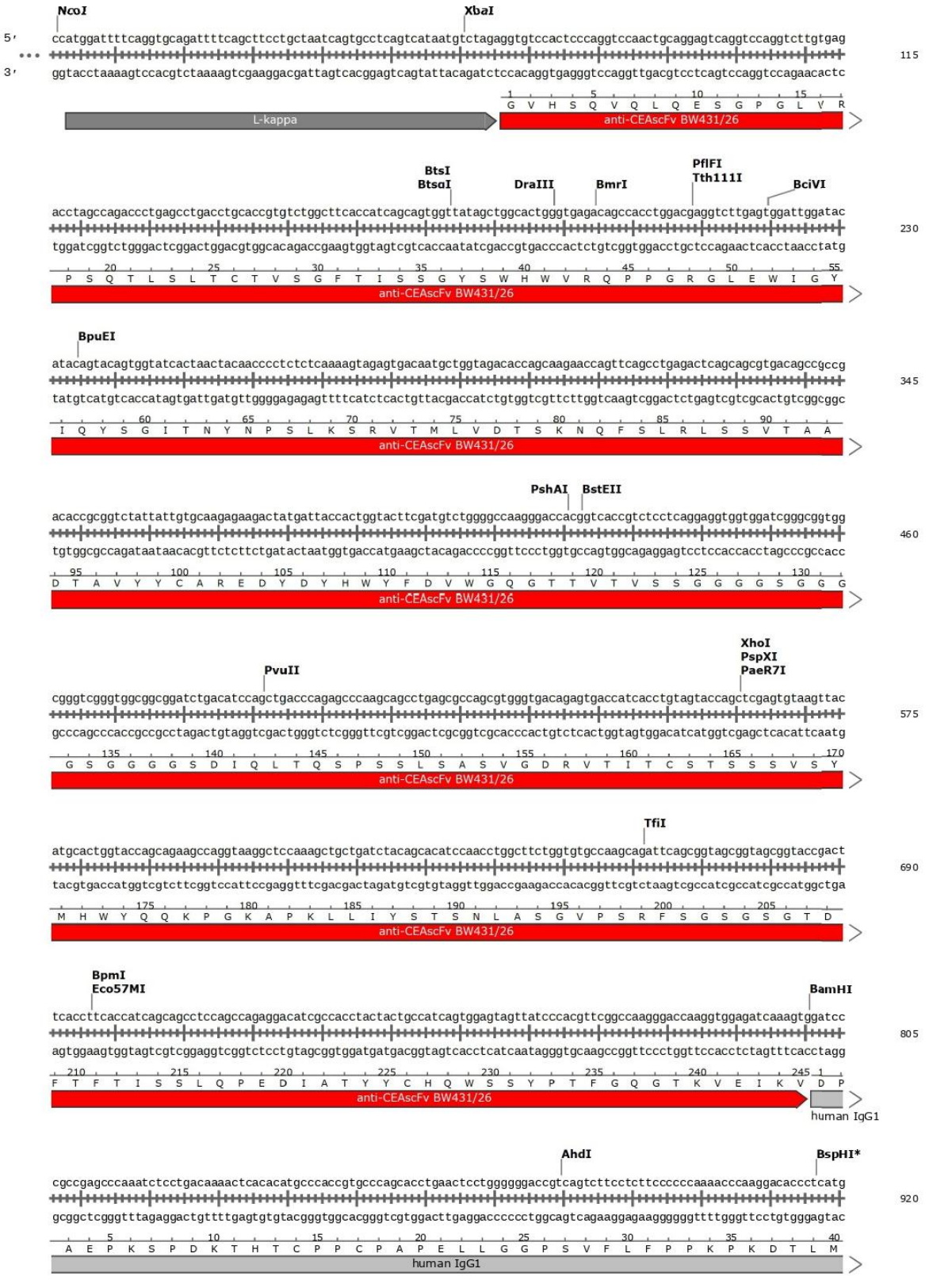

Printed from SnapGene®: 1. Apr 2024 14:40

Page 1

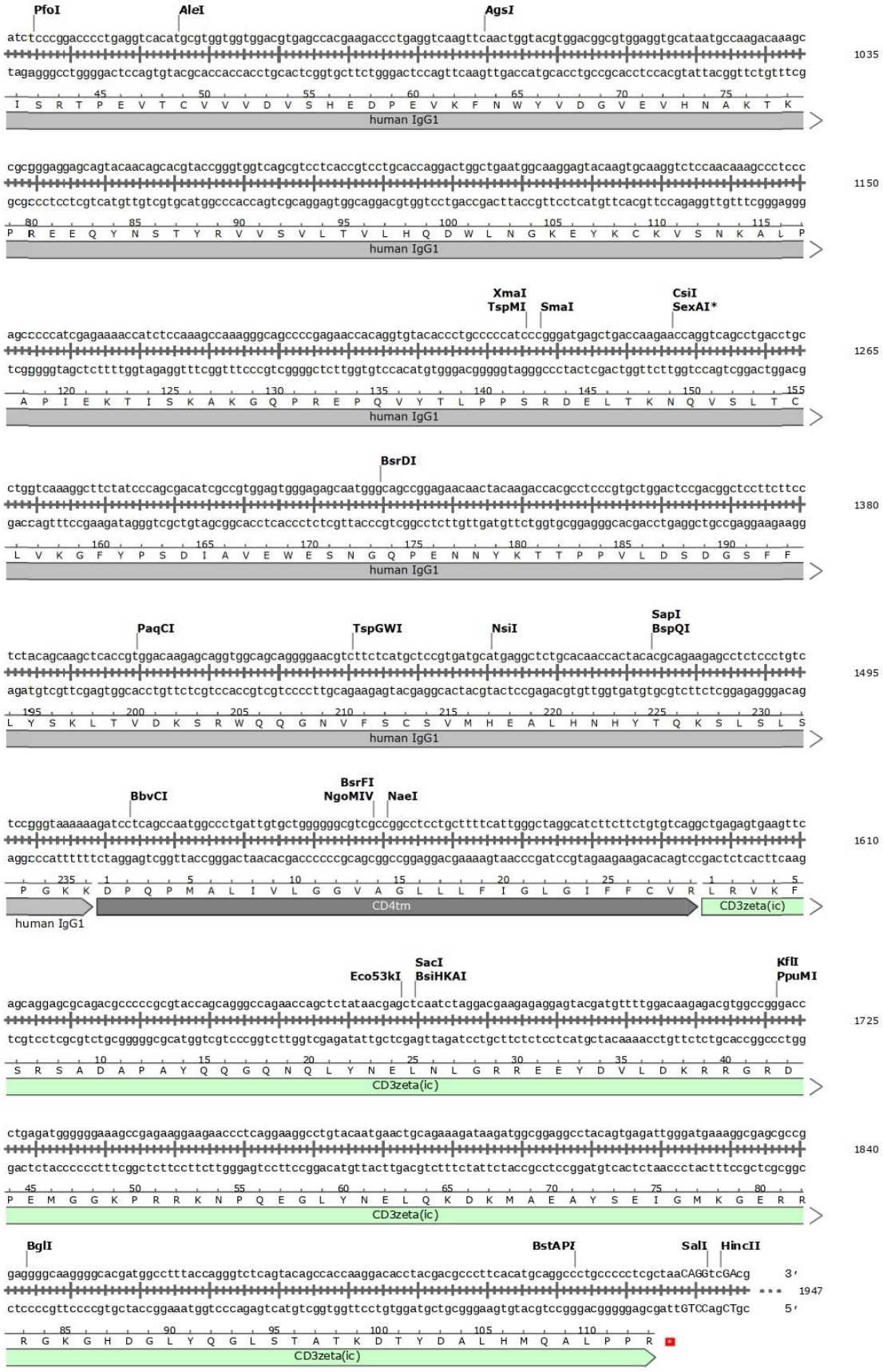
PfoI
AleI
AgsI
1035
1150
XmaI
TspMI
SmaI
CsiI
SexAI*
1265
BsrDI
1380
PaqCI
TspGWI
NsiI
SapI
BspQI
1495
BbvCI
BsrFI
NgoMIV
NaeI
1610
human IgG1
CD4tm
CD3zeta(ic)
Eco53kI
SacI
BsiHKAI
KflI
PpuMI
1725
1840
BglI
BstAPI
SalI
HincII
1947
3′
5′

5.5.8. #2739 pBullet_Lk_BW431/26scFv_IgG1Fc_CD4TM

Sequence: #2739 pBullet-Lk-BW431-26-scFv-hIgG1Fc-CD4 (no stim at all).dna (Circular / 2062 bp)
Features: 7 total

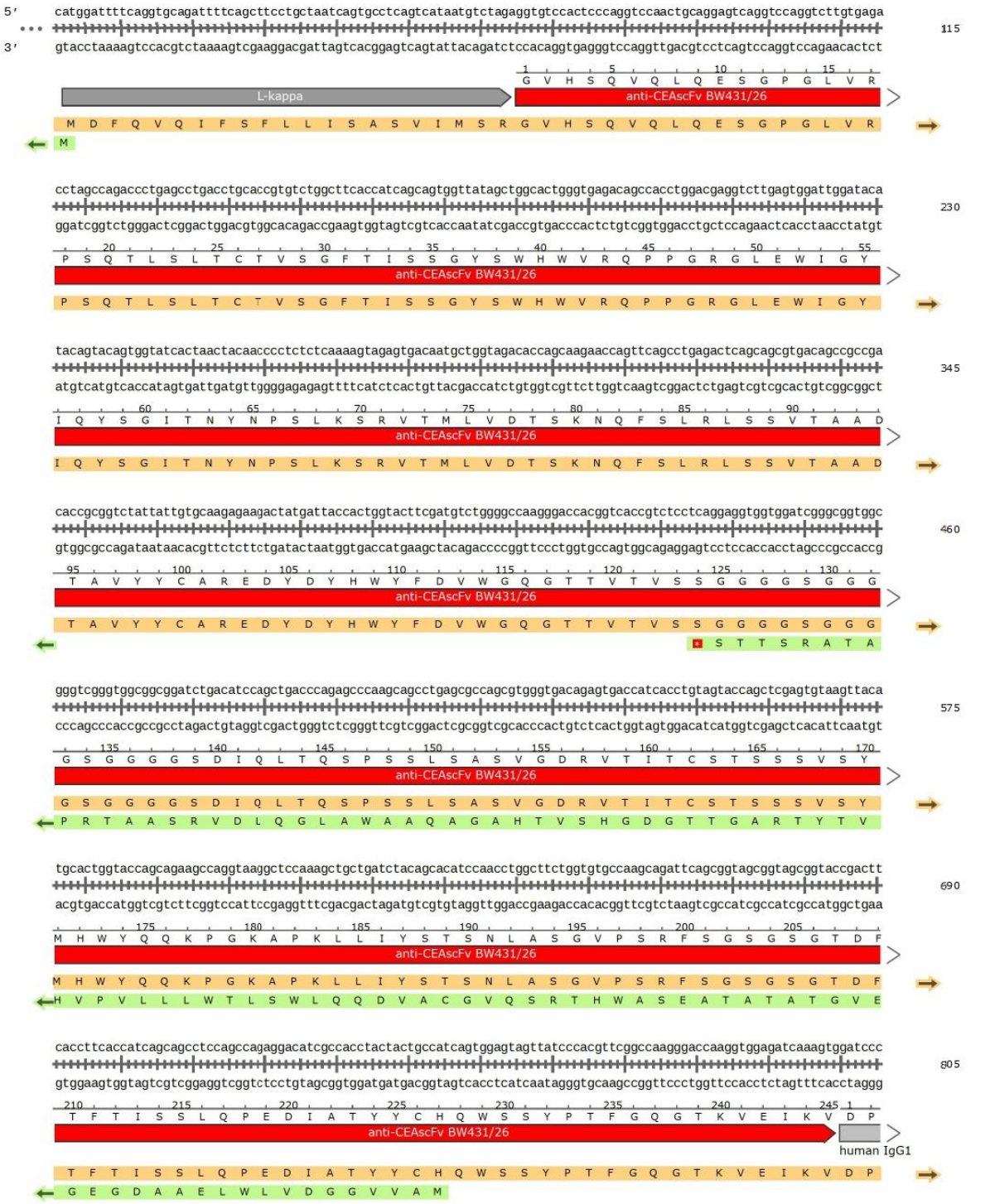


human IgG1
CD4tm
4-1BB(ic)
t haben2

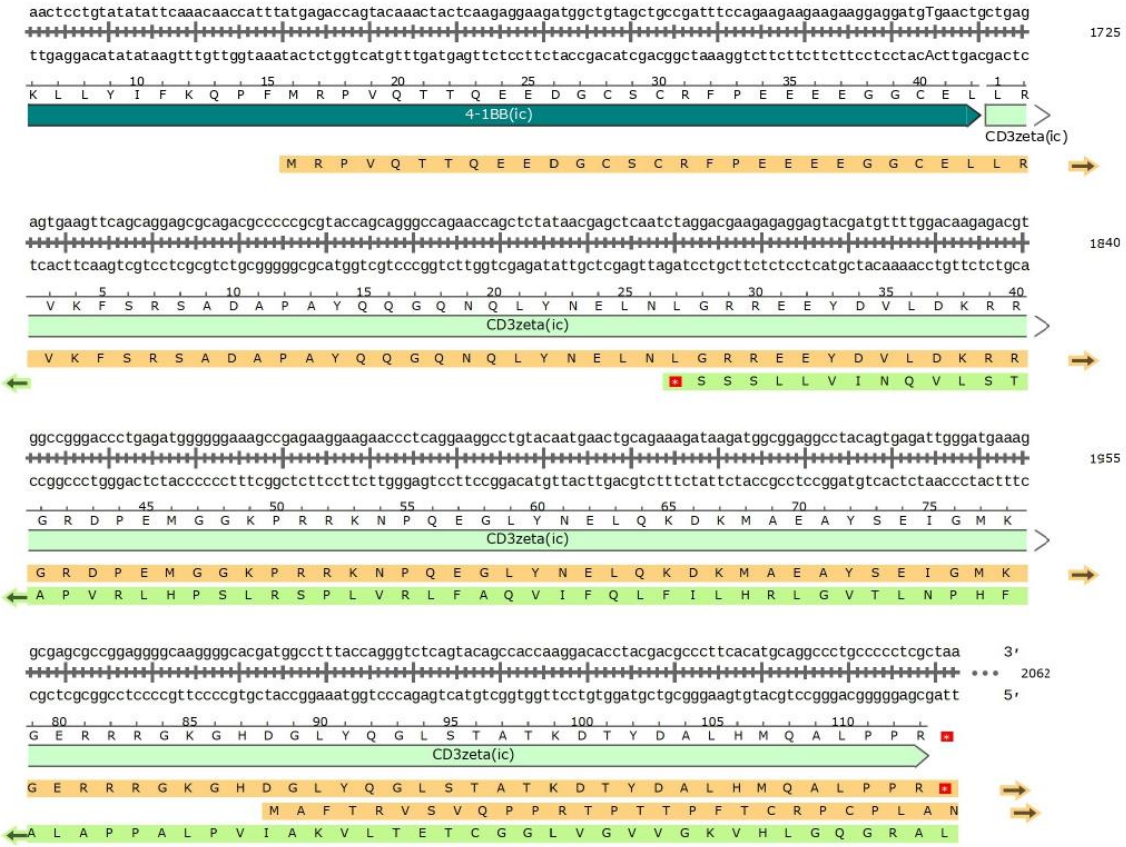
aactcctgtatatattcaaacaaccatttatgagaccagtacaaactactcaagaggaagatggctgtagctgccgatttccagaagaagaagaaggaggatgTgaactgctgag
1725
ttgaggacatatataagtttgttggtaaatactctggtcatgtttgatgagttctccttctaccgacatcgacggctaaaggtcttcttcttcttcctcctacActtgacgactc
K L L Y I F K Q P F M R P V Q T T Q E E D G C S C R F P E E E E G G C E L L R
4-1BB(ic)
CD3zeta(ic)
M R P V Q T T Q E E D G C S C R F P E E E E G G C E L L R
agtgaagttcagcaggagcgcagacgccccgcgtaccagcagggccagaaccagctctataacgagctcaatctaggacgaagagaggagtacgatgttttggacaagagacgt
1840
tcacttcaagtcgtcctcgcgtctgcgggggcgcatggtcgtcccggtcttggtcgagatattgctcgagttagatcctgcttctctcctcatgctacaaaacctgttctctgca
V K F S R S A D A P A Y Q Q G Q N Q L Y N E L N L G R R E E Y D V L D K R R
CD3zeta(ic)
V K F S R S A D A P A Y Q Q G Q N Q L Y N E L N L G R R E E Y D V L D K R R
S S S L L V I N Q V L S T
ggccgggaccctgagatgggggaaagccgagaaggaagaaccctcaggaaggcctgtacaatgaactgcagaaagataagatggcggaggcctacagtgagattgggatgaaag
1955
ccggccctgggactctacccccctttcggctcttccttcttgggagtccttccggacatgttacttgacgtctttctattctaccgcctccggatgtcactctaaccctactttc
G R D P E M G G K P R R K N P Q E G L Y N E L Q K D K M A E A Y S E I G M K
CD3zeta(ic)
G R D P E M G G K P R R K N P Q E G L Y N E L Q K D K M A E A Y S E I G M K
A P V R L H P S L R S P L V R L F A Q V I F Q L F I L H R L G V T L N P H F
gcgagcgccggaggggcaaggggcacgatggcctttaccagggtctcagtacagccaccaaggacacctacgacgcccttcacatgcaggccctgccccctcgctaa
3′
2062
cgctcgcggcctccccgttccccgtgctaccggaaatggtcccagagtcatgtcggtggttcctgtggatgctgcgggaagtgtacgtccgggacgggggagcgatt
5′
G E R R R G K G H D G L Y Q G L S T A T K D T Y D A L H M Q A L P P R
CD3zeta(ic)
G E R R R G K G H D G L Y Q G L S T A T K D T Y D A L H M Q A L P P R
M A F T R V S V Q P P R T P T T P F T C R P C P L A N
A L A P P A L P V I A K V L T E T C G G L V G V V G K V H L G Q G R A L

- The End -